RLk

REPORT NO. FRA/ORD-78/25

PB 285559

AN EXPERIMENTAL EVALUATION OF TECHNIQUES FOR MEASURING THE DYNAMIC COMPLIANCE OF RAILROAD TRACK

JULY 1978
FINAL REPORT
PHASE I

Prepared for

U.S. DEPARTMENT OF TRANSPORTATION
FEDERAL RAILROAD ADMINISTRATION
Office of Research and Development
Washington, D.C. 20590

NOTICE

The contents of this report reflect the views of Battelle's Columbus Laboratories, which is responsible for the facts and the accuracy of the data represented herein. The contents do not necessarily reflect the official views of the Department of Transportation. This report does not constitute a standard, specification, or regulation.

NOTICE

The United States Government does not endorse products or manufacturers. Trade or manufacturers' names appear herein solely because they are considered essential to the object of this report.

Technical Report Documentation Page

1. Report No.	2. Government Accession No.	3. Recipient's Catalog No.
FRA/ORD-78/25		

4. Title and Subtitle

AN EXPERIMENTAL EVALUATION OF TECHNIQUES FOR MEASURING THE DYNAMIC COMPLIANCE OF RAILROAD TRACK

5. Report Date: July 1978

6. Performing Organization Code

7. Author(s)

G. L. Nessler, R. H. Prause, W. D. Kaiser

8. Performing Organization Report No.

9. Performing Organization Name and Address

Battelle Columbus Laboratories
505 King Avenue
Columbus, Ohio 43201

10. Work Unit No. (TRAIS)

11. Contract or Grant No.

DOT-FR-30051

12. Sponsoring Agency Name and Address

U. S. Department of Transportation
Federal Railroad Administration
400 Seventh Street, S.W.
Washington, D C. 20591

13. Type of Report and Period Covered

Final Report Phase I
May 1975-Sept. 1977

14. Sponsoring Agency Code

15. Supplementary Notes

NONE

16. Abstract

SUMMARY

This report covers the initial track measurement task of a 3-phase program to design and fabricate equipment for measuring track dynamic characteristics. The objective of this task was to evaluate techniques for measuring the dynamic compliance and to identify general trends in the behavior of the track structure. Some of the results obtained were a high degree of nonlinearity of vertical track stiffness with vertical preload and a settling phenomenon of the track structure due to the constant preload and dynamic excitation. This settling yields a stiffer track structure for a constantly applied preload as compared to a cyclic preload.

MANAGEMENT REVIEW STATEMENT

The information in this report is intended for use by research personnel who have an interest in railroad track performance as related to vehicle/track interaction and track maintenance, and in the measurement of track deflections and dynamic characteristics for developing track analysis models and evaluating track structure condition.

17. Key Words	18. Distribution Statement
Track, track modulus, track dynamic compliance, track impedance, track dynamics, track stiffness	Document is available to the public through the National Technical Information Service, Springfield, Virginia 22161

19. Security Classif. (of this report)	20. Security Classif. (of this page)	21. No. of Pages	22. Price
UNCLASSIFIED	UNCLASSIFIED		

Form DOT F 1700.7 (8-72)

PREFACE

This report discusses some track dynamic response measurements which were made by Battelle's Columbus Laboratories (BCL) as a part of the Phase I work on Contract DOT-FR-30051 from the Office of Research and Development of the Federal Railroad Administration (FRA). The overall objective of this 3-phase program is to design and build equipment for measuring the dynamic compliance of railroad track. A previous interim report entitled "A Review of Measurement Techniques, Requirements, and Available Data on the Dynamic Compliance of Railroad Track" presents the results from a review of the literature and some preliminary concepts for measurement techniques.

Mr. Thomas P. Woll was the FRA technical monitor for this contract. The authors are grateful for the encouragement provided by Mr. Woll, the cooperation of several persons at the Ohio Railway Museum, and the contributions made by several members of the BCL staff during the long hours of the measurement program.

TABLE OF CONTENTS

	Page
SUMMARY OF RESULTS AND CONCLUSIONS	1
RECOMMENDATIONS FOR FUTURE WORK	7
TECHNICAL DISCUSSION	8
EQUIPMENT DESCRIPTION	8
Shaker Control System	13
Motion Transducers	13
Data Analysis	15
Random and Pulse Response Analysis	19
Track Compliance	20
TRACK MEASUREMENT LOCATIONS	27
RESULTS OF TRACK COMPLIANCE MEASUREMENTS	30
Sinusoidal Excitation	30
Effect of Preload	33
Single Versus 2-Rail Excitation	35
Increase in Dynamic Amplitude	35
Random Excitation in Vertical Direction	35
Effect of Preload	40
Single Versus 2-Rail Excitation	40
Increase in Dynamic Amplitude	46
Track Condition	46
Random Excitation in Lateral Direction	46

TABLE OF CONTENTS - Continued

Effect of Vertical Preload 46

Effect of Lateral Preload. 53

High Frequency Response. 61

Pulse Excitation in Vertical Direction. 61

Pulse Shape Spectra. 61

Effect of Pulse Duration 72

Effect of Preload. 76

Pulse Excitation at Location 3 in the Vertical Direction 86

Pulse Excitation in Lateral Direction 86

Comparison of Track Stiffness from Static and Dynamic Measurements. 86

Development of a Cyclic Preload/Pulse Excitation Technique. 95

Track Lateral Static Stiffness at Location 1 . . . 101

Effect of a Defective or Missing Tie. 105

Load Affected Zone 111

REFERENCES. 121

Page

APPENDIX A

Table A-1. Summary Table of Static Stiffness Measurements. A-1

Table A-2. Summary Table of Dynamic Stiffness Measurements A-2

Table A-3. Summary of Track Vertical and Lateral Dynamic Characteristics A-3

LIST OF FIGURES

Figure 1. Hydraulic Shaker System Mounted on Car Frame. 9

Figure 2. Vertical Hydraulic Cylinder Mounted to Underframe of Car and to Rail Head. 11

Figure 3. Mounting Configuration of the Hydraulic Shaker System . . . 12

Figure 4. Schematic of Actuator Control and Data Analysis Systems . . 14

Figure 5. Antenna Tower Used As Reference Beam For Relative Displacement Measurements 16

Figure 6. Fourier Analyzer Inside Railroad Car. 17

Figure 7. Single Degree-of-Freedom Model for a Vibratory System . . . 22

Figure 8. Theoretical Compliance Magnitude and Phase Curves as a Function of Frequency for a Single Degree-of-Freedom Model. 24

Figure 9. Track Lateral Dynamic Compliance (Phase and Coherence) Obtained by Using Random Excitation with a 5000-LB Vertical Preload at Location 1. 26

Figure 10. Averaged Force Power Spectral Density of the Random Excitation at Location 1. 28

Figure 11. Location No. 1 Test Site and Measurement Car 31

TABLE OF CONTENTS - Continued

Page

Figure 12. Location No. 2 Test Site. 32

Figure 13. Track Vertical Dynamic Compliance Obtained by Using Sinusoidal Excitation at Location 1 for Three Vertical Preloads. 34

Figure 14. Track Vertical Dynamic Stiffness at Location 1 Using Sinusoidal Excitation 37

Figure 15. Track Vertical Dynamic Compliance Obtained by Using Sinusoidal Excitation on a Single Rail and on Both Rails at Location 1 38

Figure 16. Track Vertical Dynamic Compliance Obtained by Using Sinusoidal Excitation to Determine the Effect of Doubling the Dynamic Excitation Level at Location 1. 39

Figure 17. Track Vertical Dynamic Compliance Obtained by Using Random Excitation for Three Vertical Preloads at Location 1. 41

Figure 18. Track Vertical Dynamic Compliance at Location 1 Obtained by Using Sinusoidal and Random Excitation for Two Different Vertical Preloads. 43

Figure 19. Track Vertical Dynamic Stiffness at Location 1 Using Sinusoidal and Random Excitation. 44

Figure 20. Track Vertical Dynamic Compliance Obtained by Using Random Excitation on a Single Rail and on Both Rails At Location 1 For Two Vertical Preloads 45

Figure 21. Track Vertical Dynamic Compliance Obtained by Using Random Excitation to Determine the Effect of Doubling the Dynamic Excitation Level at Location 1 47

TABLE OF CONTENTS - Continued

Page

Figure 22. Track Vertical Dynamic Compliance Obtained by Using Random Excitation for Three Vertical Preloads at Location 2. 48

Figure 23. Track Vertical Dynamic Stiffness at Locations 1 and 2. 51

Figure 24. Track Lateral Dynamic Compliance (Phase and Coherence) Obtained by Using Random Excitation with a 2500-lb Vertical Preload at Location 1. 52

Figure 25. Track Lateral Dynamic Stiffness, Effective Mass, and Natural Frequency at Location 1 as a Function of Vertical Preload. 54

Figure 26. Averaged Force Power Spectral Density of the Random Excitation at Location 1 55

Figure 27. Track Lateral Dynamic Compliance (Phase and Coherence) Obtained by Using Random Excitation with a 5000-lb Vertical Preload at Location 1. 56

Figure 28. Track Lateral Dynamic Compliance (Phase and Coherence) Obtained by Using Random Excitation with a 15,000-lb Vertical Preload at Location 1. 57

Figure 29. Track Lateral Dynamic Compliance Obtained By Using Random Excitation At Location 1 for Three Vertical Preloads 59

Figure 30. Track Lateral Dynamic Compliance Obtained By Using Random Excitation with and without a Lateral Preload For Two Vertical Preloads at Location 2. 60

Figure 31. Track Lateral Dynamic Compliance Obtained by Using Random Excitation for two Different Maximum Frequencies at Location 1. 63

Page

Figure 32. Track Lateral Dynamic Compliance to Demonstrate the Effect of Averaging Using Random Excitation at Location 1. 64

Figure 33. Input Rectangular Pulse Shapes to the Control System 66

Figure 34. Theoretical And Measured Frequency Content of the 10 Millisecond Rectangular Pulse. 67

Figure 35. Theoretical and Measured Frequency Content of the 15 Millisecond Rectangular Pulse 68

Figure 36. Theoretical and Measured Frequency Content of the 20 Millisecond Rectangular Pulse 69

Figure 37. Measured Unloading Pulse Input to the Rail Structure with 15,000-lb Vertical Preload. 70

Figure 38. Measured Unloading Pulse Input to the Rail Structure with 7500-lb Vertical Preload. 71

Figure 39. Track Vertical Dynamic Compliance Obtained by Using Pulse Excitation at a Fixed Vertical Preload and Variable Pulse Durations at Location 1 73

Figure 40. Comparison Between an Unloading and a Loading Pulse Shape. 75

Figure 41. Track Vertical Dynamic Compliance Obtained by Using a Loading Pulse and an Unloading Pulse at Location 2. 77

Figure 42. Track Vertical Dynamic Compliance Obtained by Using a 25 Millisecond Unloading Pulse for Three Preloads at Location 1 79

Figure 43. Track Vertical Dynamic Stiffness at Location 1 Using Three Methods of Excitation. 80

Figure 44. Track Vertical Dynamic Compliance Obtained by Using a Loading Pulse for Two Different Preloads at Location 2 82

TABLE OF CONTENTS - Continued

		Page
Figure 45.	Track Vertical Dynamic Stiffness at Location 2 for Two Methods of Dynamic Excitation.	85
Figure 46.	Track Vertical Dynamic Compliance (Phase and Coherence) Obtained by using Loading Pulse Excitation with a 2500-Lb Vertical Preload at Location 3	87
Figure 47.	Averaged Force Power Spectral Density of the Pulse Excitation at Location 3	88
Figure 48.	Track Vertical Dynamic Stiffness at Location 3 Using a Loading Pulse.	90
Figure 49.	Track Vertical Dynamic Compliance to Demonstrate the Effect of Averaging Using Pulse Excitation with 15,000-lb Preload at Location 1	91
Figure 50.	Track Lateral Dynamic Compliance Obtained by Using Loading Pulse Excitation at Location 1	92
Figure 51.	Track Lateral Dynamic Stiffness at Location 1 for Two Methods of Excitation.	94
Figure 52.	Vertical Load Deflection Curve for Location 2.	96
Figure 53.	Track Vertical Static and Dynamic Stiffness at Location 1.	98
Figure 54.	Vertical Load Deflection Curves for the Three Test Locations	99
Figure 55.	Comparison Between Two Methods of Excitation, One Using a Constant Static Preload with Pulse Excitation, and the Other Using a Cyclic Preload with Pulse Excitation.	100
Figure 56.	Track Vertical Dynamic Compliance Obtained by Using a Cyclic Preload/Pulse and a Constant Preload Pulse at Location 1.	102
Figure 57.	Typical Data for Vertical Tieplate Force for a 4-Car Train.	103
Figure 58.	Lateral Load Deflection Curves for Location 1.	104

Page

Figure 59. Track Vertical Dynamic Compliance Measured at Location 3 with and without the Tieplate. 107

Figure 60. Track Vertical Dynamic Stiffness for Nominal Track and Track with Tieplates on One Tie Removed at Location 3. 108

Figure 61. Vertical Load Deflection Curves for Location 3 with and without Tieplates 109

Figure 62. Track Vertical Dynamic Compliance Obtained by Using a Cyclic Preload/Pulse to Determine the Effect of a Missing Tieplate at Location 3 110

Figure 63. Track Lateral Dynamic Compliance with the Tieplates Removed. 112

Figure 64. Static Load Deflection Curves in the Lateral Direction for three vertical preloads at Location 3 114

Figure 65. Track Lateral Static and Dynamic Stiffness at Location 3 with the Tieplate Removed 115

Figure 66. Vertical Transfer Compliance Values at Specific Frequencies as a Function of Distance along the Rail 116

Figure 67. Track Vertical Transfer Dynamic Compliance at Four Locations Along the Rail. 119

Figure 68. Vertical Transfer Compliance Phase Angle for the Four Distances along the Rail. 120

Page

LIST OF TABLES

Table 1. Measurement Location Description. 29

Table 2. Summary of Vertical Compliance Measurements Using Sinusoidal Excitation at Location 1 36

Table 3. Summary of Vertical Compliance Measurements Using Random Excitation at Location 1 42

Table 4. Summary of Vertical Compliance Measurements Using Random Excitation at Location 2 49

Table 5. Summary of Vertical Dynamic Stiffnesses Measured at Locations 1 and 2. 50

Table 6. Summary of Lateral Compliance Measurements Using Random Excitation at Location 2 58

Table 7. Summary of Lateral Compliance Parameters for a Preloaded and Unpreloaded condition in the Lateral Direction Using Random Excitation at Location 1 62

Table 8. Summary of Vertical Compliance Measurement Using Pulse Excitation with 15,000 lb Vertical Preload for 5 Pulse Durations 74 74

Table 9. Summary of Vertical Compliance Parameters Comparing Loading Pulse Against An Unloading Pulse at Location 2 of 20 ms Duration 78

Table 10. Summary of Vertical Compliance Measurements Using Unloading Pulse Excitation at Location 1 81

Table 11. Summary of Vertical Compliance Characteristics Measured at Location 1 Using Three Methods of Excitation 83

Table 12. Summary of Vertical Compliance Characteristics Measured at Location 2 Using Two Methods of Excitation 84

Table 13. Summary of Vertical Loading Compliance Measurements at Location 3 Using Loading Pulse Excitation (20 ms) . . . 89

Page

LIST OF TABLES

Table 14. Comparison of Lateral Compliance Parameters Obtained Using Random and Pulse Excitation at Location 1. 93

Table 15. Summary of the Vertical Static and Dynamic Stiffness Data Obtained at Location 1. 97

Table 16. Comparison of the Static and Dynamic Lateral Stiffness Measured at Location 1 106

Table 17. Summary of Track Lateral Compliance Parameters at Location 3 Using Random Excitation. 113

Table 18. Transfer Compliance Values Along the Rail 117

SUMMARY OF RESULTS AND CONCLUSIONS

Several different techniques for measuring the dynamic characteristics of railroad track were evaluated during this relatively brief measurement program. These included sinusoidal, random and pulse excitation applied in the lateral and vertical directions at the rail head. Static load-deflection measurements were also made for comparison.

Measurements were made at three different locations on the track at the Ohio Railway Museum. The track at two of these locations was in relatively good condition with one location having tie plates and the other location having the rail spiked directly on the ties. The track at the third location had some split ties and was in a low area with water on both sides. All of the museum track is light construction (85 lb/yd rail), and the service loading consists of infrequent, low-speed tourist rides. Therefore, the quantitative results reported herein are not intended to represent the characteristics of typical mainline railroad track. However, the general behavior of the museum track is believed to be sufficiently typical of cross-tie track construction for the evaluation of measurement techniques and the identification of trends.

Hydraulic actuators mounted underneath and near the center of a railroad car were used to apply static preloads and dynamic excitation to the track. Two actuators were used to load both rails vertically, and a single actuator was used to apply a lateral load to one rail. The excitation force and track response were measured at the rail head. Pulse, sinusoidal and random dynamic loads were superimposed with constant vertical preloads up to 15,000 pounds on each rail to measure track dynamic compliance (ratio of track displacement to input force as a function of frequency). A fixed reference beam was used to determine track stiffness (static) from load-deflection curves for comparison with the dynamic data.

Detailed descriptions of the equipment, procedures, and results of the track measurements are included in the Technical Discussion section of this report. However, the most important results are summarized briefly in the following paragraphs.

Track Vertical Stiffness. An important conclusion from all of the measurements is that the nonlinear behavior of the track for vertical loads is quite significant. Vertical measurements show an initial low-stiffness region before the free-play between track components and in the ballast is removed by increasing preload. The vertical load range of 4000 to 8000 pounds per rail represented a transition region between the low and high stiffness regions. The tangent stiffness from static load-deflection measurements varied from 12,500 to 88,800 lb/in. per rail with a light preload of 2500 pounds, and from 158,000 to 258,000 lb/in. for a 15,000 pound preload--an order of magnitude difference. This verifies the necessity for using vertical loads representative of typical wheel loads in order to measure track characteristics which are valid for railroad service.

Track Lateral Stiffness. Lateral track load-deflection measurements with constant vertical preloads also show a significant nonlinear behavior. The initial lateral stiffness for low lateral loads is relatively high. The stiffness is reduced considerably when the lateral load is increased sufficiently to make the rail slide sideways. The track lateral stiffness is almost directly proportional to the vertical preload, so realistic wheel loads are also required for these measurements.

Track Dynamic Characterisitcs. Data on dynamic stiffness, resonant frequency, effective mass, and damping were measured to characterize the behavior of track under dynamic loading. As would be expected from the previous discussion, vertical preload had a significant effect on these results. In general, the data showed that increasing the vertical preload increased the stiffness, effective mass, and damping of the track structure. In most cases, increasing the preload also increased the resonant frequency. But the increase in effective mass partially compensated for the large increase in stiffness, so the relative change in resonant frequency was less than the variation for the other parameters.

Typical results for vertical track dynamic characteristics with a 15,000 pound vertical preload were:

- Resonant Frequency: 30 to 45 Hz.
- Effective Mass: 2500 to 5500 lbm per rail
- Damping: 15 to 45 percent critical.

The damping measured on this track was surprisingly high because data values reported in the literature generally show damping of 10 to 25 percent of critical. The higher measured damping values minimize the dynamic amplification effects at resonance; however, the dynamic response of the vehicle/track system is affected by the addition of the unsprung mass of the vehicle to the effective mass of the track. This addition would be expected to reduce the natural frequencies and the damping ratios below the data reported here for the bare track.

The measurements of track dynamic compliance indicate that data on the stiffness, resonant frequency, and damping are probably adequate to characterize track dynamic response over the frequency range of 0 to 80 Hz. This frequency range is of primary interest for vehicle/track design and analysis. Higher frequency data will be needed for acoustics and for predicting the track and vehicle response to impact forces from flat wheels or bolted rail joints. A frequency resolution of 1-2 Hz. will be adequate for defining the track dynamic characteristics, although much better resolution was used for this measurement program.

Variations in Track Condition. Stiffness measurements at the three different track locations selected for this program showed a significant variation resulting from the roadbed condition even though the track had the same size rail and nearly the same tie size and tie spacing. As expected, the greatest differences occurred for the light preloads where the track behavior is governed by the amount of free-play in the components. However, the stiffness at the higher preloads showed a 2:1 variation between the track in the low, wet region (Location 2) and the other locations (Locations 1 and 3). Also, as much as a 40 percent difference in vertical stiffness was measured between the two rails at one track location, so individual rail measurements rather than average track measurements are of considerable value.

The effect of removing the tie plates from one tie to simulate a missing of defective tie also produced a measurable change in stiffness. The vertical stiffness was reduced by about 20 to 40 percent for the 15,000 pound preload. This variation was well within the resolution capability for the equipment and procedures used for these measurements.

Measurement Techniques. A comparison of the results from using sinusoidal, random, or pulse excitation superimposed on a constant preload showed that these three different techniques for making dynamic measurements usually gave similar, but not identical, data for track dynamic characteristics. The results from the pulse excitation showed the greatest variation from the other measurements because the force amplitude needed to get sufficient energy in the pulse was much larger than the force level needed for the random or sine excitation. These larger force amplitudes for the pulse measurements increased the influence from the nonlinear track behavior.

However, a more surprising and significant result was that the vertical track stiffness determined by the low frequency (5-10 Hz.) response of the track to any of the three dynamic force excitations was considerably higher than the tangent stiffness determined from the slope of the static load-deflection measurement at the corresponding preload. This stiffness as measured with these dynamic techniques was as much as a factor of two greater than the static stiffness as determined by load-deflection measurements. Further investigation of this result indicated a considerable compaction or settling effect when the track is loaded by a constant preload with repeated vertical dynamic excitation. This hysteresis effect was also confirmed by the difference in the results obtained from an unloading and loading pulse. In this test, the only significant variation was that the sequencing of the tension and compression portions of a nearly symmetrical dynamic pulse were reversed. This would not affect the response for a linear system, but the track response was noticeably different.

The conclusion that the track has significant settling is quite important for selecting a measurement technique. When the objective is to measure the vertical track characteristics which are relevant to those seen by a passing wheel, it will be necessary to duplicate the service loading environment for the track in much greater detail than was previously expected. The vertical track loads from a passing train are characterized by a series of loading pulses for each truck. The load variations from individual axles are only noticeable on some track, but these variations are relatively small compared to the total truck load.

The important part of the track loading in service is that the track is nearly unloaded between trucks of adjacent cars (when the coupler passes), and it is always unloaded between the passage of the front and rear trucks of each car. The measurement results in this report indicate this periodic unloading is very important. This was confirmed by changing the constant preload with multiple pulses or random excitation superimposed to an excitation having a slowly varying cyclic preload (1 pulse every 5 seconds) with a single pulse superimposed at the maximum loading point. This type of cyclic preload/pulse excitation unloaded the track between each dynamic measurement and much closer agreement was obtained between the static and dynamic stiffness measurements. It appears that this type of loading is a much better simulation of the track loads from a moving train. And the track hysteresis in the vertical direction makes this more realistic simulation necessary to obtain valid data for analytical models or for the Wheel/Rail Dynamics Laboratory being constructed at Pueblo, Colorado. The results from lateral measurements showed much closer agreement between the static and dynamic stiffness measurements, so it is concluded that settling effects are not as significant in the lateral direction.

The results from this measurement program have revealed that track behavior under dynamic loads is quite complex and that settling effects cannot be neglected. It should also be mentioned that other research investigations where track dynamic measurements have been made in the U.S. and in Europe, utilize a constant preload with repetitive dynamic loading (usually sinusoidal) superimposed. Results from these measurements may differ considerably from realistic service loading, depending on track conditions. It is important to understand that the data which showed large hysteresis effects were measured on wet track. Some other measurements showed relatively little settling effects, and it is believed that the ballast and subgrade may have been frozen during this time period. Therefore, it is conjectured that wet track may exhibit maximum settling effects and frozen or quite dry track may have relatively little settling. Additional measurements are needed to fully evaluate the effect of these different climatic conditions.

RECOMMENDATIONS FOR FUTURE WORK

The results in this report, which were summarized in the previous section, show that the techniques and equipment used to measure track dynamic characteristics must be capable of simulating realistic track loads from passing trains. The use of a cyclic vertical preload which varies from zero to full wheel loads as high as 36,000 pound at a rate representing passing cars is recommended to simulate track loading using stationary equipment. Random or pulse excitation superimposed on the cyclic preload can be used to measure track dynamic compliance. However, the track measurement equipment should have the versatility for evaluating other measurement techniques. The advantage of having this capability was demonstrated during the brief measurement program covered by this report.

It is recommended that the development of a track compliance measurement system for the Phase II and Phase III efforts of this program should be based extensively on the successful experience using the Phase I measurement system. A similar capability for applying vertical loads to both rails and lateral loads to one rail should be provided. It is expected that the measurement system will operate primarily from a stationary railroad car, but the equipment must include the capability for rapid alignment and retraction so that it can be moved quickly to different track locations.

In addition to the stationary measurements, it is recommended that a limited capability for evaluating moving measurements be included by using wheels instead of a stationary fixture to load the track. This concept could be used to determine the effects of "noise" from track geometry irregularities and any additional hysteresis effects from a moving vehicle during low-speed measurements. Data on these effects are needed before the feasibility of developing a measurement system capable of operating at normal train speeds can be fully evaluated.

TECHNICAL DISCUSSION

The principal objectives of the brief measurement program discussed in this report were to obtain some realistic data on track dynamic characteristics to supplement the limited data found in the literature. The measurement program was also planned to determine the advantages and disadvantages of sinusoidal, pulse, and random excitation techniques for making track measurements. The effects of typical track defects and variations in preload, dynamic force amplitude, and excitation frequency were also investigated to provide a better basis for the Phase II feasibility study of track test equipment.

Much of the equipment and instrumentation used for this measurement program was selected from that available at BCL, or rented. This was done to avoid purchasing additional equipment which might be unsuitable for the prototype device to be developed during Phases II and III of the program. The entire measurement program was conducted on the track at the Ohio Railway Museum in Worthington, Ohio. This location was selected for its convenience to BCL, the availability of a railroad car for mounting the equipment, and the cooperation of the museum staff in providing access to their facilities for a research program of this type.

EQUIPMENT DESCRIPTION

Servo-controlled hydraulic actuators were used to apply excitation forces at the rail head. Motion transducers were used to measure the rail response at the forcing location and at other locations on the track in the vicinity of the shakers. Figure 1 shows the excitation system consisting of three hydraulic cylinders mounted to the underframe of a combination passenger-baggage car (Car 1511). The actuators were located a distance of 15 feet from the nearest wheel to minimize the influence of the cylinder reaction forces being transmitted through the car body and truck to the track. Rail response measurements discussed later in this report verified that the influence of the car wheels was negligible in the vicinity of the shaker system.

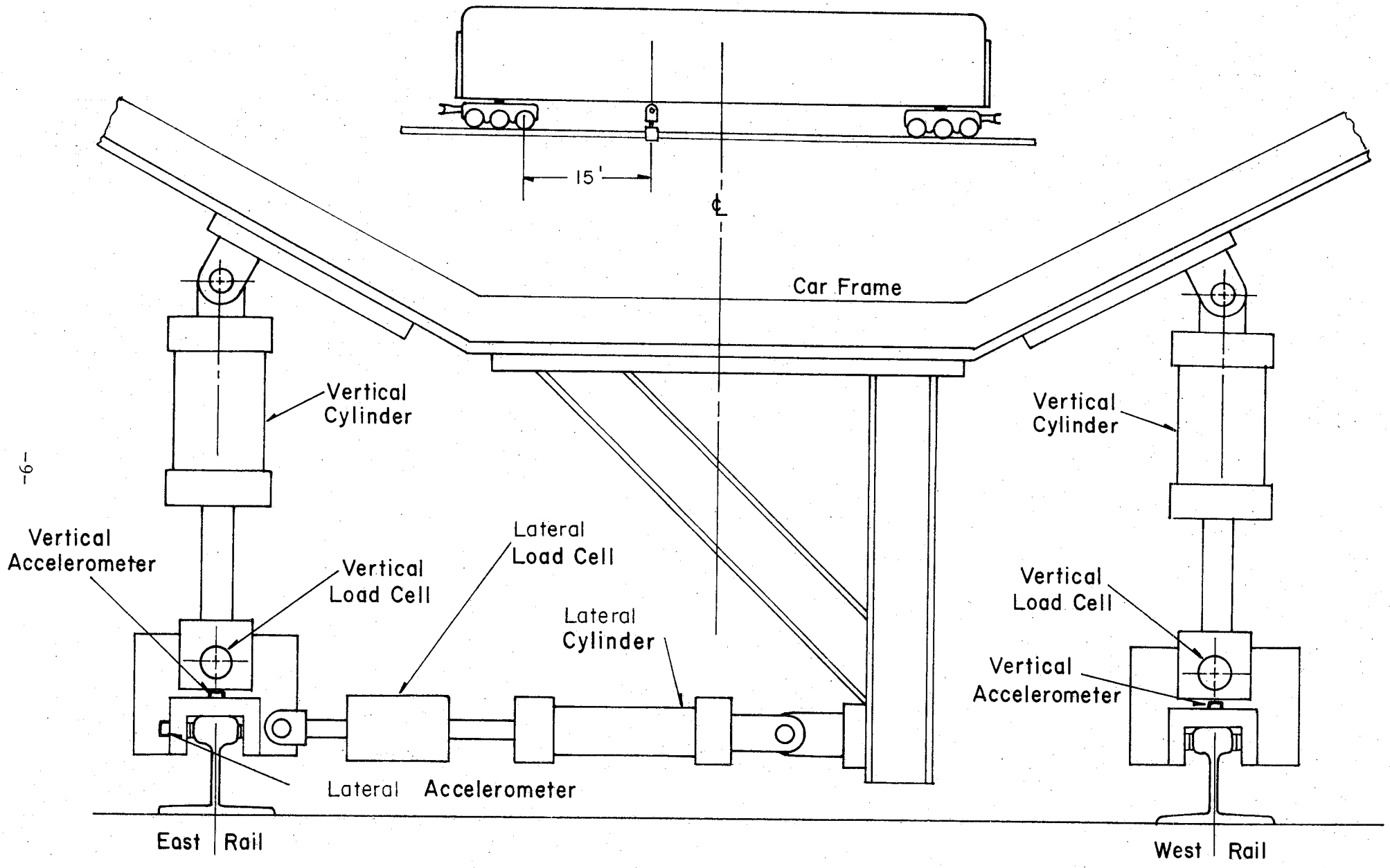

FIGURE 1. HYDRAULIC SHAKER SYSTEM MOUNTED ON CAR FRAME

Three hydraulic cylinders were used to apply static and dynamic loads to both rails in the vertical direction, and to one rail in the lateral direction. The cylinders were attached to a rail clamping fixture with rod end bearings, and they were attached to the car frame with clevis pins to eliminate any restraint on rail deflections by the cylinders. The two vertical cylinders had a 4-inch bore with a 5-inch stroke. At 3000 psi, the vertical cylinders could each generate 30,000 lb to simulate car wheel loads. The lateral cylinder had 2-1/2 inch bore with a 12-inch stroke, providing a maximum force capability of 12,000 lb.

Figure 2 is a photograph of one of the vertical cylinders mounted on the car. This photograph shows the servovalve, the clevis pin load cell, the rail clamping fixture, and an accelerometer. The horizontal cylinder and bracket are visible in the background. The antennae structure shown is the displacement reference beam which is supported 15 feet either side of the rail. Ice and snow were covering the gravel ballast when this photograph was made.

Figure 3 is a photograph that is similar to the sketch shown in Figure 1. This shows the mounting configuration of the two vertical and the one lateral cylinders. The small angle of the vertical cylinders is due to the car being on a slight curve which shifts the center of the car to one side, relative to the track center.

The power supply for the hydraulic system was a 3000 psi, 23 gpm axial piston pump with pressure compensation. A 24-hp, 2-cylinder gasoline engine was used to drive the pump. The system was normally operated at a supply pressure of 2000 psi, and a maximum flow rate of 15 gpm, which required about 20 hp. This limited the maximum vertical force to about 20,000 lb. A hydraulic accumulator was mounted underneath the car close to the cylinders to reduce supply pressure fluctuations.

Electrohydraulic flow-control servovalves were used to drive each cylinder. The two vertical cylinders each had a Moog 76-104 (15 gpm) valve, and a Moog 74-114 (15gpm) valve was used on the lateral cylinder. The frequency response of the shaker system was relatively flat up to about 70 Hz., and some low amplitude excitation could be obtained as high as about 250 Hz.

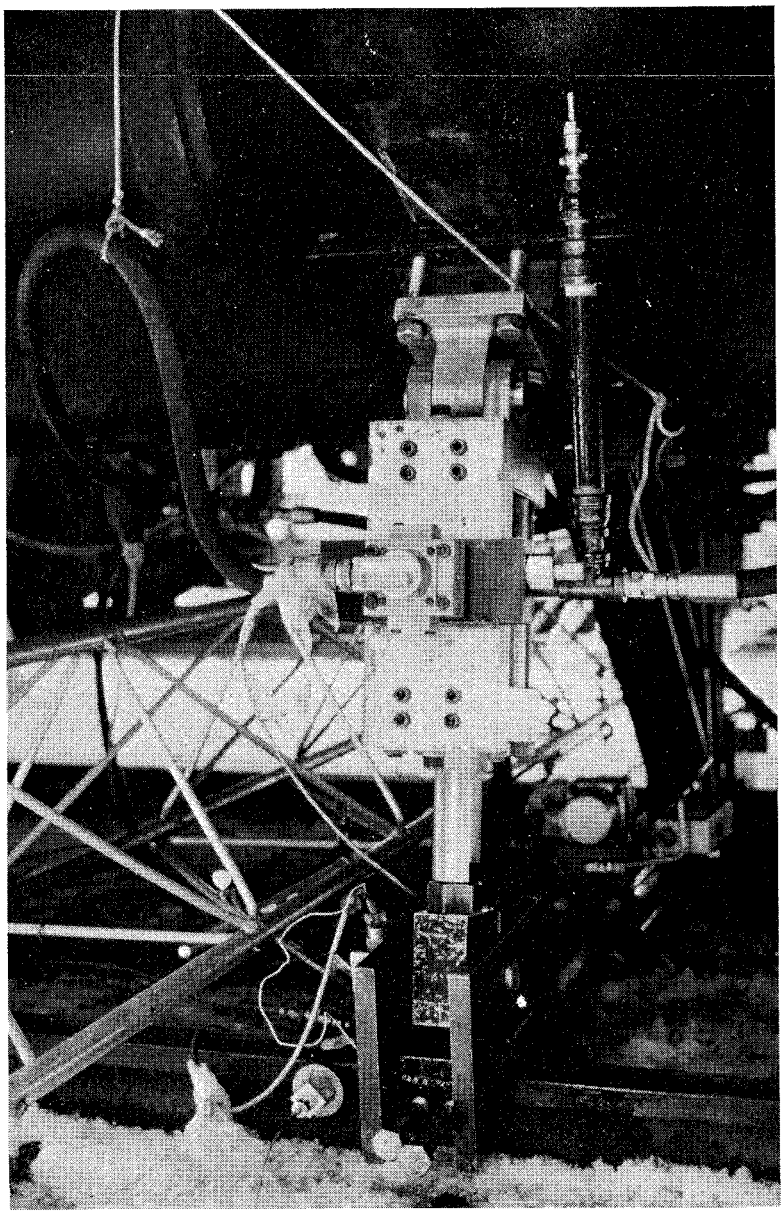

FIGURE 2. VERTICAL HYDRAULIC CYLINDER MOUNTED TO UNDERFRAME OF CAR AND TO RAIL HEAD

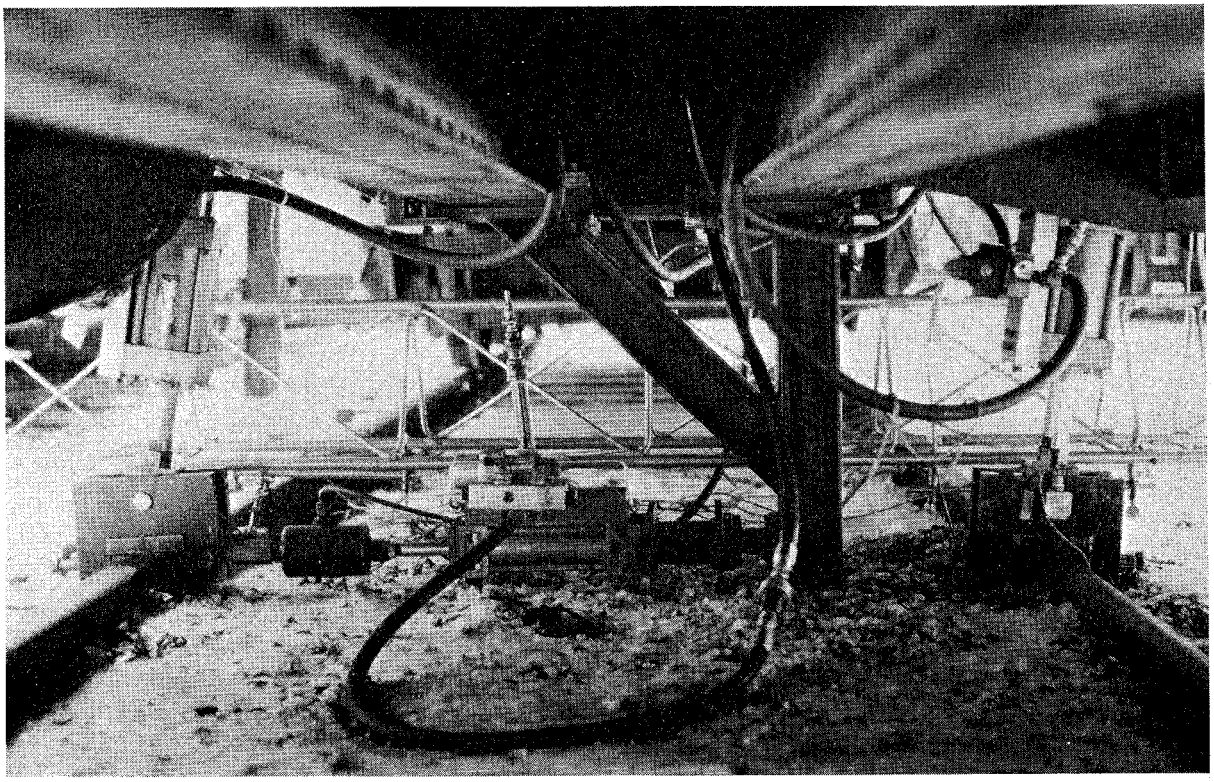

FIGURE 3. MOUNTING CONFIGURATION OF THE HYDRAULIC SHAKER SYSTEM

Shaker Control System

The actuator control and data analysis systems are shown in Figure 4. A force feedback system was used to generate a force proportional to the amplitude of the electrical input signal from the oscillator, the random noise generator, or the analyzer. A high pass filter in series with the random generator was used to limit the magnitude of the forces applied to the car body at low frequencies which tended to excite car body modes. This system was used to control the static preload and the superimposed dynamic excitation using a separate control system for each actuator.

Strain-gage load cells built into the clevis pins were used to measure the vertical force applied to the rail and to control the vertical cylinders. These load cells were rated for a 25,000 lb maximum force. A standard axial-force strain-gage load cell rated at 10,000 lb maximum force was used to measure and control the lateral rail force.

Three different methods of dynamic excitation were used; sinusoidal, random, and pulse. The sinusoidal (swept sine) tests consisted of the servo system being driven by a sine-sweep oscillator between 1 and 100 Hz at a sweep rate varying from 1 to 2 Hz/sec. This was done for various static preloads and amplitudes of the dynamic force.

The random excitation signal came from a General Radio Random Noise generator. The output from the generator was high-pass filtered to eliminate the frequency content below the range of interest. This filtered signal was fed into the shaker control system. A continuing random signal was used so that several record lengths of the input and response could be analyzed and averaged to improve the accuracy of the track compliance data.

Impulse excitation was obtained using digital techniques to program pulse widths ranging from 10 to 25 milliseconds. These pulses were then processed through the digital-analog converter to drive the shaker system.

Motion Transducers

Accelerometers and displacement transducers were used to measure rail motions. The accelerometers were the piezoelectric-type having

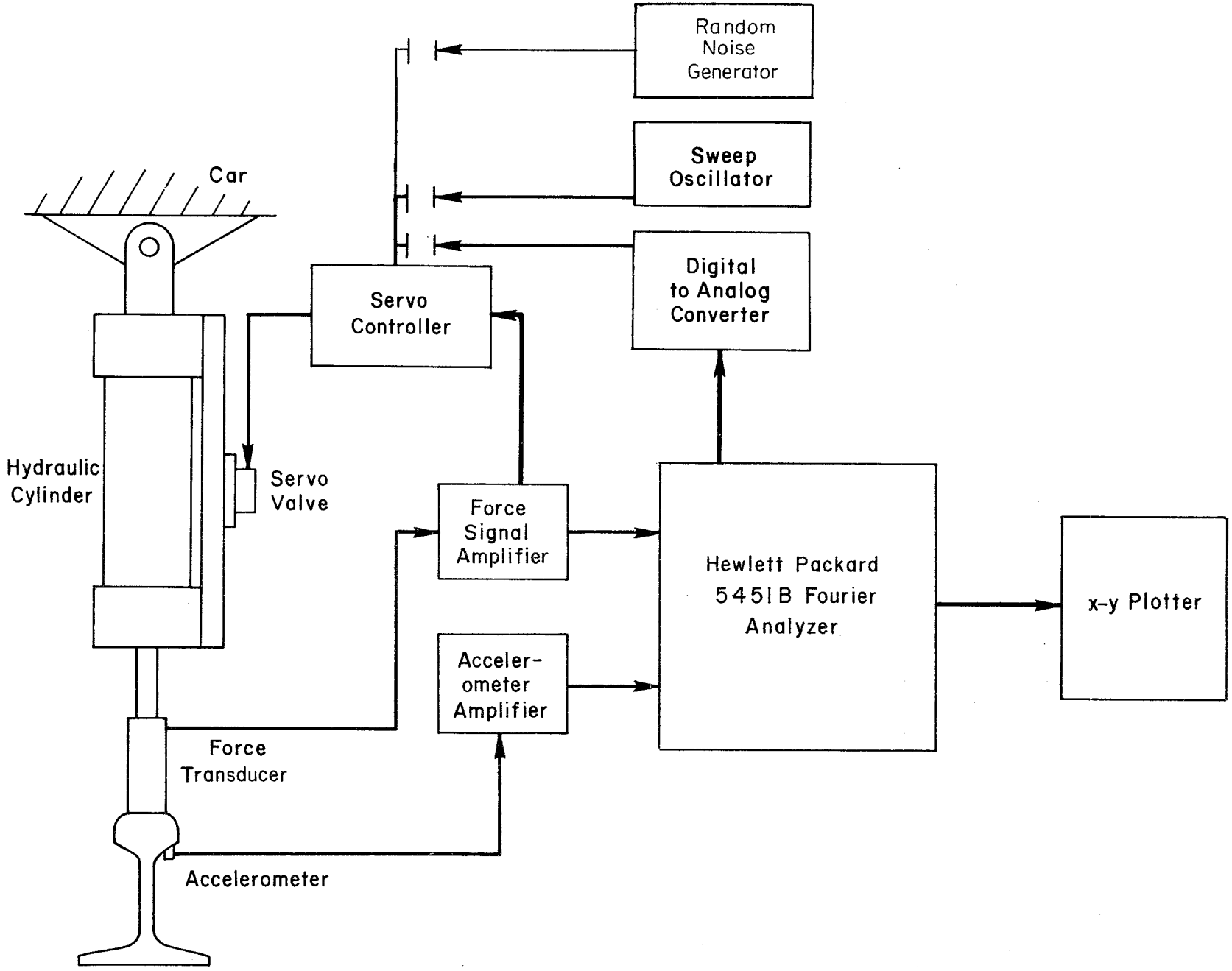

FIGURE 4. SCHEMATIC OF ACTUATOR CONTROL AND DATA ANALYSIS SYSTEMS

frequency response down to about 0.1 Hz. The acceleration signals were integrated to provide a displacement measurement that was accurate above about 1 Hz. The accelerometers were attached to magnets so they could be moved easily to any location on the rail.

Log-frequency and static displacement measurements were made using either a Linear Variable Differential Transformer (LVDT) or a linear potentiometer. These displacement transducers measured rail displacements relative to a fixed reference consisting of a 40-foot lightweight truss structure (aluminum radio antenna tower) which spanned the track and was supported at its ends on the ground, see Figure 5. The support points located at about 15 feet from each rail were well away from the load-affected zone for static loads on the track.

Data Analysis

A Hewlett Packard Model 5451B Fourier Analyzer was used to analyze the data and plot the results from the swept sine, random and pulse excitations. The Fourier Analyzer consists of a dedicated mini-computer with 32K of core memory which uses a Fast Fourier Transform (FFT) algorithm to transform time series data to the frequency domain. The input force and track-response measurements were used to determine the force-displacement transfer function (compliance) between any two selected locations. Figure 6 is a photograph of the Fourier Analyzer inside the railroad car.

The cross-spectral method of determining transfer functions was used to calculate track dynamic compliance for this program. Equation (1),

$$\bar{C}(jw) = \frac{\bar{G}_{yf}(jw)}{\bar{G}_{ff}(jw)} , \qquad (1)$$

determines the compliance $\bar{C}(jw)$ from the ratio of the averaged cross-spectral density $\bar{G}_{yf}(jw)$ between the track displacement y and input force f and the averaged power spectral density $\bar{G}_{ff}(jw)$ of the input force. The cross and power spectral density functions in the frequency (w) domain are computed from the Fourier Transforms S of the measured force and displacement time signals using

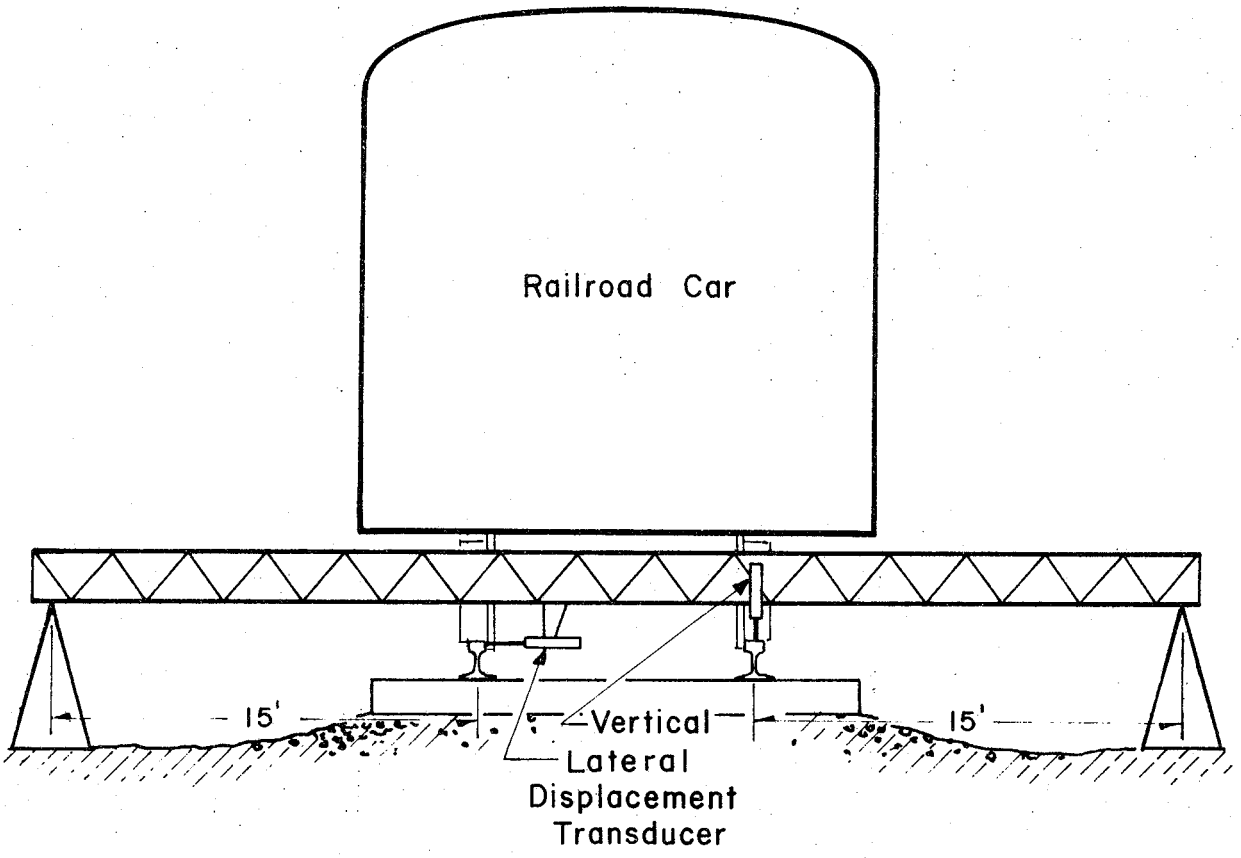

FIGURE 5. ANTENNA TOWER USED AS REFERENCE BEAM FOR RELATIVE DISPLACEMENT MEASUREMENTS

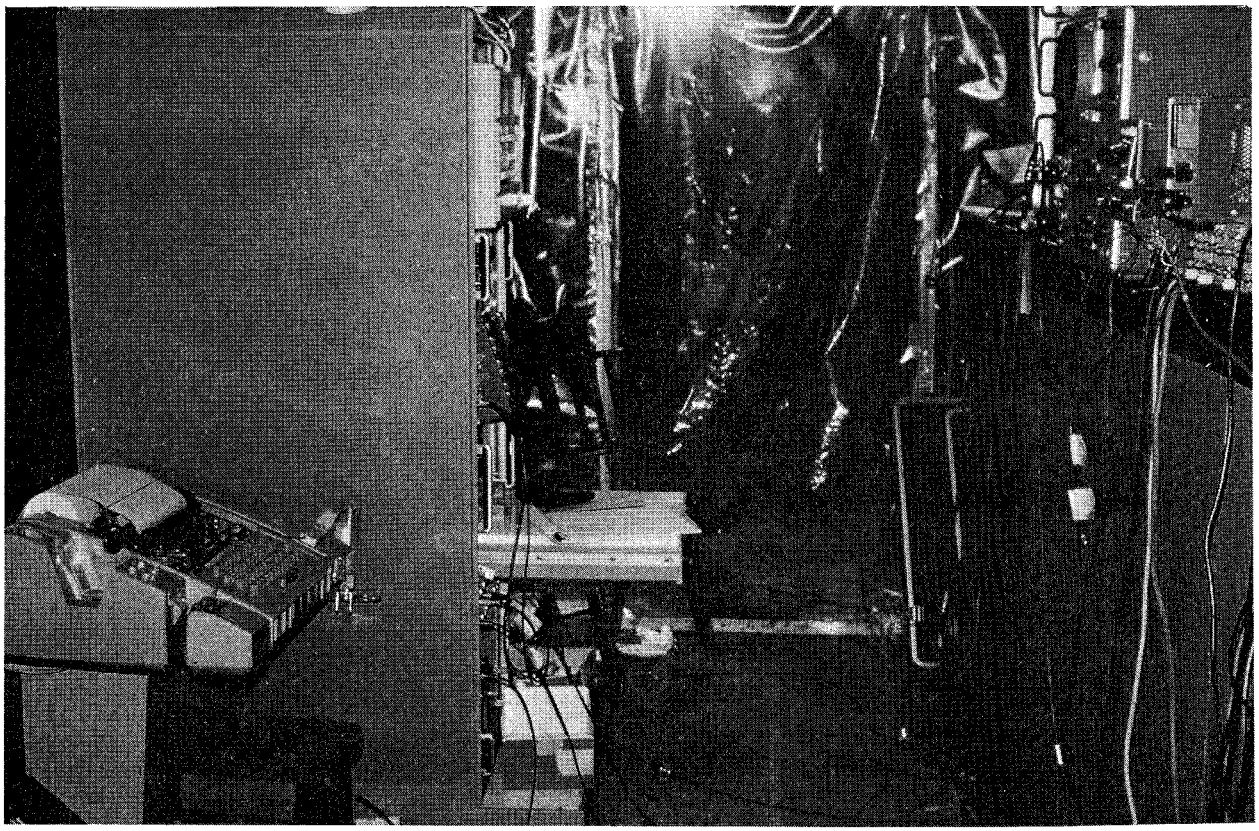

FIGURE 6. FOURIER ANALYZER INSIDE RAILROAD CAR

$$\bar{G}_{yf}(jw) = \overline{S_y S_f^*} \tag{2}$$

and

$$\bar{G}_{ff}(jw) = \overline{S_f S_f^*} \tag{3}$$

where * denotes the complex conjugate.

The advantage of using the cross-spectral method for determining transfer functions instead of the classical definition where $C(jw) = S_y(jw)/S_f(jw)$ is that the cross-spectra can be averaged to reduce the effects of external noise which does not have a fixed phase relative to the exciting force. It is also important to realize that the compliance function given by Equation (1) is a complex quantity, so both real and imaginary components are required for a complete description. These parameters were displayed in the form of a magnitude (absolute value) and phase angle as a function of frequency for the track measurements.

In addition to calculating track compliance, the coherence function was also determined for the different measurement techniques. The coherence function $\gamma(jw)$ estimate is obtained from

$$\gamma^2_{yf}(jw) = \frac{\left|\bar{G}_{yf}\right|^2}{(\bar{G}_{ff})\ (\bar{G}_{yy})}, \quad 0 \leq \gamma^2_{yf} \leq 1. \tag{4}$$

The coherence function is a quantitative indication of the accuracy of the track compliance measurement. For a constant parameter linear system with a single input, the coherence function will be 1. If the input and output are completely unrelated, the coherence function will be zero.

Therefore, when the coherence function is close to unity, good data can be assumed.

When the coherence function is less than unity, the most likely explanation is one or more of the following[1]*:

(a) Extraneous noise is present in the measurements.

(b) The track structure is non-linear

(c) The track response is due to more than one exciting force that is not being measured.

The coherence function was calculated for each of the compliance function measurements in order to determine the frequency range over which

---

* Numbers in brackets [] refer to References.

Random and Pulse Response Analysis

Digital techniques for analyzing pulse and random response data impose certain restrictions due to the sampling relationships that determine the frequency resolution (Δf), total sampling time (T), the maximum frequency F_{max}, and the time interval between samples (Δt). Also, the total number of data points (N) is governed by the computer size. For these tests, all data were taken in the range of 0 to 100 Hz or) to 256 Hz. Therefore, F_{max} was equal to either 100 or 256 Hz, and a block size N of 1024 points of time data was used (N). With F_{max} and N fixed in value, Δt, T, and Δf are given by the following relationships:

$$\Delta t = \frac{1}{2 F_{max}} \tag{5}$$

$$T = N\Delta t \tag{6}$$

$$\Delta f = \frac{F_{max}}{N/2} \tag{7}$$

Therefore, with F_{max} = 100 Hz and N = 1024, the time between samples Δt is 5 milliseconds, and the total sampling time T was 5.12 seconds. The resolution Δf was 0.195 which was a greater resolution than necessary to define the resonance characteristics of the relatively heavily damped track structure.

For F_{max} equal to 256 Hz, the analysis parameters were: Δt = 1.95 milliseconds, T = 2 seconds, and Δf = .5 Hz.

In order to increase the signal to noise ratio, the power and cross spectra of the input and response were averaged. As a general guide, the signal to noise ratio will improve by about 3 dB each time the number of averages is doubled, i.e., averaging two signals will improve the signal to noise by about 3dB and averaging 16 signals will improve the ratio by about 12 dB. For the pulse and random excitation 20 averages were used for most cases, so about 100 seconds of data was required for F_{max} = 100 Hz and 41 seconds of data were used for F_{max} = 256 Hz. However, the effect of

different numbers of averaging was evaluated during the measurement program.

Track Compliance

The nomenclature and definitions of terms used to describe the static and dynamic characteristics of railroad track can be quite confusing to persons having a varied background. Therefore, only a few descriptive terms have been selected for this report, and they have been used according to the definitions which follow.

Track Modulus is a term commonly used in railroad engineering to describe the average elastic support of the foundation under the rail base. The track modulus is determined by the effective support from discretely spaced ties on a roadbed composed of ballast and subgrade. This is strictly a static parameter with units of lb/in. per inch of rail (or track) length. It is not intended to include any dynamic effects such as frequency dependent damping or mass. Since the measurements in this report are all related to deflections of the rail head and include the rail as part of the track assembly, the term track modulus has not been used in this report.

Track Stiffness is used to describe the static (low-frequency) chacteristics of the track. Track stiffness as used herein refers to the load deflection ratio (lb/in.) for a point load applied to the rail head, so this track stiffness includes contributions from both the rail and foundation stiffnesses.

Track Dynamic Compliance is based on the definition of compliance that is commonly used in vibration analysis--the complex ratio of displacement to force representing the frequency dependent transfer function (amplitude and phase) for steady-state sinusoidal excitation. A measurement of dynamic compliance over a selected frequency range describes the dynamic characteristics of structural behavior such as resonant frequencies, anti-resonant frequencies, and energy dissipation (damping). The term compliance, or track compliance has been used to indicate forces and displacements measured at the rail head. Therefore, if the frequency of interest is well below the natural frequency of the system, the track dynamic compliance approaches in magnitude the inverse of the track stiffness. Also, the inverse of the dynamic compliance at low frequencies is sometimes identified as the track dynamic stiffness to differentiate the results from a static and dynamic measurement.

All measurements were made from a stationary railroad car. The term dynamic refers to the force excitation, but it does not imply a moving vehicle.

These definitions can perhaps be understood better by considering the response characteristics of the single degree-of-freedom system shown in Figure 7. This represents a very simplified, linear model of the track where

M_r = effective mass of the rail, ties and roadbed
K_r = effective stiffness for a point load at the rail
C_r = effective damping of the rail, ties, and roadbed
$F(t)$ = time dependent rail force
$y(t)$ = time dependent rail deflection.

The equation of motion for this model is

$$M_r \ddot{y}(t) + C_r \dot{y}(t) + K_r y(t) = F(t). \tag{8}$$

For steady-state sinusoidal excitation at frequency ω,

$$F = F_o e^{j\omega t} \tag{9}$$

and

$$y = y_o e^{j\omega t},$$

and the solution is given by

$$\left[(K_r - M_r \omega^2) + j C_r \omega\right] y_o e^{j\omega t} = F_o e^{j\omega t} \tag{10}$$

The compliance function $\bar{C}(\omega)$ for this model can be determined from the displacement force ratio as

$$\bar{C}(\omega) = \frac{y_o}{F_o} = \frac{1}{(K_r - M_r \omega^2) + j C_r \omega}. \tag{11}$$

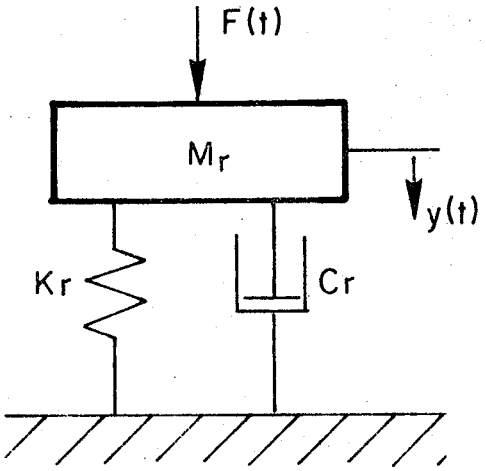

FIGURE 7. SINGLE DEGREE OF FREEDOM MODEL FOR A VIBRATORY SYSTEM

This complex quantity can be written in an alternate form to give the magnitude $|C(\omega)|$ and a phase angle θ as

$$\overline{C}(\omega) = \frac{1}{\left[(K_r - M_r \omega^2)^2 + (C_r \omega)^2\right]^{1/2}} \angle\theta \qquad (12)$$

where $\theta = \tan^{-1} \dfrac{C_r \omega}{K_r - M_r \omega^2}$ is the phase lag for the displacement response relative to the excitation force.

Equation 12 can be rewritten in terms of the system natural frequency which is defined as

$$\omega_n^2 = \frac{K_r}{M_r} \qquad (13)$$

and the percent of critical damping defined as

$$\zeta = \frac{C_r}{C_c} \quad , \qquad (14)$$

where C_c is the critical damping coefficient given by

$$C_c = 2 M_r \omega_n$$

This alternate form for Equation 12 is

$$\overline{C}(\omega) = \frac{1/K_r}{\left[\left(1 - \frac{\omega^2}{\omega_n^2}\right)^2 + \left(2\zeta \frac{\omega}{\omega_n}\right)^2\right]^{1/2}} \cdot \angle\theta \qquad (15)$$

Three regions of particular interest are the stiffness region, the resonance region, and the mass region, see Figure 8. When the excitation frequency is much less than the undamped resonant frequency given by Equation 13, the compliance function is a straight, horizontal line determined by the stiffness

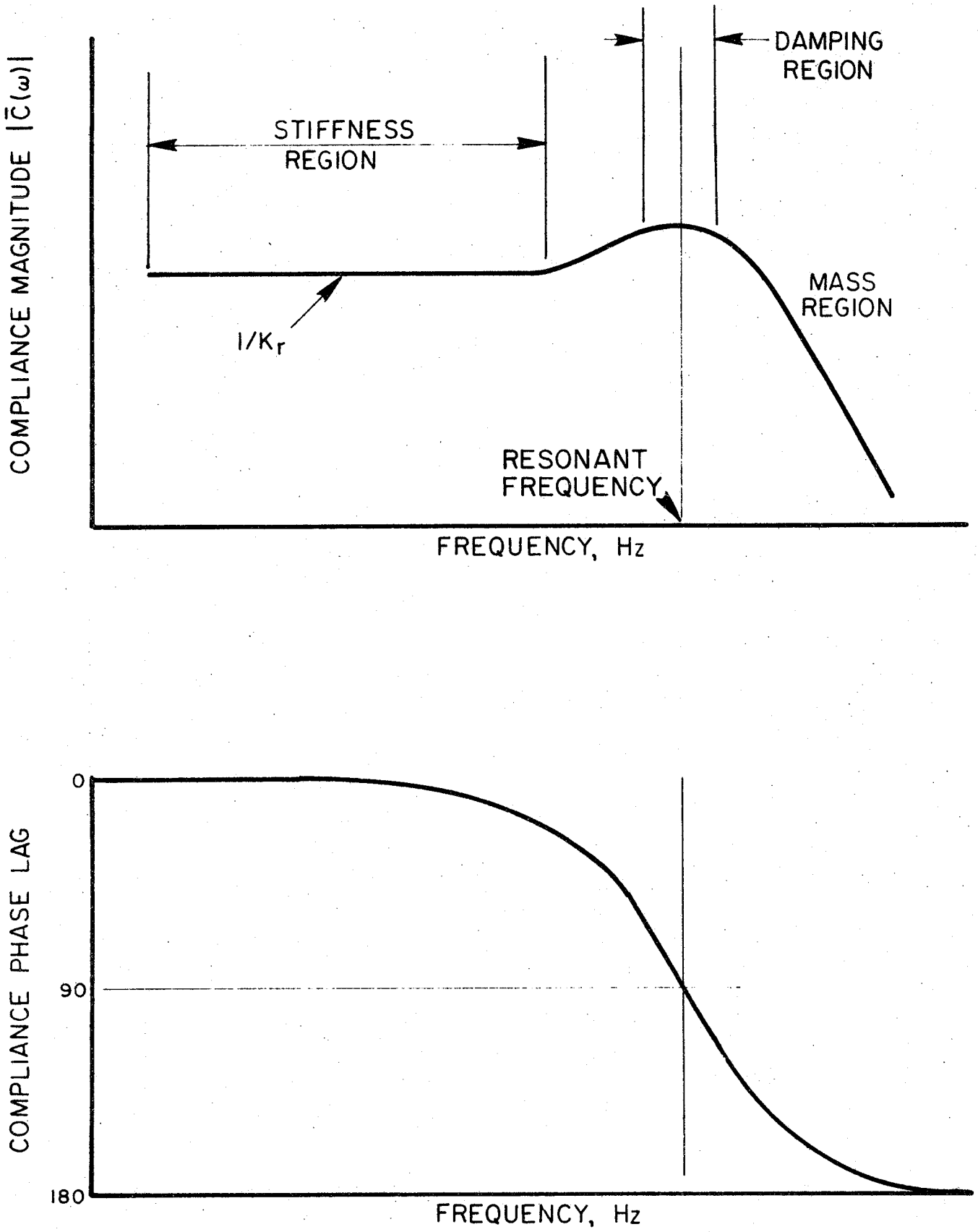

FIGURE 8. THEORETICAL COMPLIANCE MAGNITUDE AND PHASE CURVES AS A FUNCTION OF FREQUENCY FOR A SINGLE DEGREE OF FREEDOM MODEL

$$\left|\bar{C}\ (\omega)\right| \approx \frac{1}{K_r} \quad \omega << \omega_n \tag{16}$$

and the phase l g is quite small.

At the natural frequency, or resonant frequency, the compliance is controlled by the damping (energy dissipation) and the phase lag is 90^o for all values of damping. The compliance at the natural frequency is given from Equation 12 by

$$\left|\bar{C}\ (\omega)\right| \approx \frac{1}{C_r \omega_n} \qquad \omega = \omega_n. \tag{17}$$

Therefore, the damping can be estimated in terms of a percent of critical damping ζ, at resonance, from Equation 15 by the equation

$$\zeta = \frac{C_r}{2M_r \omega_n} = \frac{1}{2 K_r \left(y_o/F_o\right)_{\omega_n}} \tag{18}$$

where $\left(y_o/F_o\right)_{\omega_n}$ is the compliance magnitude at the natural frequency.

When the excitation frequency is much higher than the resonant frequency, the response of a single degree-of-freedom system is controlled by the mass, as seen by

$$\left|\bar{C}\ \ (\omega)\right| \approx \frac{1}{M_r \omega^2} \qquad \omega << \omega_n. \tag{19}$$

The track dynamic compliance measurements for this report were made over a selected frequency range in order to describe the dynamic characteristics of the track structure in terms of resonant frequencies, damping (energy dissipation), and stiffness. Figure 9 is shown here as a typical example of compliance data. This is a lateral track dynamic compliance plot obtained with 15,000-lb vertical preload and random excitation in the lateral direction. This plot looks very similar to the single degree

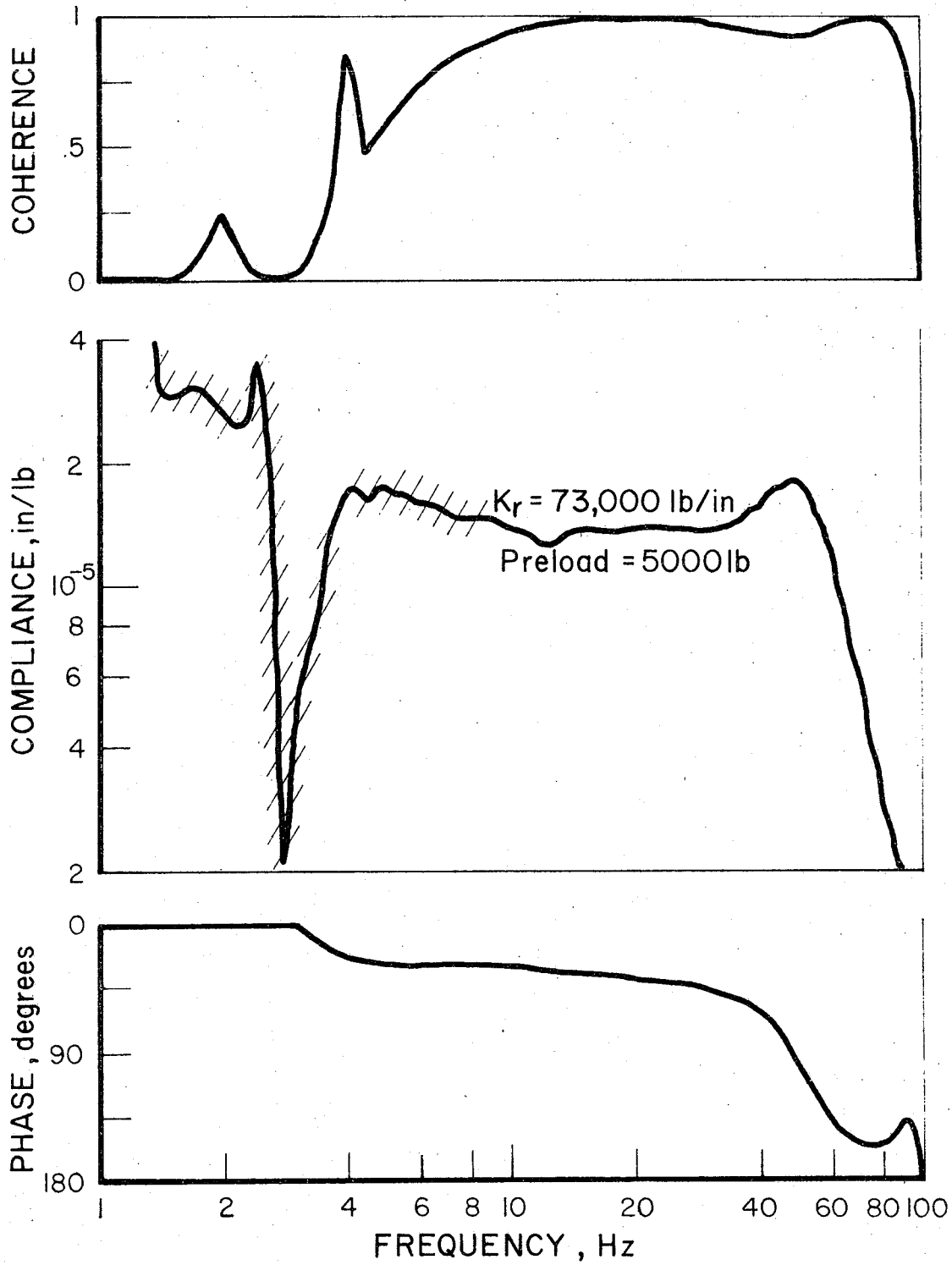

FIGURE 9. TRACK LATERAL DYNAMIC COMPLIANCE (PHASE AND COHERENCE) OBTAINED BY USING RANDOM EXCITATION WITH A 5,000-LB VERTICAL PRELOAD AT LOCATION 1

of freedom system shown in Figure 8. The value of the compliance in the stiffness region is 1.37×10^5 in/lb. which is a stiffness of $K_r = 73{,}000$ lb/in. A resonance at 50 Hz is indicated by the peak in the compliance plot and also by the 90^o crossing of the phase angle plot. The coherence function indicates the data is valid over the frequency range of about 8-80 Hz, since the coherence function has a value close to 1. The cross hatched area of the compliance plot indicates bad data based on poor coherence. The percent of critical damping (ζ) has a value of 37.5 percent, and the effective mass is 289 pounds as determined from Equations (18) and (13), respectively.

A power spectrum of the random force input to the track structure is shown in Figure 10. This plot shows the frequency content of the input to the track structure to indicate the level of excitation at each frequency. The force excitation rolls off at both ends of the spectrum. The high-frequency roll off is due to the characteristics of the excitation system. The low frequency roll off is due to an electronic filter inserted in the circuit to remove the low frequency excitation near the natural frequencies of the car suspension and body modes.

TRACK MEASUREMENT LOCATIONS

All of the track measurements for this program were made during the period of March 5 through March 14, 1975, at the Ohio Railway Museum in Worthington, Ohio. The museum is located about 10 miles north of Battelle's Columbus Laboratories. There is about 1-1/2 miles of interurban track that is used during the summer for tourist rides on trolley cars and railroad cars pulled by a steam or electric locomotive. The track is in good condition for this low-speed, infrequent traffic, and none of the usual problems such as pumping joints and sunken ties caused by high tonnage are visible.

Table 1 summarizes the track construction for the three locations selected for this program. Worn 85-lb/yd. rail and gravel ballast is used at all locations. Location 1 was a siding in good condition. Figure 11 is a

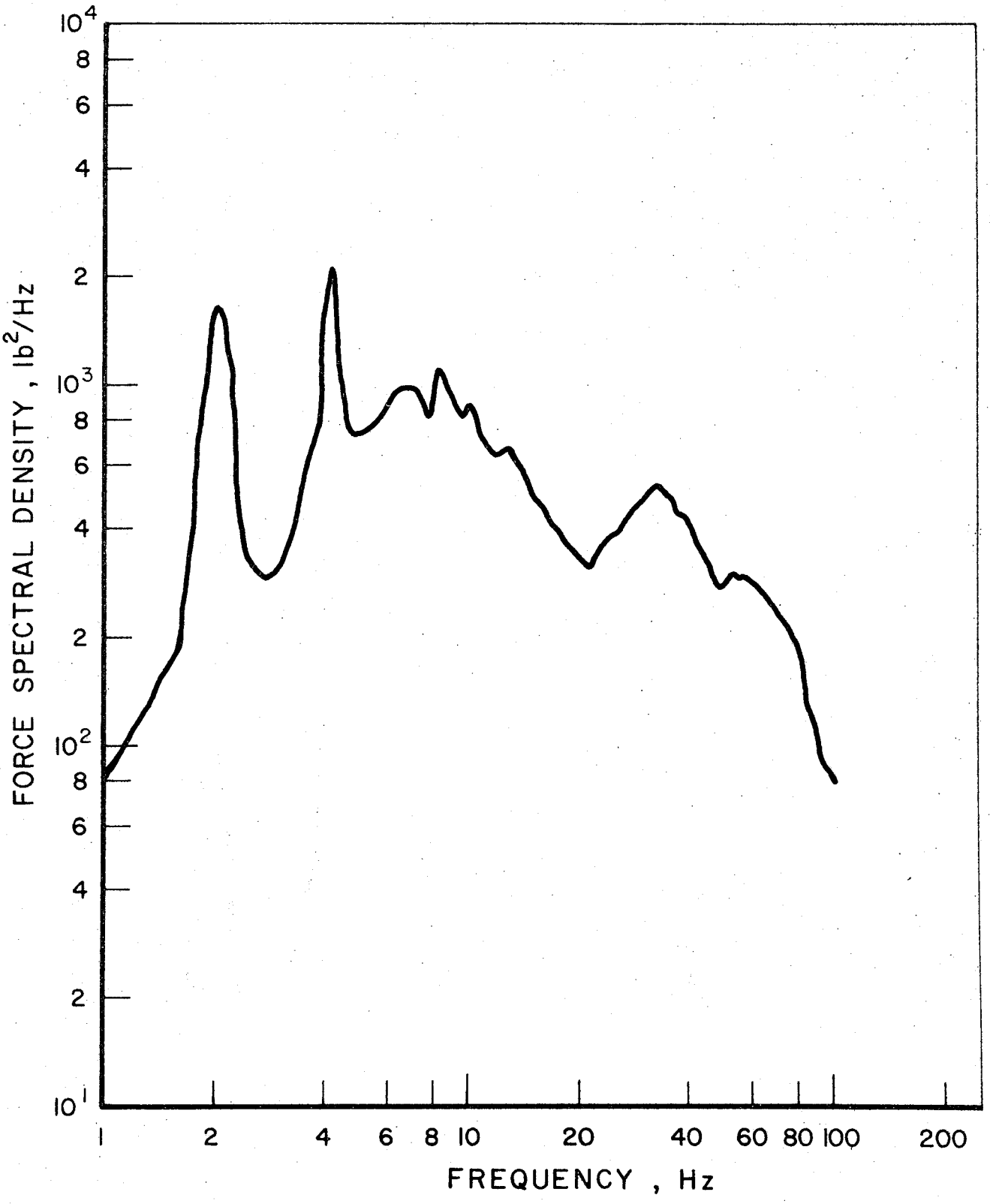

FIGURE 10. AVERAGED FORCE POWER SPECTRAL DENSITY OF THE RANDOM EXCITATION AT LOCATION 1

TABLE 1. MEASUREMENT LOCATION DESCRIPTION

Location Number	Rail Size (lb/yd)	Tie Spacing in. (1)	Tie Size (2)	General Description
1	85	25	6-in. x 7-3/4 in. x 8 ft 6 in.	Good track, sound ties, full ballast crib, no tie plates
2	85	25-1/2	6.5-in. x 8 in. x 7 ft 11 in.	Poor track, some split ties, minimal ballast shoulders, no tie plates
3	85	20-1/2	6.25 in. x 8.25 in. x 8 ft 6 in.	Good track, sound ties, with tie plates

(1) Tie spacing was averaged over a 50-ft length of track.

(2) Tie size is the average of 5 ties.

photograph of Location 1 and the test car. The track at Location 2 crossed a low, wet region and water was standing on both sides of the track at a level close to the tie bottoms during the measurements. Some ties were split and there was very little ballast at some of the tie ends. Figure 12 is a photograph of Location 2 showing the standing water on the side of the track.

The track at Location 3 was in good condition. This site was selected because there were tie plates that could be removed to simulate a defective tie support condition. The ballast in all three locations was insufficient to elevate the track very far above the ground level. However, although no borings were made to inspect the roadbed, this site was previously used as an interurban track during the early 1900's, so there may be a mixture of cinders and gravel much deeper than indicated by visual inspection.

RESULTS OF TRACK COMPLIANCE MEASUREMENTS

This section of the report gives a detailed discussion of the procedures and results from the track measurements. Measured data from the different track locations have been selected to demonstrate the effects of preload, dynamic force amplitude, and frequency range on the results obtained using sinusoidal, random, and pulse excitation. The important advantages and disadvantages for the measurement techniques have been evaluated with regard to the dynamic characteristics of the different track selected for this program.

Sinusoidal Excitation

The classical method for measuring the frequency response of a structure is to use sinusoidal force excitation and measure the acceleration velocity, or displacement response at selected locations. This is usually accomplished with an analog system having narrow-band tracking filters to reduce noise and log amplifers to combine the signals in the form of a transfer function. (ratio of response to excitation force) However,

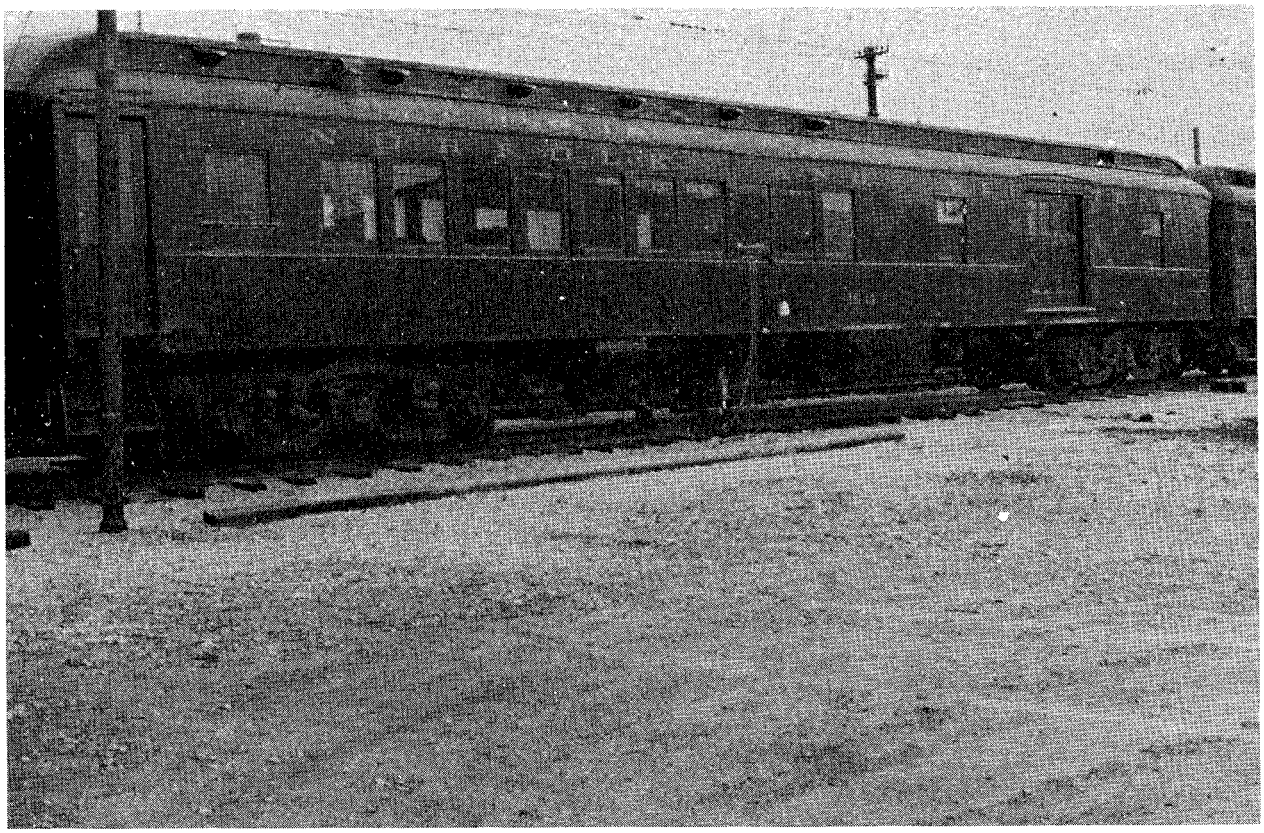

FIGURE 11. LOCATION NO. 1 TEST SITE AND MEASUREMENT CAR

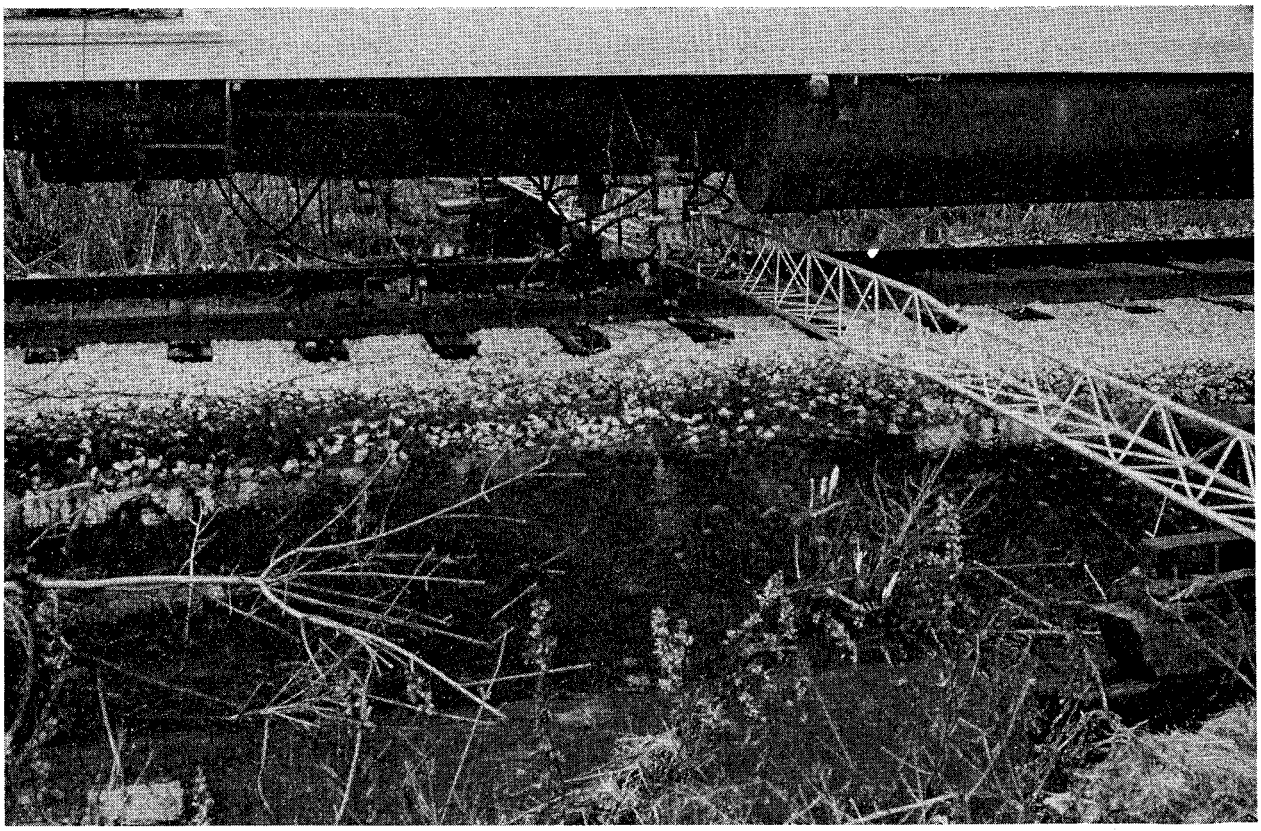

FIGURE 12. LOCATION NO. 2 TEST SITE

for this program, a digital system was used to sample data and average power spectra for 100 seconds. The sinusoidal oscillator was used to sweep from 1 to 100 Hz in 100 seconds at a 1 Hz/sec linear sweep rate. The Fourier analyzer sampled data 500 times during the sweep and averaged the spectra. Additional sine sweeps were also made out to 256 Hz. The input force amplitude was maintained constant during the sine sweeps by the force feedback control system until the control system response began to fall off at 70 Hz. The excitation level was controlled manually at frequencies above 70 Hz.

Effect of Preload

Figure 13 shows vertical track compliance measurements obtained by using sine excitation at Location 1. Both rails were preloaded vertically, but only one rail was subjected to the dynamic force. The input force and the displacement response of the driven rail were measured and used to calculate track compliance (displacement/force). These are point compliance spectra because the force and response were measured at the same point. The term transfer compliance will be used whenever the response was measured away from the forcing point.

Figure 13 shows three vertical compliance functions as a function of increasing vertical preload. The vertical preloads applied were 2500 lb/rail, 7500 lb/rail, and 15,000 lb/rail. The vertical compliance plot with 2500 lb preload had an excitation level of 200 lb peak-to-peak sine, and yielded a vertical stiffness of 17,000 lb/in. (5-7 Hz). For 7500 lb preload and 200 lb peak-to-peak dynamic excitation, the vertical dynamic stiffness increased to 400,000 lb/in. An increase in preload by a factor of 3 caused an increase in stiffness by a factor of 23. This shows a very nonlinear effect with increasing preload. This is also verified by vertical load-deflection curves which will be discussed in a later section.

When the vertical preload was increased to 15,000 lb, the vertical stiffness increased to 670,000 lb/in. In this case, a doubling of the preload caused the stiffness to increase by a factor of 1.7.

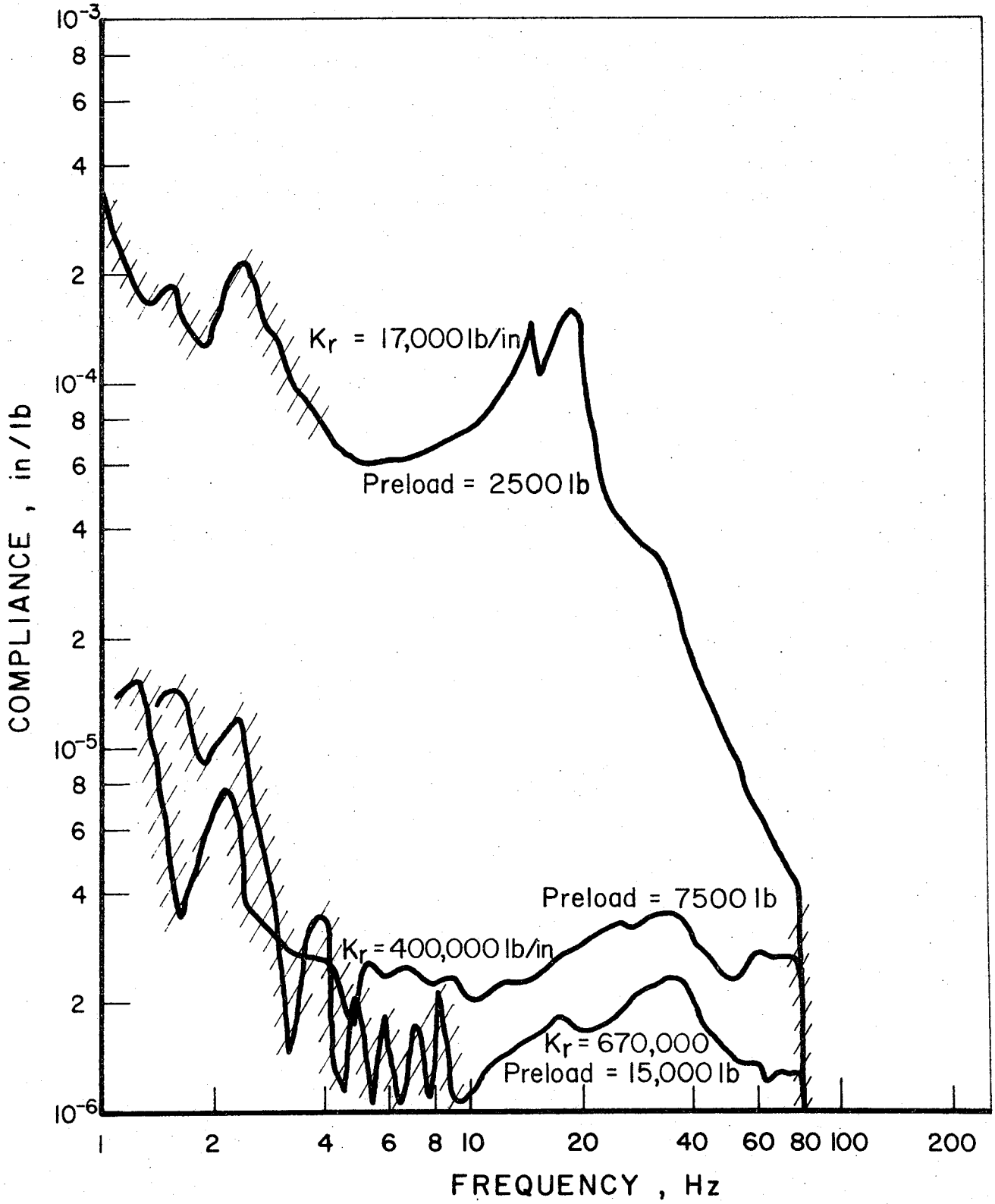

FIGURE 13. TRACK VERTICAL DYNAMIC COMPLIANCE OBTAINED BY USING SINUSOIDAL EXCITATION AT LOCATION 1 FOR THREE VERTICAL PRELOADS

Table 2 summarizes these curves in terms of the parameters needed for a single degree-of-freedom model; stiffness K_r, natural frequency W_n, damping (ζ) and mass (M_r). Where no natural frequency value is listed, this indicates there was no 90^o phase shift in the phase plot. The stiffness values reported in Table 2 are plotted in Figure 14.

Single Versus 2-Rail Excitation

Figure 15 is a comparison of driving one rail sinusoidally, and then driving both rails simultaneously using the same dynamic level and 2500 lb vertical preload for both. Driving one rail yielded a stiffness of 17,000 lb/in., and driving both rails showed a small increase in vertical stiffness to 20,000 lb/in. Therefore, there is a small stiffening effect from driving both rails, due to the coupling of the track structure through the ties. These results show that the coupling is relatively small for this track location.

Increase in Dynamic Amplitude

Figure 16 shows two compliance plots with the same static preload of 2500 lb, but for one plot the amplitude of the sinusoidal excitation was doubled to 400 lbs. peak-to-peak. The compliance is nearly identical for the two force amplitudes, which indicates the track behaves as a linear system within this small dynamic range. As will be shown in a later section, the track structure shows a large degree of nonlinearity when the dynamic excitation becomes large relative to the preload.

Random Excitation in Vertical Direction

The second method of obtaining dynamic compliance data was to use random excitation. The procedure was similar to the sine sweep except a random noise generator was used to drive the system. The Fourier analyzer was used to compute the track compliance from the average power spectra from a specified number of record lengths using the cross-spectra method discussed previously.

TABLE 2. SUMMARY OF VERTICAL COMPLIANCE MEASUREMENTS USING SINUSOIDAL EXCITATION AT LOCATION 1.

Preload 16	Stiffness K_r 16/14	Natural Frequency W_n Hz	Damping %	Mass M M_r
2500	17,000	18	18	513
7500	400,000	35	35	3200
15,000	670,000	37	30	4780

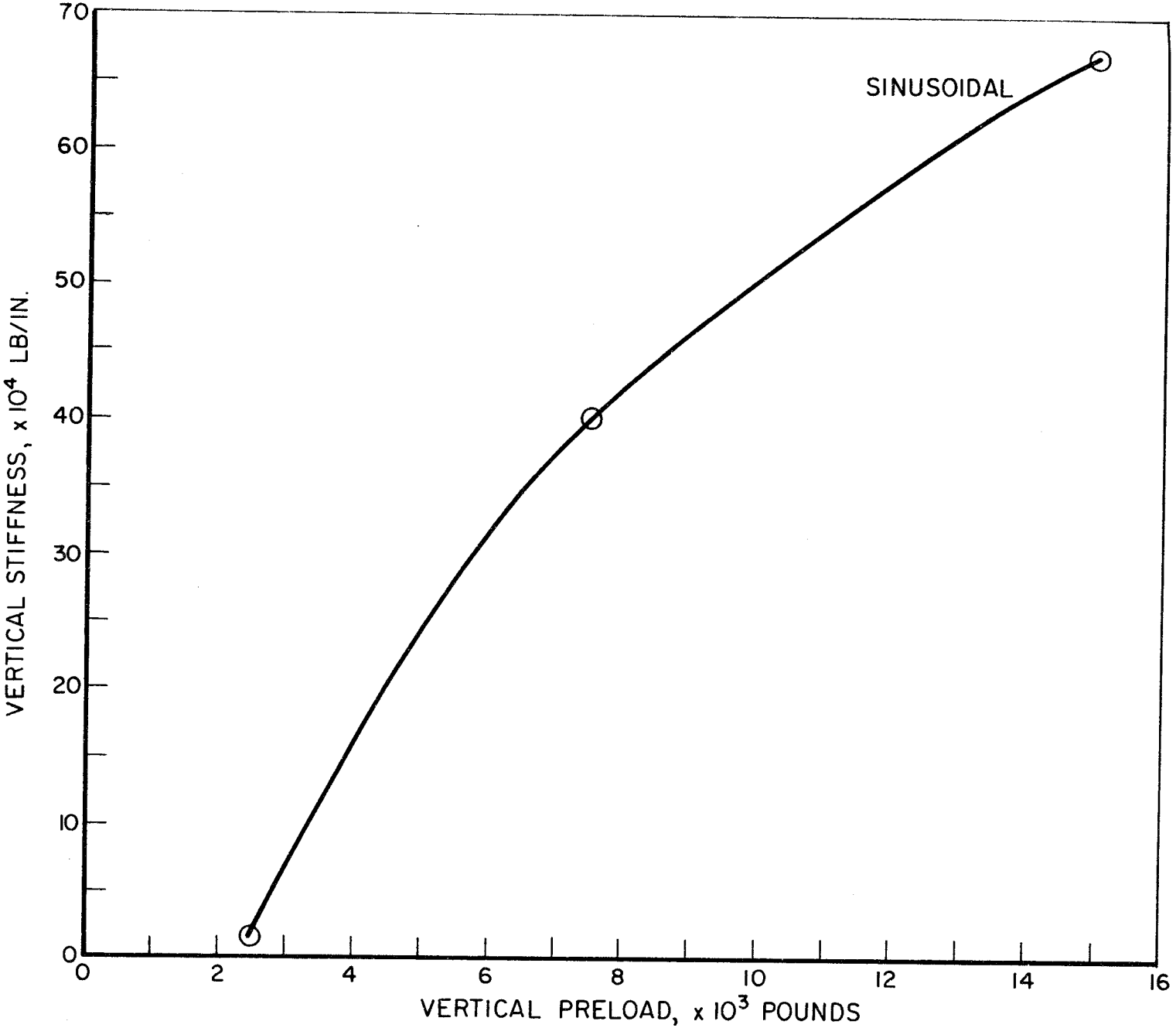

FIGURE 14. TRACK VERTICAL DYNAMIC STIFFNESS AT LOCATION 1 USING SINUSOIDAL EXCITATION

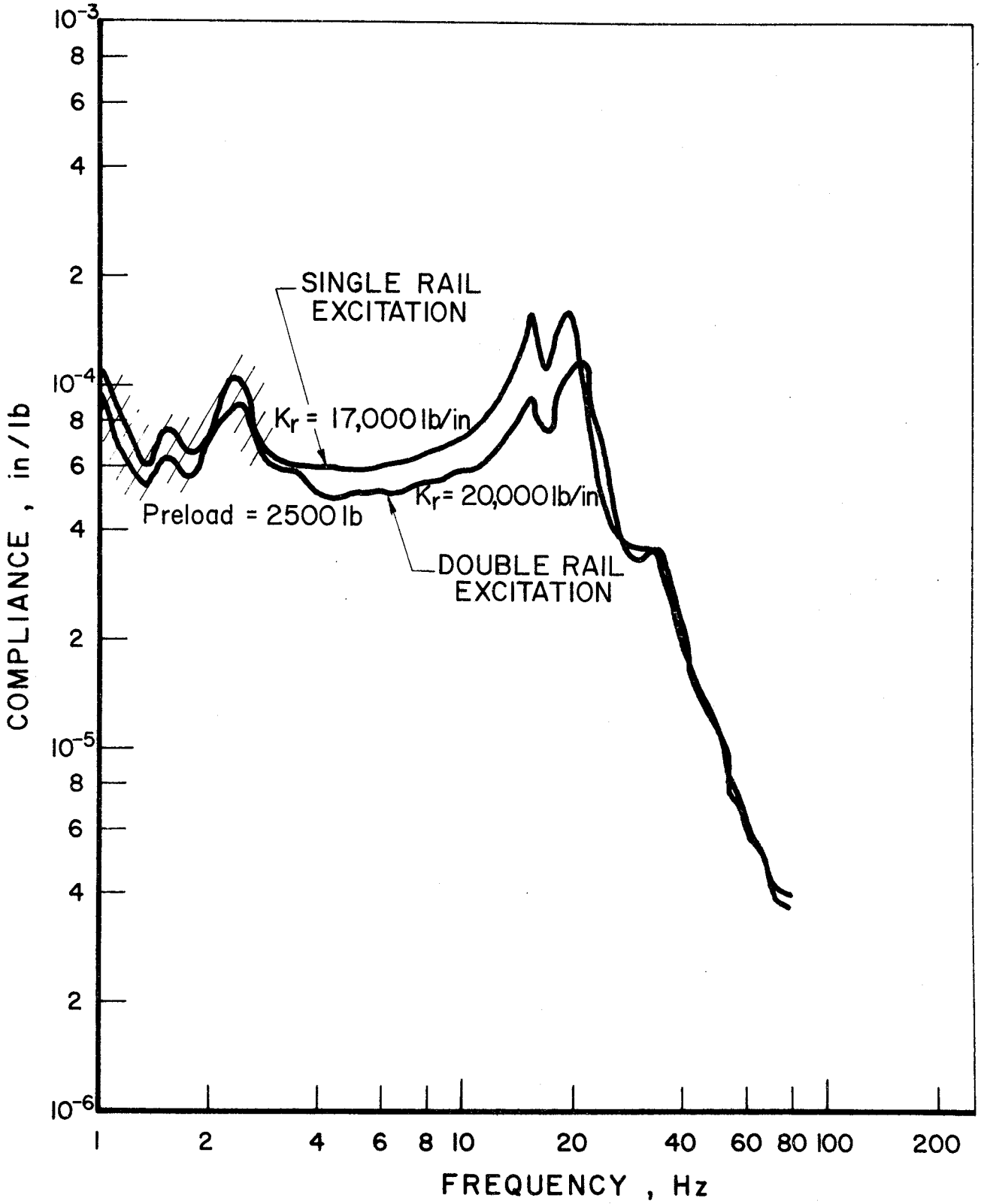

FIGURE 15. TRACK VERTICAL DYNAMIC COMPLIANCE OBTAINED BY USING SINUSOIDAL EXCITATION ON A SINGLE RAIL AND ON BOTH RAILS AT LOCATION 1

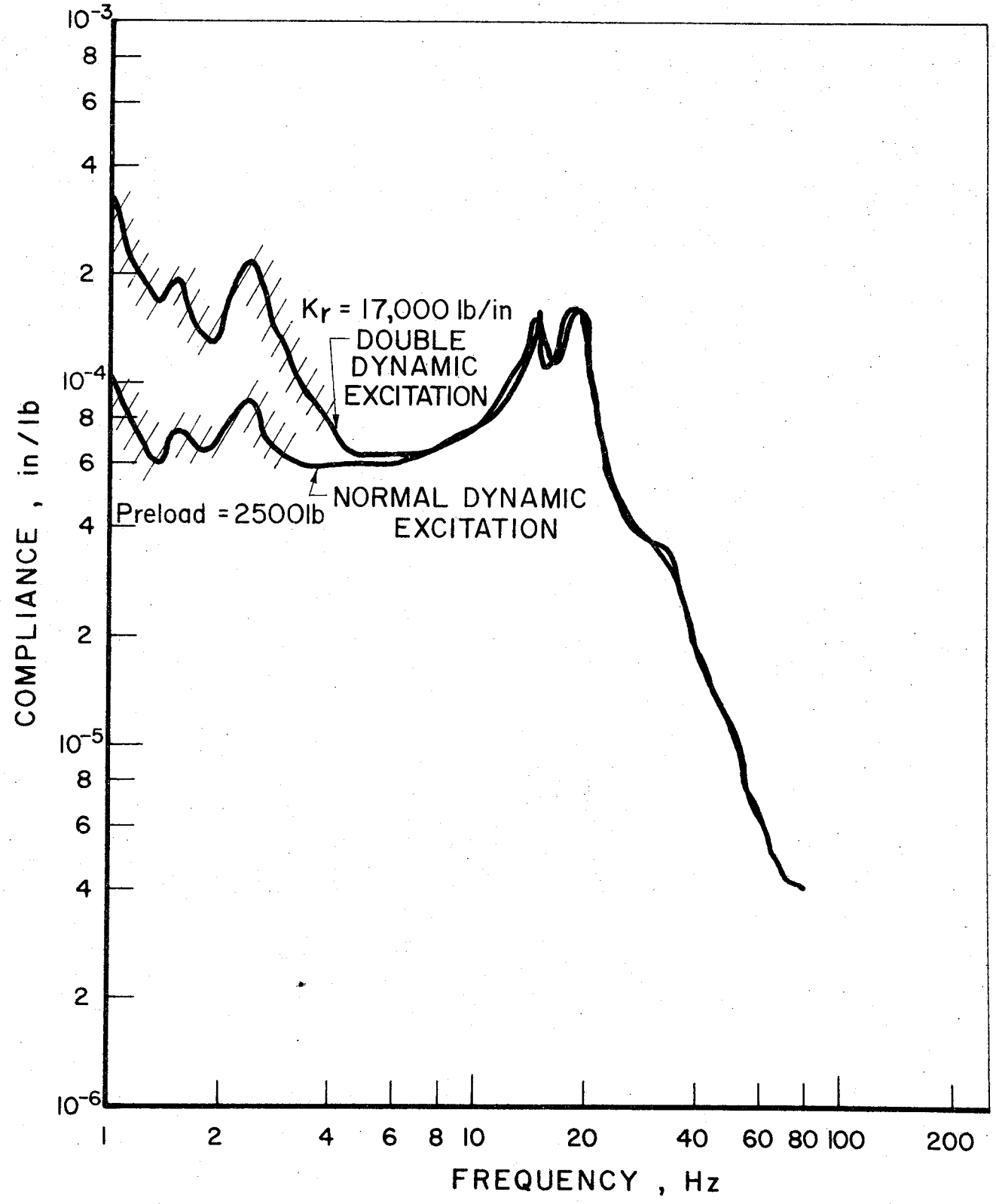

FIGURE 16. TRACK VERTICAL DYNAMIC COMPLIANCE OBTAINED BY USING SINUSOIDAL EXCITATION TO DETERMINE THE EFFECT OF DOUBLING THE DYNAMIC EXCITATION LEVEL AT LOCATION 1

Effect of Preload

Figure 17 shows the track vertical compliance measurements at Location 1 which were obtained by preloading both rails and driving one rail. Preloads of 2500, 7500, and 15,000 lb/rail were used. The vertical stiffness for 2500 lb preload is 15,000 lb/in.; 160,000 lb/in. for 7500 lb load. For a 15,000 lb/rail preload, the stiffness measured is 526,000 lb/in.; a factor of six increase in preload caused an increase of a factor of 35 in stiffness. This is very similar to the effect of preload using sinusoidal excitation.

Table 3 is a summary of the parameters measured at Location 1 using random excitation. A comparison of the data from Figures 13 and 17 is shown in Figure 18. The low preload vertical compliance functions show good agreement using both methods of excitation, but the high preload of 15,000 lb/rail shows a factor of 1.2 increase in stiffness using the sinusoidal method of excitation. These additional data points are added to the previous stiffness curve and are shown in Figure 19. One possible reason for this difference in stiffness value is that measurements were not done on the same day, and it had rained after the sinusoidal measurements. Other data also show a softening of the track after a rain.

Single Versus 2-Rail Excitation

It was shown previously with the light preload sinusoidal excitation that driving both rails or driving one rail showed only a small change in stiffness. This is also true for random excitation, as shown in Figure 20 for 2500 and 15,000 lb. preloads.

It was noted that driving one rail vertically at Location 1 showed a stiffness of 15,000 lb/in. early in the day. A stiffness of 18,000 lb/in. as shown in Figure 20 , was measured later the same day. This stiffening effect was also noted on other days. This may be a settling or compaction effect due to the continual dynamic loading.

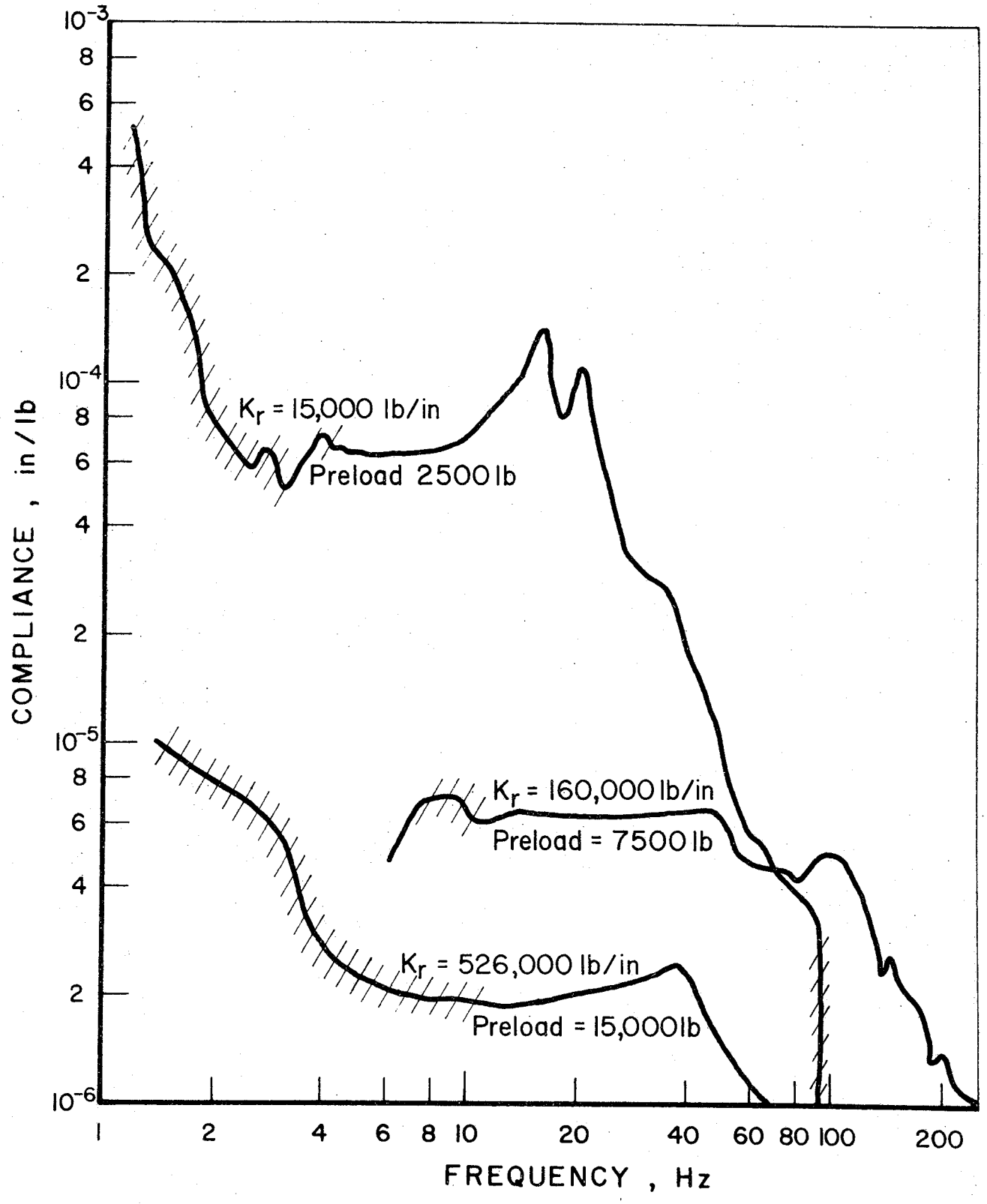

FIGURE 17. TRACK VERTICAL DYNAMIC COMPLIANCE OBTAINED BY USING RANDOM EXCITATION FOR THREE VERTICAL PRELOADS AT LOCATION 1

TABLE 3. SUMMARY OF VERTICAL COMPLIANCE MEASUREMENTS USING RANDOM EXCITATION AT LOCATION 1.

Vertical Preload 16	Vertical Stiffness K_r lb/in.	Natural Frequency W_r Hz	Damping %	Effection Mass M_r 16
2500	15,000	17.5	24	478
7500	160,000	42	46	887
15,000	526,000	37	39	3760

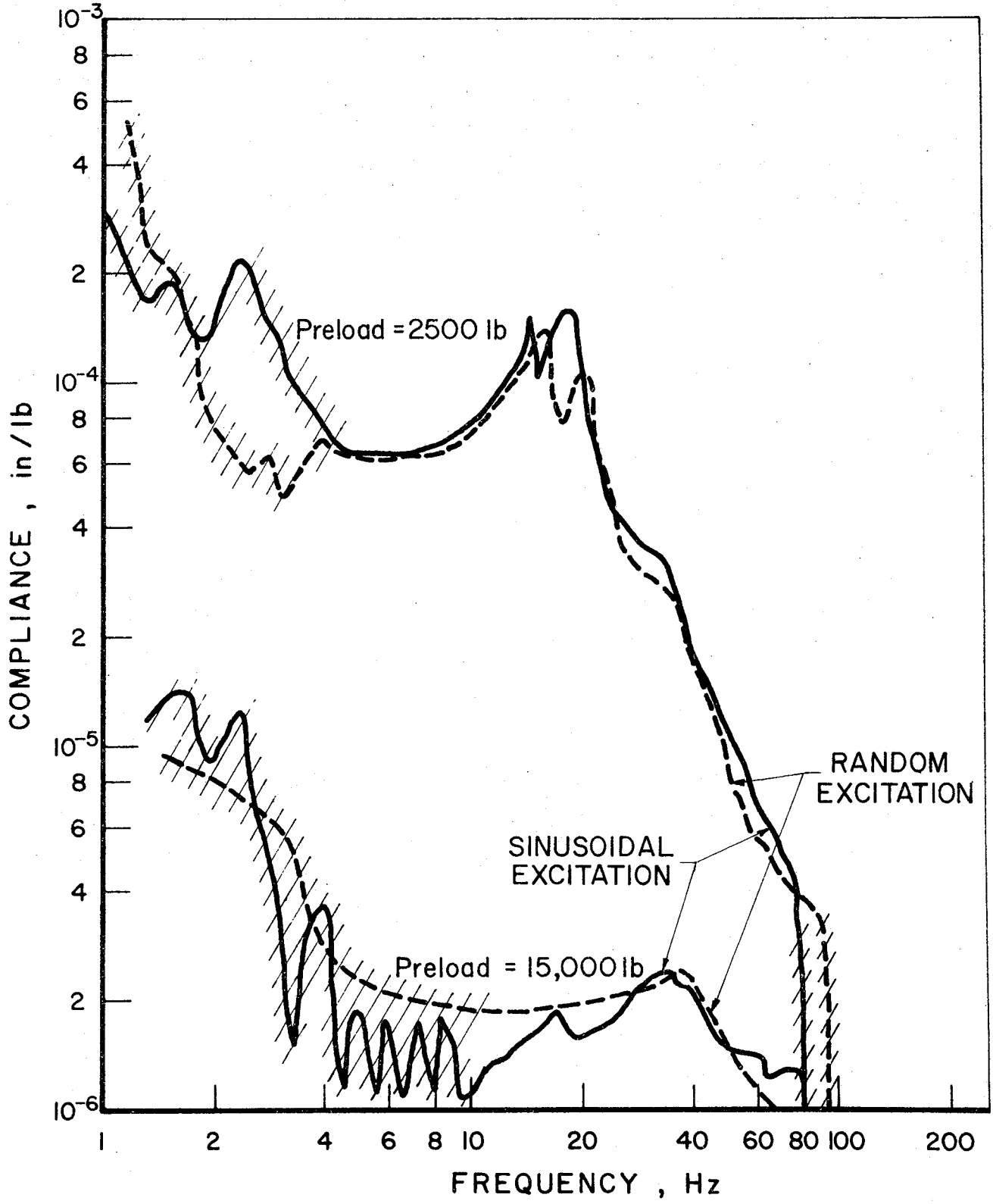

FIGURE 18. TRACK VERTICAL DYNAMIC COMPLIANCE AT LOCATION 1 OBTAINED BY USING SINUSOIDAL AND RANDOM EXCITATION FOR TWO DIFFERENT VERTICAL PRELOADS

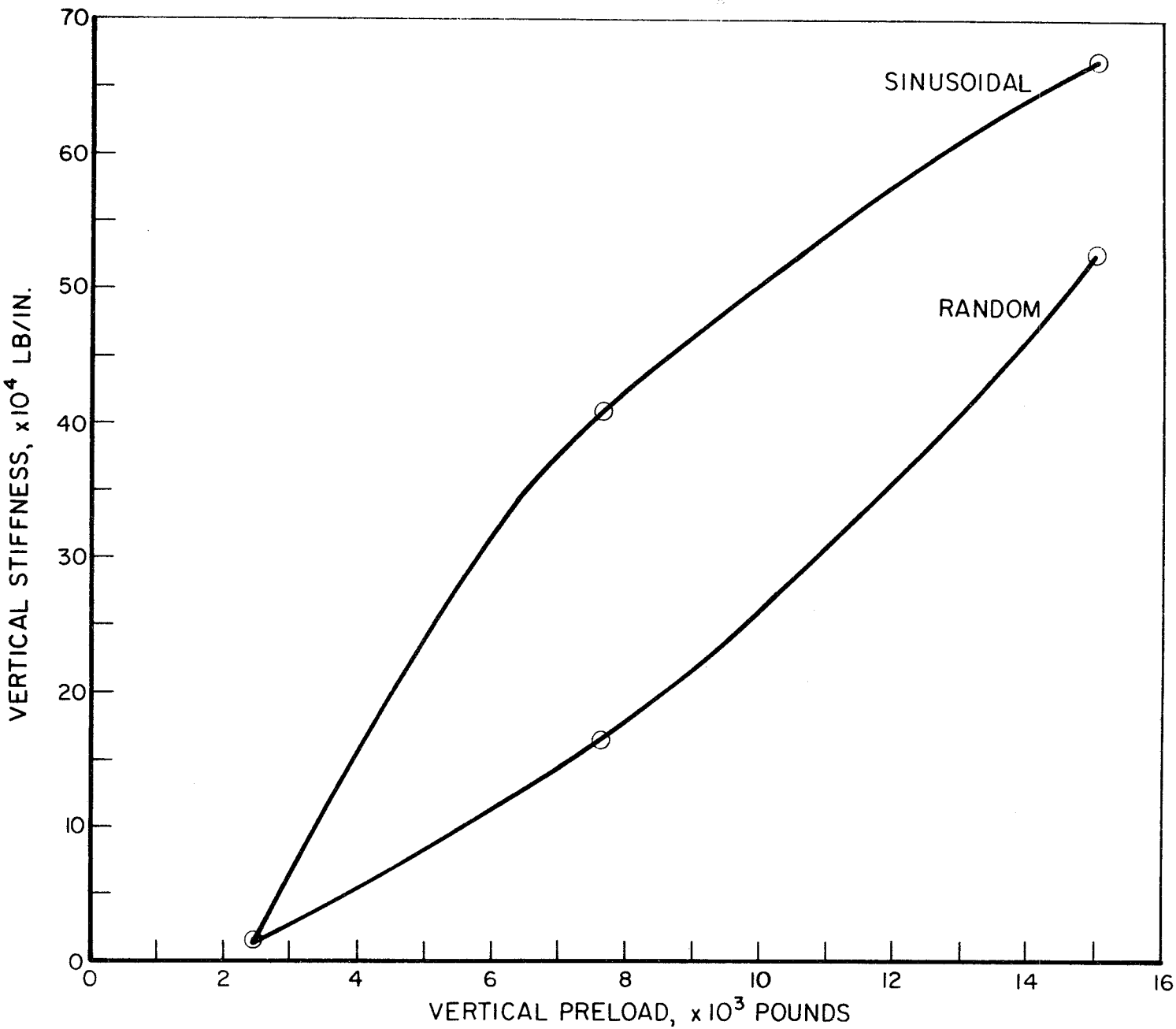

FIGURE 19. TRACK VERTICAL DYNAMIC STIFFNESS AT LOCATION 1 USING SINUSOIDAL AND RANDOM EXCITATION

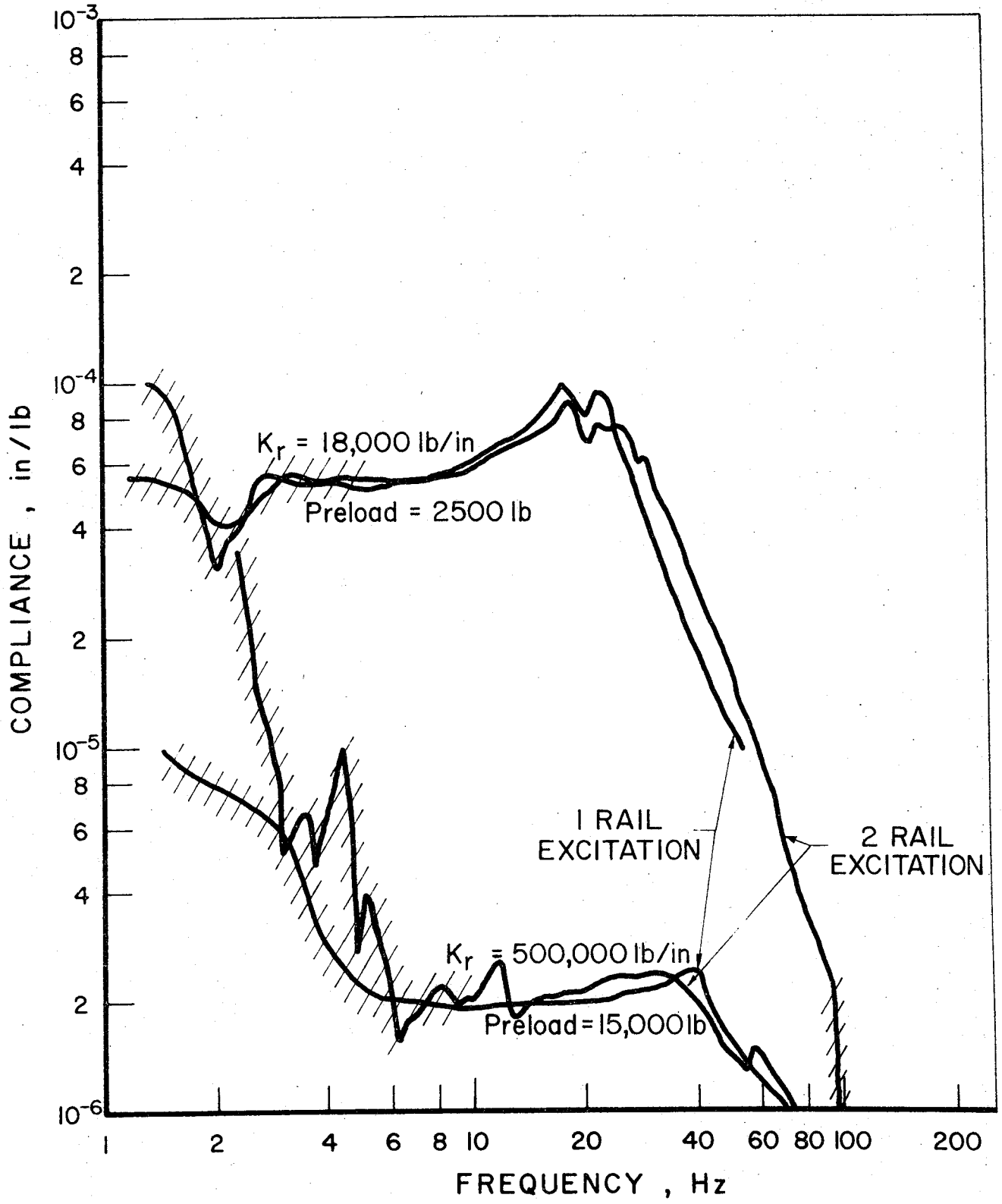

FIGURE 20. TRACK VERTICAL DYNAMIC COMPLIANCE OBTAINED BY USING RANDOM EXCITATION ON A SINGLE RAIL AND ON BOTH RAILS AT LOCATION 1 FOR TWO VERTICAL PRELOADS

Increase in Dynamic Amplitude

The rms level of the random excitation was increased to determine the degree of linearity with respect to dynamic forcing amplitude. Figure 21 shows vertical track compliance for two different vertical preloads, 5000 and 15,000 lb. For the 5000 lb preload, the lower dynamic level yielded 59,000 lb/in. The same is also true for the 15,000 lb vertical preload in that both compliance plots yield 518,000 lb/in. vertical stiffness. This indicates the system is linear within a small dynamic range and verifies the same conclusion obtained from the sinusoidal results.

Track Condition

Random excitation was also used at Location 2. Figure 22 shows the effect of vertical preloads of 2500, 7500, and 15,000 lb/rail with both rails driven simultaneously. This location yielded stiffnesses of 33,000 lb/in. at 2500 lb preload, 154,000 lb/in. at 7500 preload, and 313,000 lb/in. for 15,000 lb preload. Table 4 gives a summary of the parameters measured and calculated.

Table 5 shows a comparison between the stiffness at Locations 1 and 2 in the vertical direction, and these stiffness values are plotted in Figure 23.

Random Excitation in Lateral Direction

Effect of Vertical Preload

Lateral track compliance measurements were obtained by preloading both rails in the vertical direction and driving one rail laterally with random excitation and zero lateral preload. Figure 24 shows the lateral track compliance function at Location 1 for a 2500 lb vertical preload. Also plotted in this figure is the phase angle and the coherence function. The magnitude plot indicates a heavily damped resonance, 45 percent of critical at about 17.5 Hz. The 90^{o} phase angle crossing indicates the undamped natural frequency is at 21 Hz. The coherence function indicates

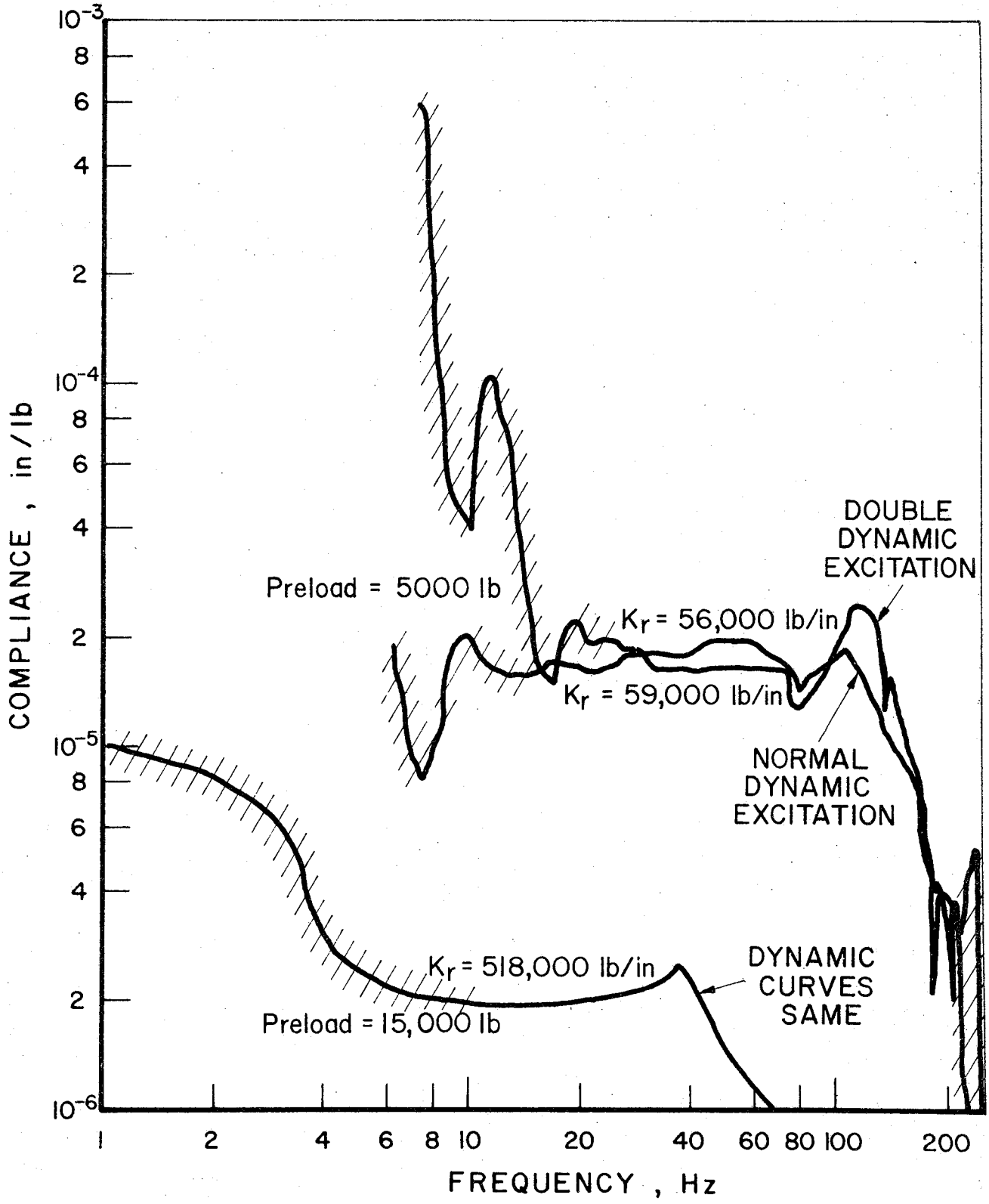

FIGURE 21. TRACK VERTICAL DYNAMIC COMPLIANCE OBTAINED BY USING RANDOM EXCITATION TO DETERMINE THE EFFECT OF DOUBLING THE DYNAMIC EXCITATION LEVEL AT LOCATION 1

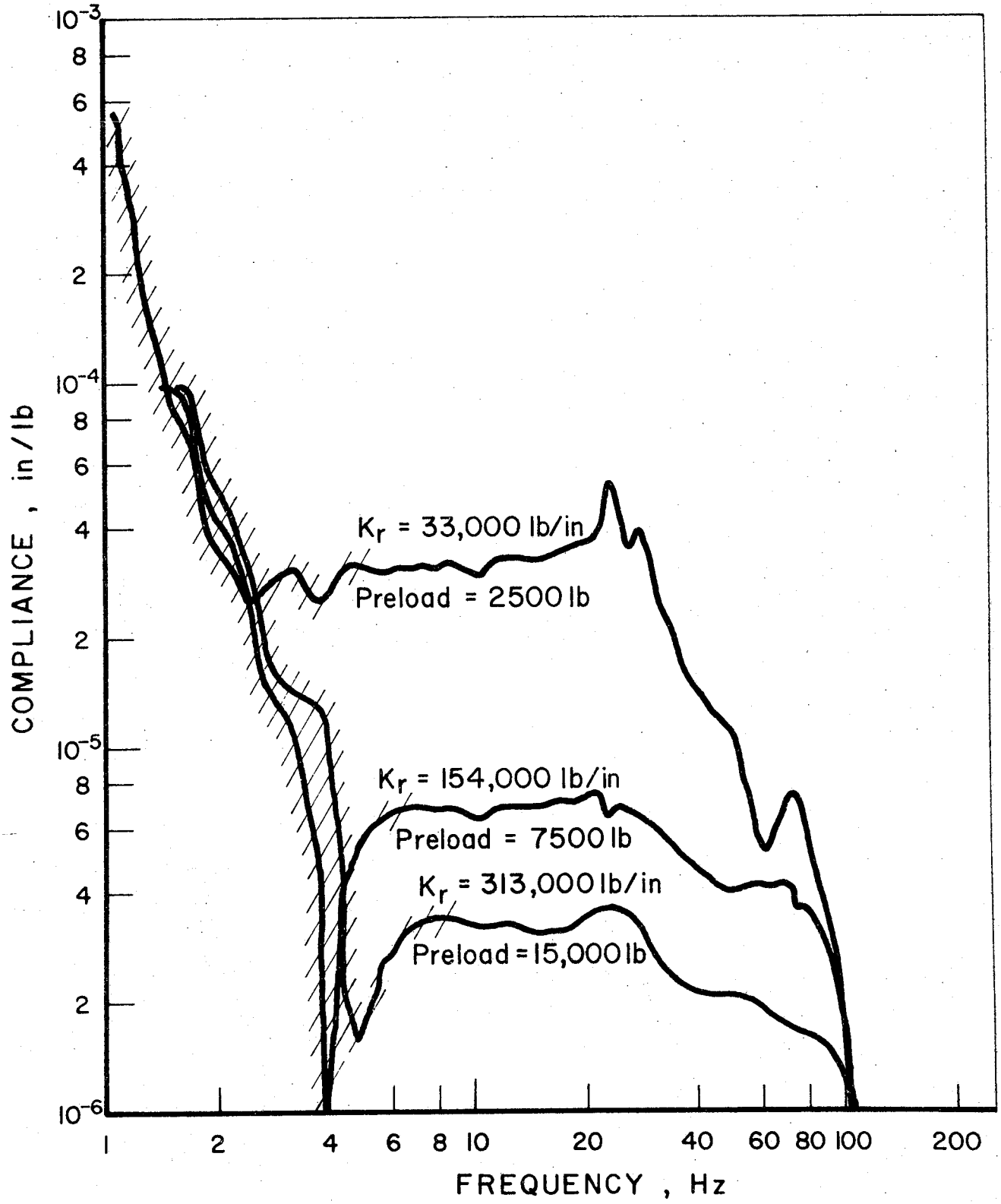

FIGURE 22. TRACK VERTICAL DYNAMIC COMPLIANCE OBTAINED BY USING RANDOM EXCITATION FOR THREE VERTICAL PRELOADS AT LOCATION 2

TABLE 4. SUMMARY OF VERTICAL COMPLIANCE MEASUREMENTS USING RANDOM EXCITATION AT LOCATION 2.

Vertical Preload	Vertical Stiffness	Natural Frequency W_n Hz	Damping %	Mass M_r
2500	33,000	23	28	610
7500	154,000	25	50	2400
15,000	313,000	25	45	4896

TABLE 5. SUMMARY OF VERTICAL DYNAMIC STIFFNESSES MEASURED AT LOCATIONS 1 AND 2.

Preload Vertical	Stiffness Location 1		Location 2
	SINE	Random	Random
2500	17,000	15,000	33,000
7500	400,000	160,000	154,000
15,000	670,000	526,000	313,000

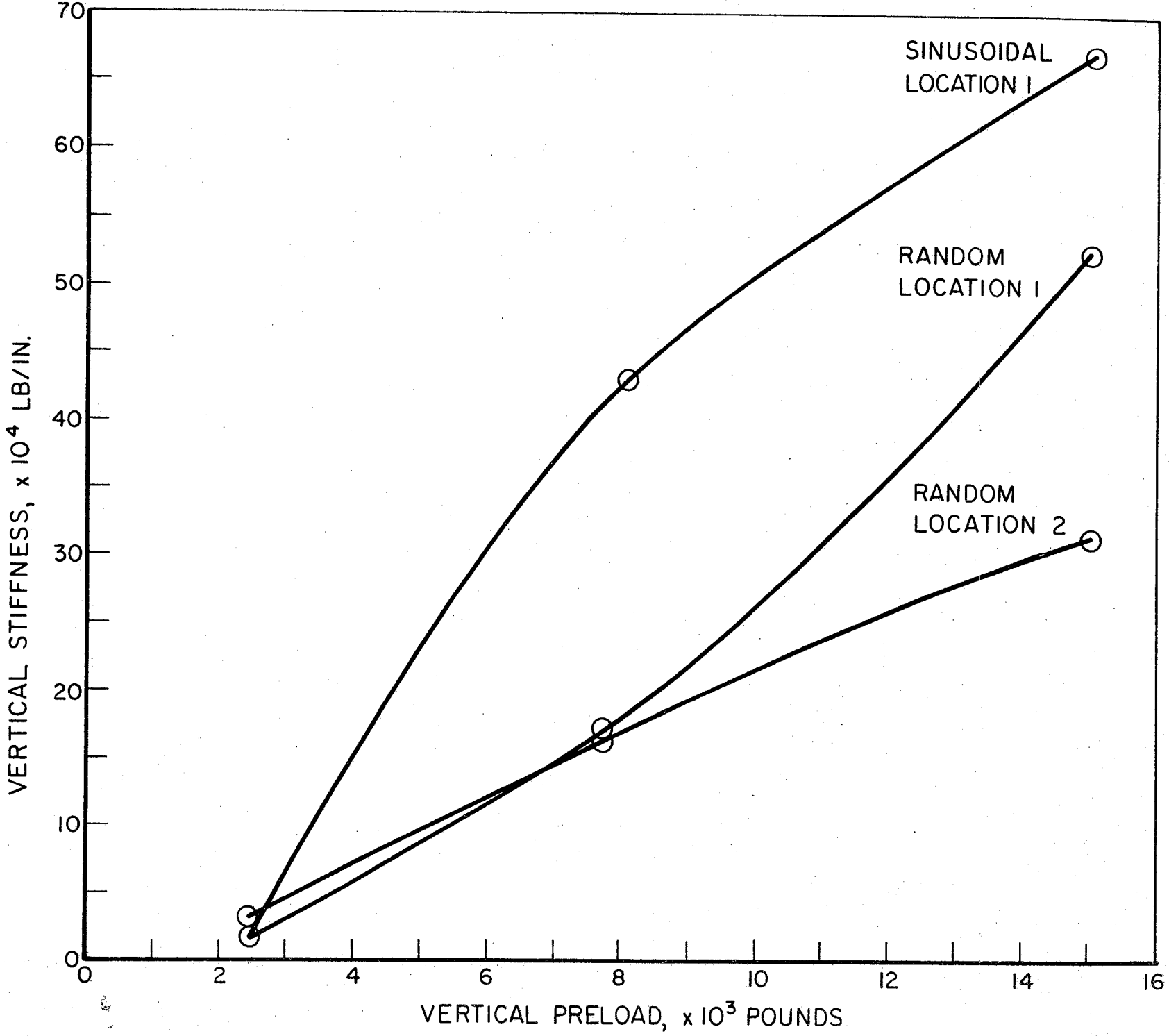

FIGURE 23. TRACK VERTICAL DYNAMIC STIFFNESS AT LOCATIONS 1 AND 2

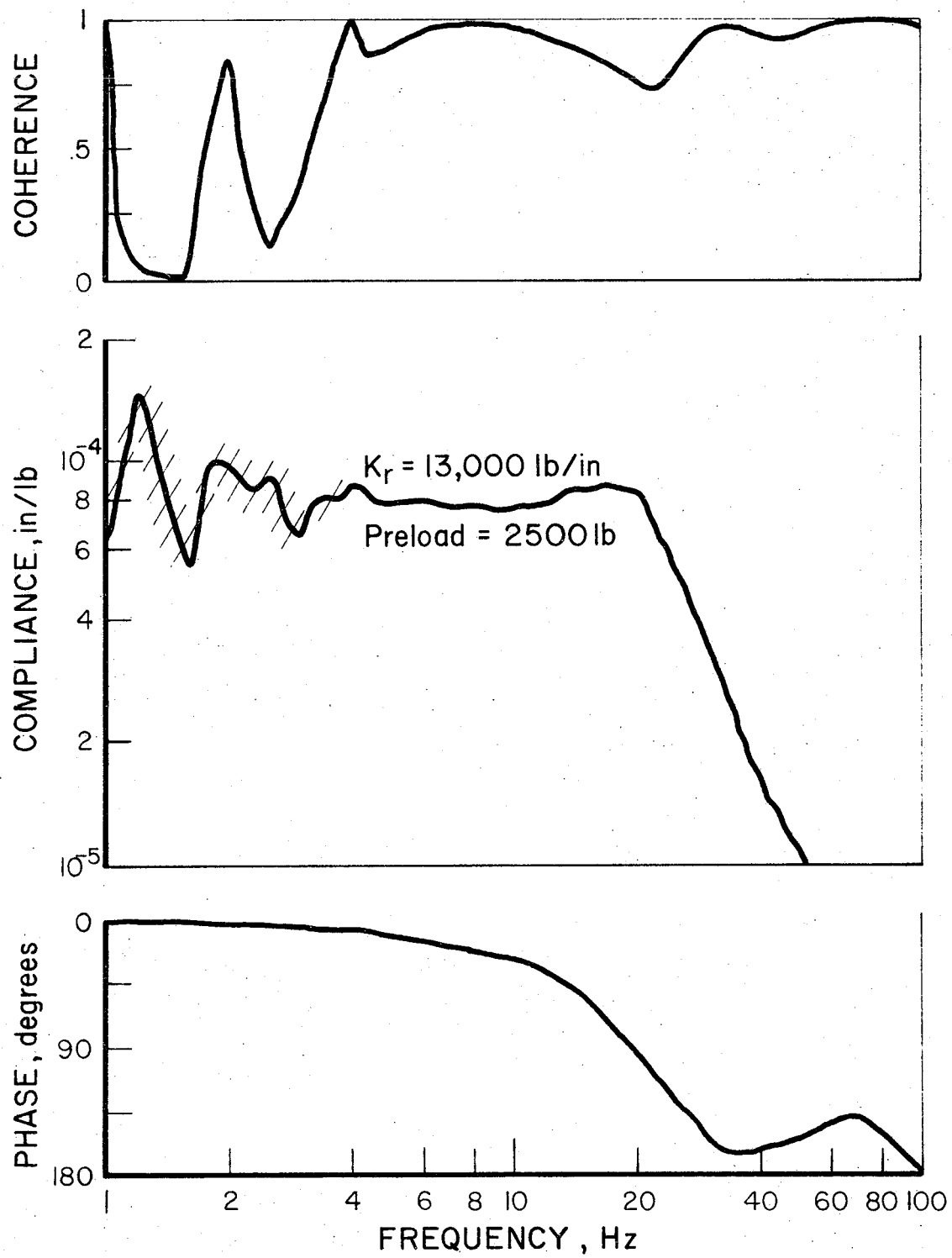

FIGURE 24. TRACK LATERAL DYNAMIC COMPLIANCE (PHASE AND COHERNECE) OBTAINED BY USING RANDOM EXCITATION WITH A 2500-LB VERTICAL PRELOAD AT LOCATION 1

the data is reliable between 10 and 90 Hz, since the coherence value is close to 1. The value of the coherance function drops near the resonance but not below 0.75. This value of the coherence could be improved by more averaging. The lateral stiffness measured is 13,000 lb/in. and the calculated effective mass is 415 lb mass. These values are compared for other preloads in Table 6. The values of stiffness, natural frequency, mass and damping are plotted against preload in Figure 25. Figure 26 is a power spectrum of the random input excitation. This shows the input force amplitude as a function of frequency. The roll off on each end of the spectrum was explained in the data analysis section.

Figure 27 shows the lateral track compliance at the same location but the vertical preload was increased to 5000 lb. The stiffness increased to 73,000 lb/in., the resonant frequency has increased to 50 Hz, and the damping has decreased to 37 percent of critical. The coherence and phase angle are also plotted in the same figure. The coherence indicates the data is valid between 10 and 90 Hz.

Increasing the vertical preload to 15,000 lb yields the compliance plot shown in Figure 28. The stiffness increased to 250,000 lb/in. and the resonant frequency has increased to 90 Hz. The coherence plot shows valid data in the range of 10 to 90 Hz. The dynamic characteristics for all three preloads are summarized in Table 6.

Figure 29 shows all three lateral compliance functions plotted together for the various preloads. This shows the nonlinear behavior of the lateral compliance function.

Effect of Lateral Preload

Lateral preload also has an effect on lateral dynamic compliance, but mostly for the light vertical preloads. Figure 30 shows a comparison between track lateral compliance for 5000 lb vertical preload with and without a lateral preload, and a 15,000 lb vertical preload with and without a lateral preload. For the 5000 lb vertical preload and no lateral preload, the stiffness was 71,000 lb/in. For 5000 lb vertical preload and 2000 lb. lateral preload, a stiffness of 222,000 lb/in. was obtained; a factor of 3 increase in stiffness. The higher vertical preloads do not

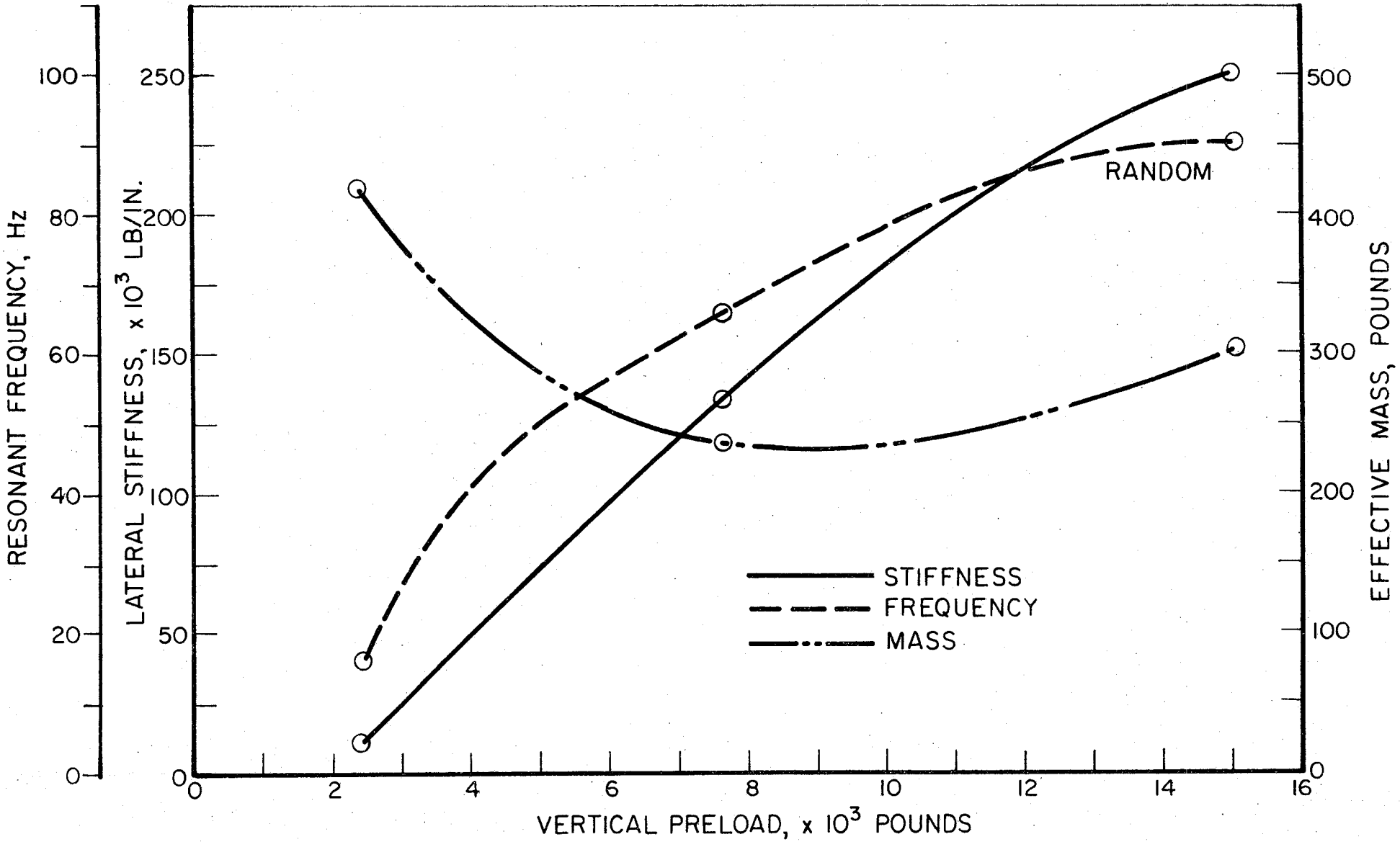

FIGURE 25. TRACK LATERAL DYNAMIC STIFFNESS, EFFECTIVE MASS, AND NATURAL FREQUENCY AT LOCATION 1 AS A FUNCTION OF VERTICAL PRELOAD

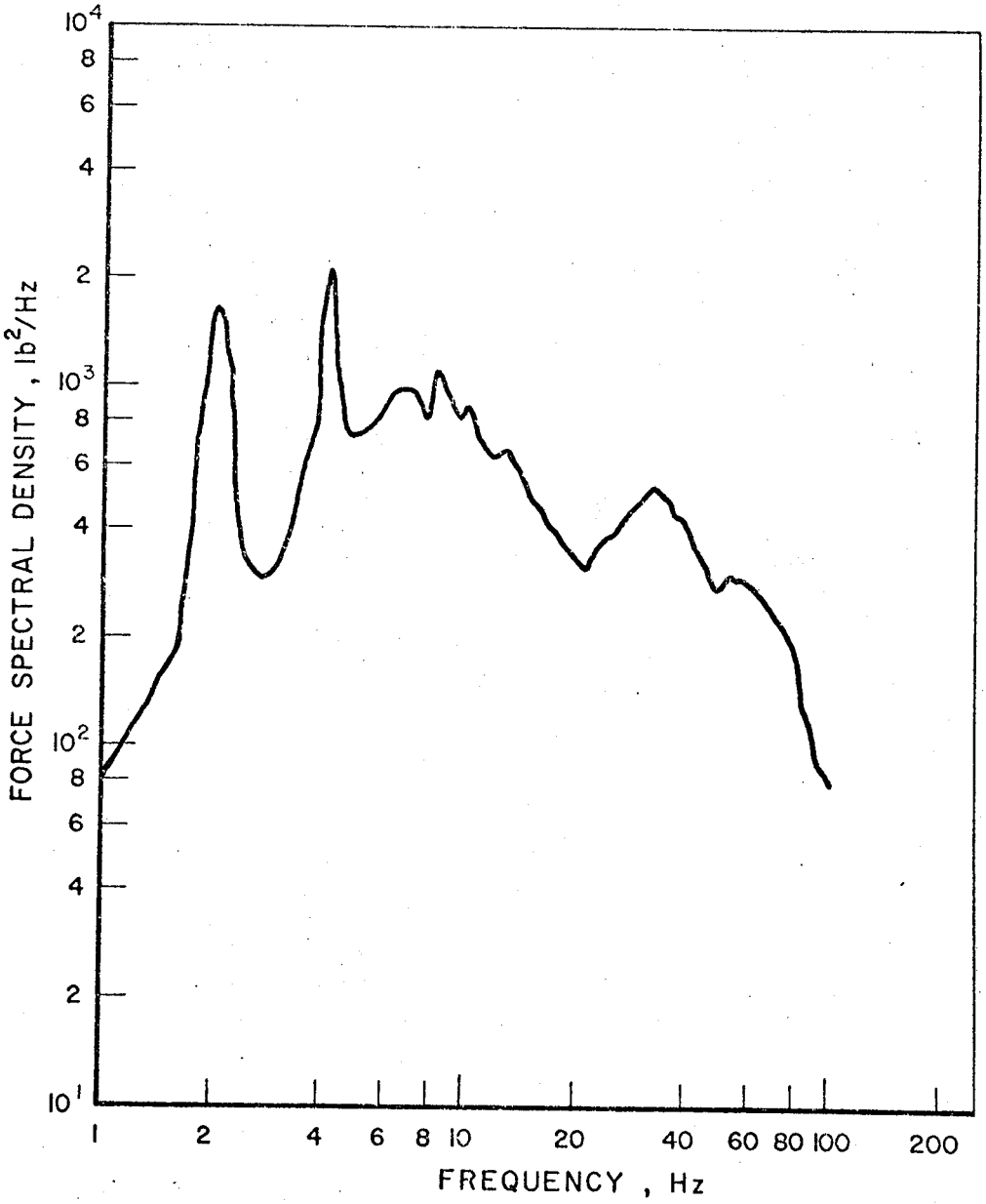

FIGURE 26. AVERAGED FORCE POWER SPECTRAL DENSITY OF THE RANDOM EXCITATION AT LOCATION 1

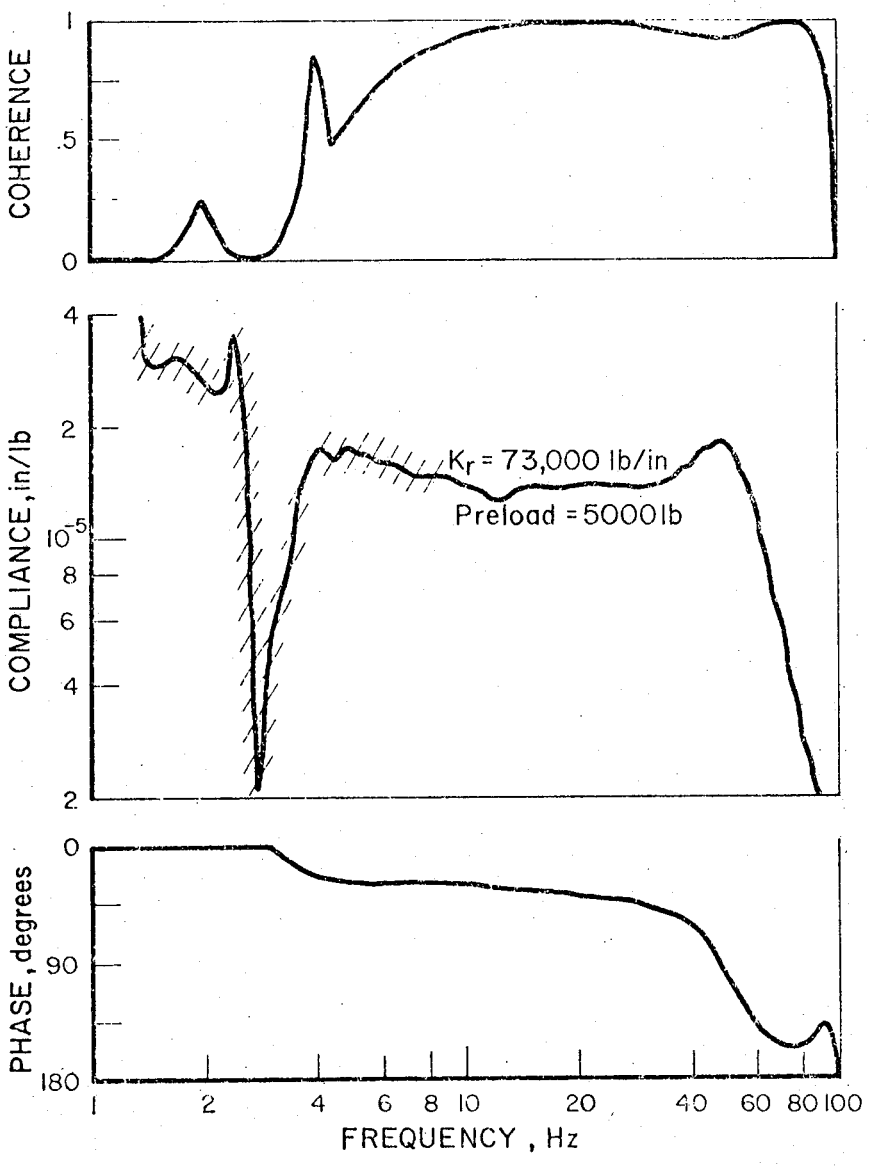

FIGURE 27. TRACK LATERAL DYNAMIC COMPLIANCE (PHASE AND COHERENCE) OBTAINED BY USING RANDOM EXCITATION WITH A 5000-LB VERTICAL PRELOAD AT LOCATION 1

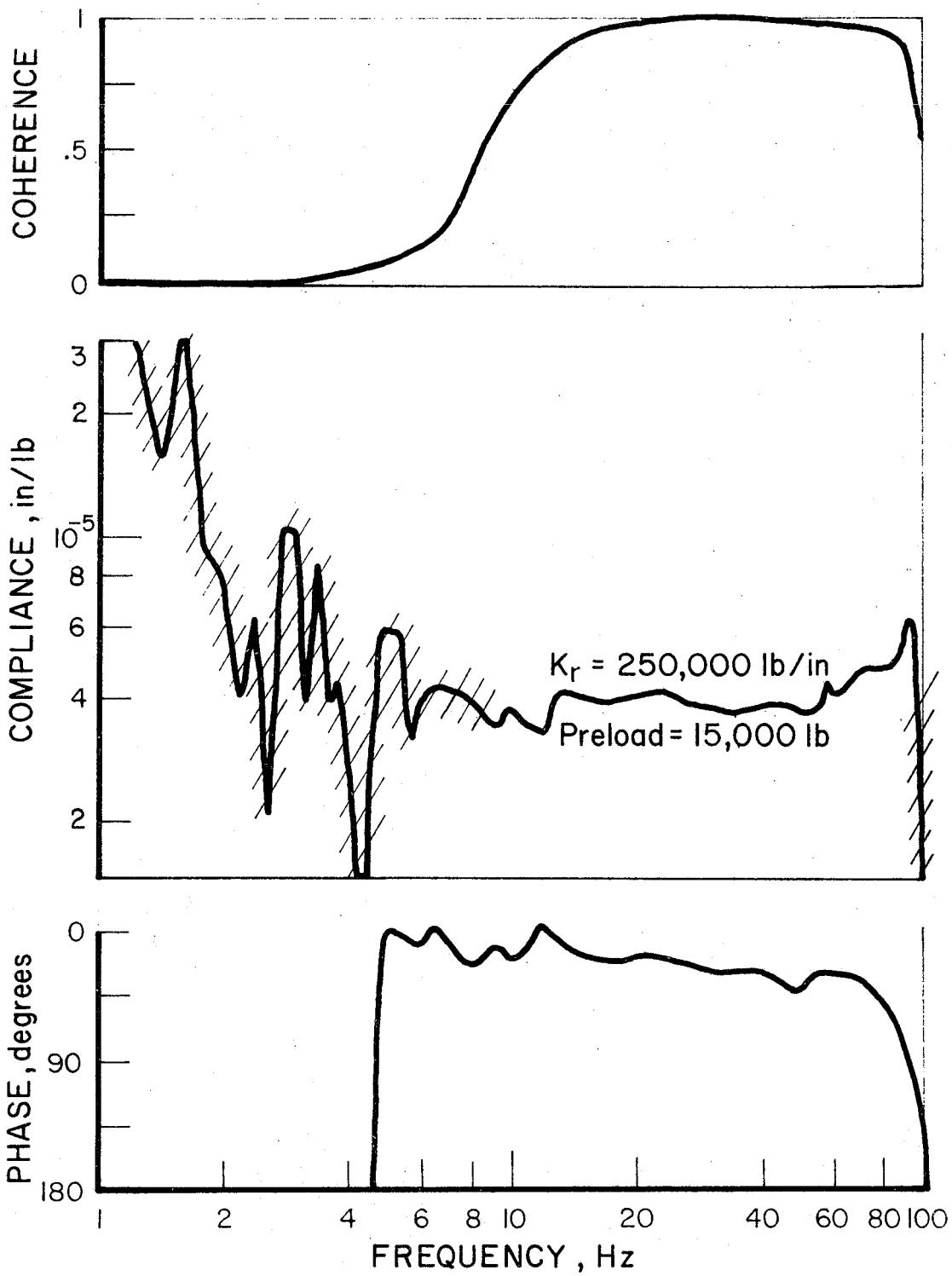

FIGURE 28. TRACK LATERAL DYNAMIC COMPLIANCE (PHASE AND COHERENCE) OBTAINED BY USING RANDOM EXCITATION WITH A 15,000-LB VERTICAL PRELOAD AT LOCATION 1

TABLE 6. SUMMARY OF LATERAL COMPLIANCE MEASUREMENTS USING RANDOM EXCITATION AT LOCATION 2.

Vertical Preload lb	Lateral Stiffness K_r lb/in.	Natural Frequency W_n Hz	Effective Mass M_r lb	Damping % Critical %
2500	13,000	17.5	415	45
5000	73,000	50	285	37
15,000	250,000	90	301	31

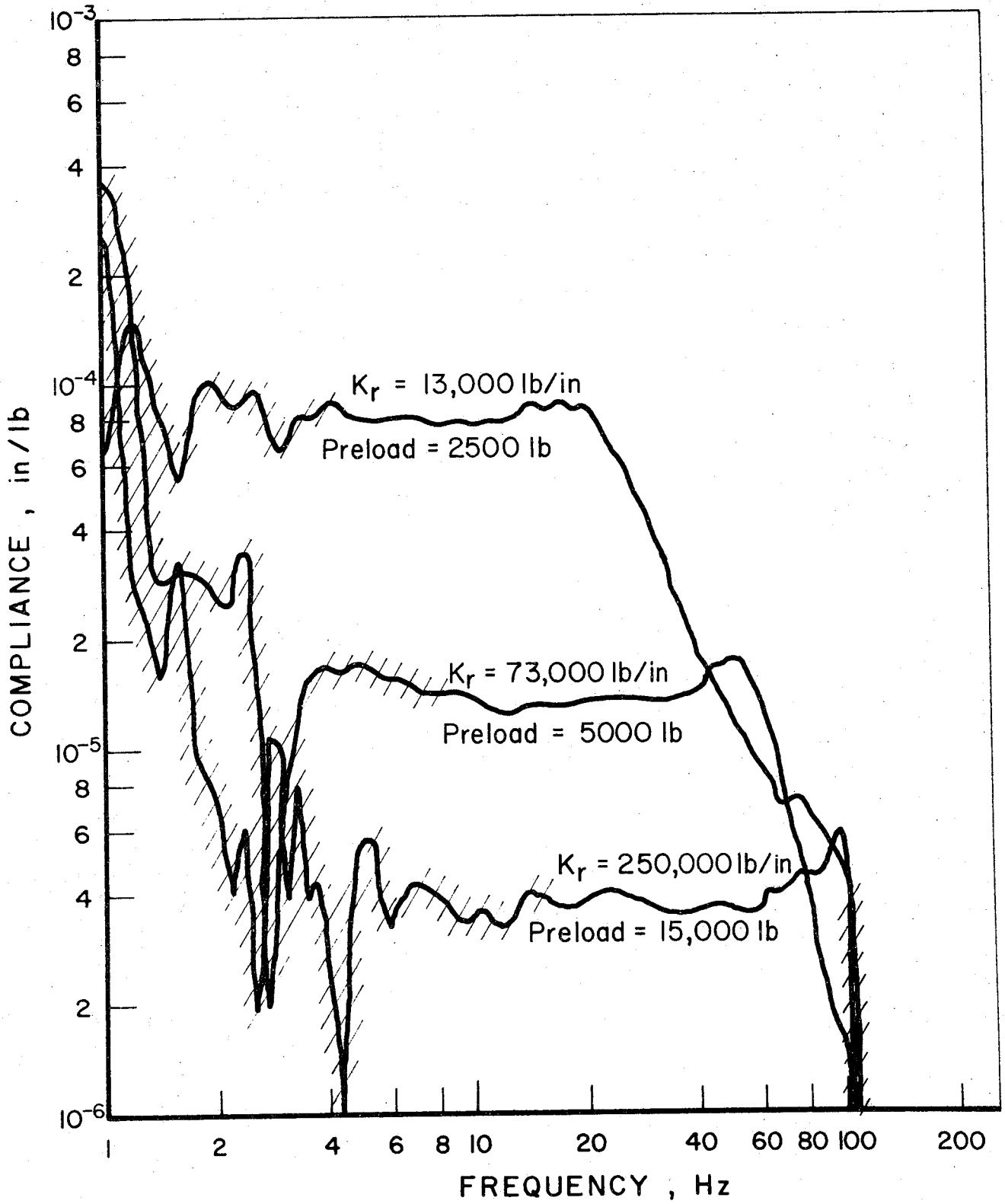

FIGURE 29. TRACK LATERAL DYNAMIC COMPLIANCE OBTAINED BY USING RANDOM EXCITATION AT LOCATION 1 FOR THREE VERTICAL PRELOADS

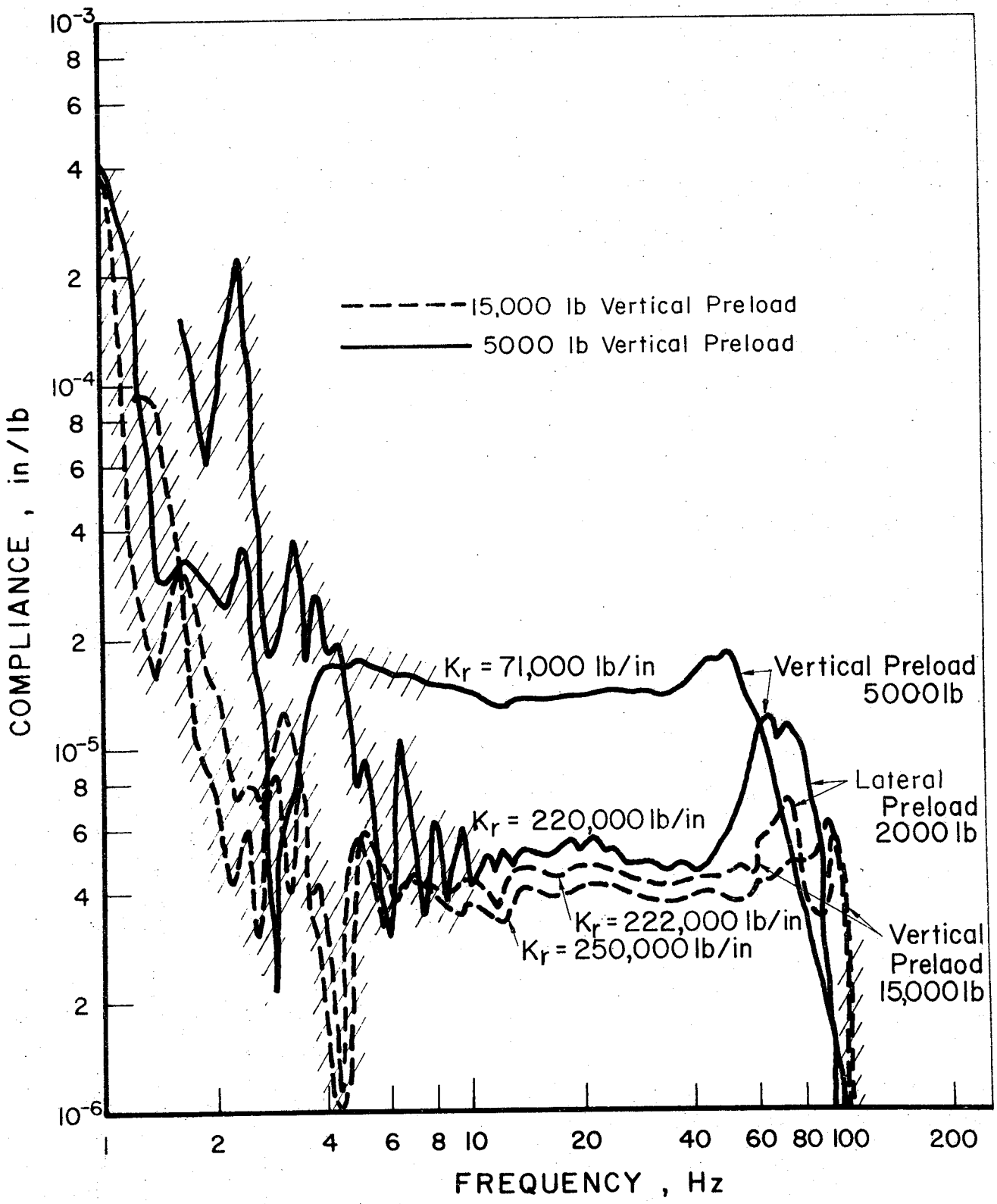

FIGURE 30. TRACK LATERAL DYNAMIC COMPLIANCE OBTAINED BY USING RANDOM EXCITATION WITH AND WITHOUT A LATERAL PRELOAD FOR TWO VERTICAL PRELOADS AT LOCATION 2

show this pronounced effect. Figure 30 shows about the same stiffness of 250,000 lb/in. for both cases of 15,000 lb vertical preload with and without a lateral preload. The reason for this effect is seen in the lateral load deflection curves discussed in a later section. Evidently, the rail begins to slide after the static friction is overcome, so there are several stiffness regions in the load deflection curve. The first is the stiffness measured before the rail slides, and the second is a less stiff region where the rail is sliding. The stiffness then increases again when the rail is forced against the spikes. For the heavy vertical preload, the rail is not able to slide due to the large normal force, and the initial high stiffness region governs. Table 7 summarizes the lateral compliance parameters.

High Frequency Response

The previous lateral data were obtained in the frequency range below 100 Hz. Some data were also measured up to 256 Hz. Figure 31 shows a comparison of the lateral track compliance for a 15,000 lb vertical preload, and zero lateral preload for maximum frequencies of 100 and 256 Hz. These data show the existence of a higher mode of vibration at 200 Hz.

To demonstrate the effect of averaging, the previous 256 Hz data, which was averaged for 41 seconds, were rerun using only one 2-second sample, see Figure 32. The static stiffness is the same, but there is a lot of noise on the compliance plot, and poor coherence at low frequencies.

Pulse Excitation in Vertical Direction

Pulse Shape Spectra

Pulse excitation was accomplished by using the Fourier analyzer to generate a rectangular pulse as an input signal for the shaker control

TABLE 7. SUMMARY OF LATERAL COMPLIANCE PARAMETERS FOR A PRELOADED AND UNPRELOADED CONDITION IN THE LATERAL DIRECTION USING RANDOM EXCITATION AT LOCATION 1

Preload Vertical lb.	Preload Lateral lb.	Stiffness Lateral lb/in.	Natural Frequency W_n Hz	Effective Mass M_r lb	Percent Critical Damping ξ
5000	0	71,000	50	278	38
5000	2000	222,000	65	509	21
15000	-	250,000	90	301	33
15000	2000	244,000	70	486	29

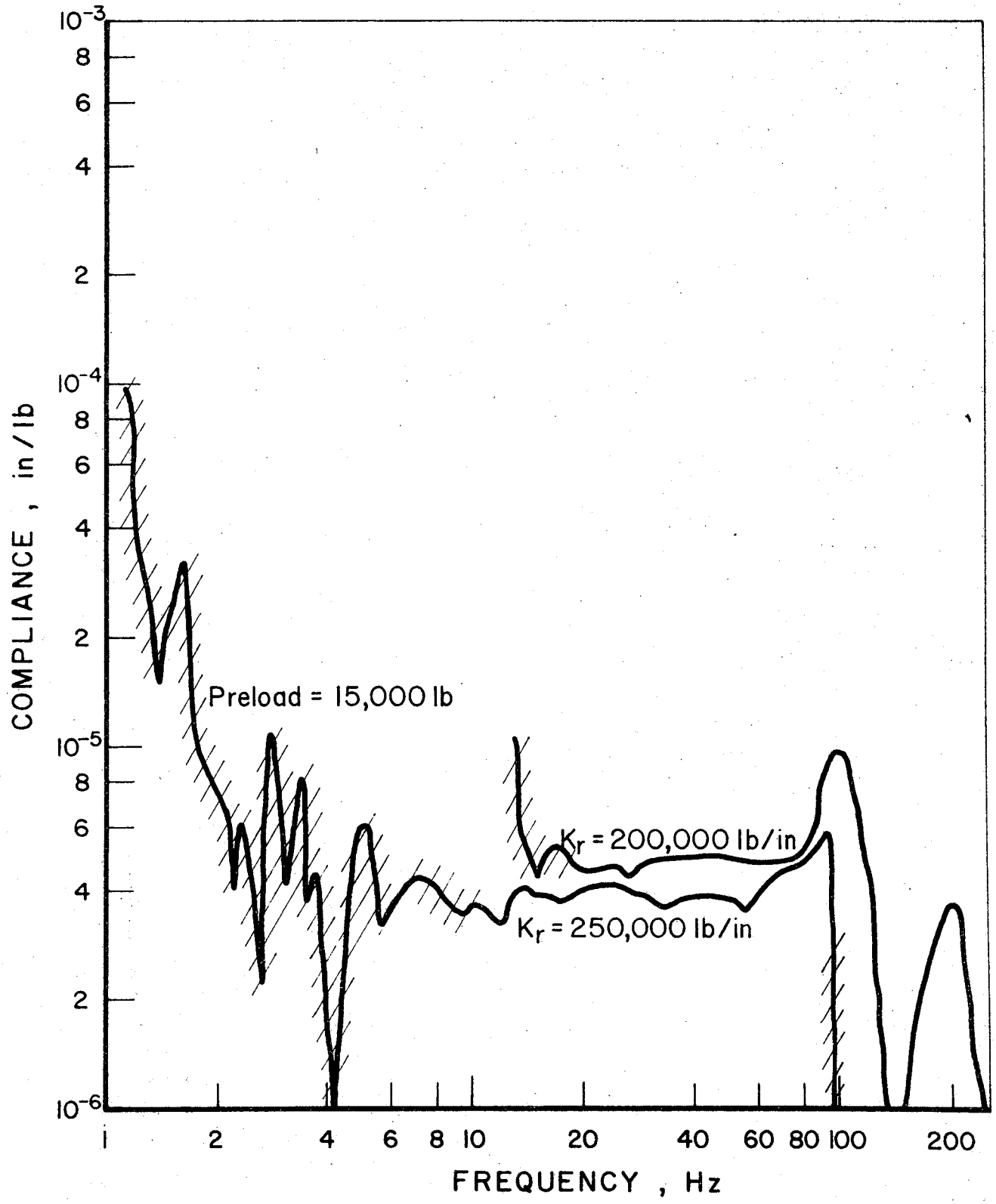

FIGURE 31. TRACK LATERAL DYNAMIC COMPLIANCE OBTAINED BY USING RANDOM EXCITATION FOR TWO DIFFERENT MAXIMUM FREQUENCIES AT LOCATION 1

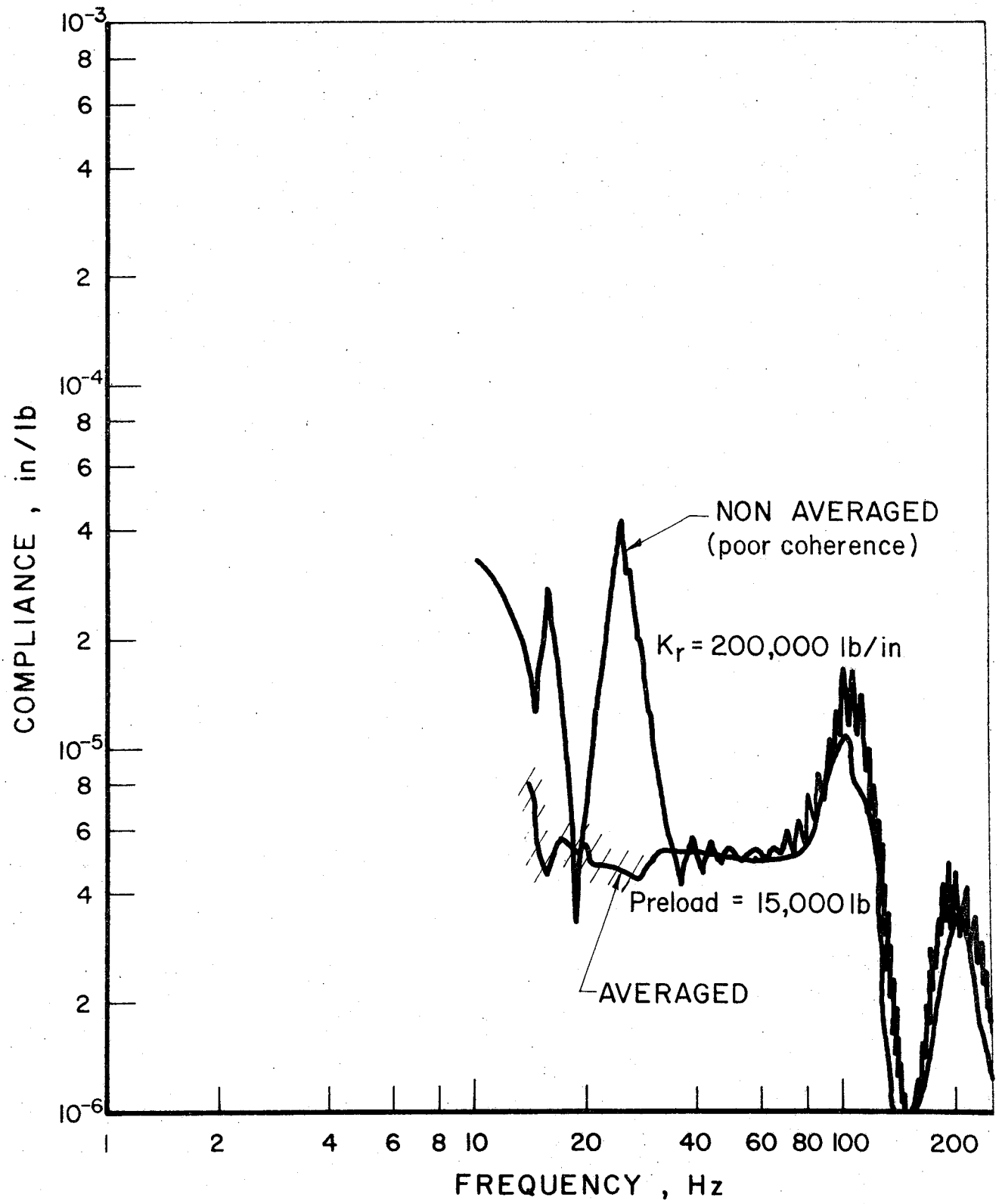

FIGURE 32. TRACK LATERAL DYNAMIC COMPLIANCE TO DEMONSTRATE THE EFFECT OF AVERAGING USING RANDOM EXCITATION AT LOCATION 1

system. The response data for 20 pulses was averaged to obtain track compliance measurements. Pulse durations of 10, 15, 20, and 25 milliseconds were used to evaluate changes in the frequency content of the excitation. Figure 33 shows the input command signal to the control system. These are rectangular pulse shapes of 10, 15, 20, and 25 milliseconds in duration. The frequency content of these rectangular pulse shapes are shown in Figures 34, 35, and 36. In these figures, the curve labeled "theoretical" is the frequency content of the input command signal to the control system. Figure 37 shows the actual measured force from the rectangular pulse input to the system control with 15,000 lb vertical preload measured by the load cell. This is an unloading pulse. The reason the measured force did not follow the input command signal is the servo control system was in saturation. This was done in order to obtain a high amplitude input pulse which was necessary to obtain a response from the track structure. The actual input frequency content of these measured pulse shapes are shown in Figures 34, 35, and 36. These curves are labeled "measured", as compared to the command signal labeled "theoretical". Figure 38 shows the measured input pulse to the track with a 7,500 lb vertical preload. There is a difference in pulse amplitude between the 15,000 lb vertical preload, and the 7,500 lb vertical preload. The 15,000 lb vertical preload with an unloading pulse yielded force amplitude of 3,950 lb for 10 millisecond duration, 5,100 lb for 15 millisecond duration, 6,000 lb for a 20 millisecond duration and 6,300 lb for a 25 millisecond duration input command pulse. For the 7,500 lb vertical preload with an unloading pulse, the input force measured was 2,000 lb for 10 millisecond duration, 2,250 lb for 15 millisecond duration, and 2,450 for 25 millisecond duration input command pulse. This result shows the unloading pulse amplitude is a function of the vertical preload. These spectra shown in Figures 34,35, and 36 indicate the frequency content of the track excitation force. The theoretical spectrum for a 10 millisecond rectangular pulse, Figure 34, shows good frequency content up to 60 Hz, where the magnitude is 3dB down. The spectrum of the actual force on the track indicates a frequency band of 2.5 to 35 Hz for the low and high frequency 3dB down points. There is also excitation at other frequencies, but the level of excitation is low.

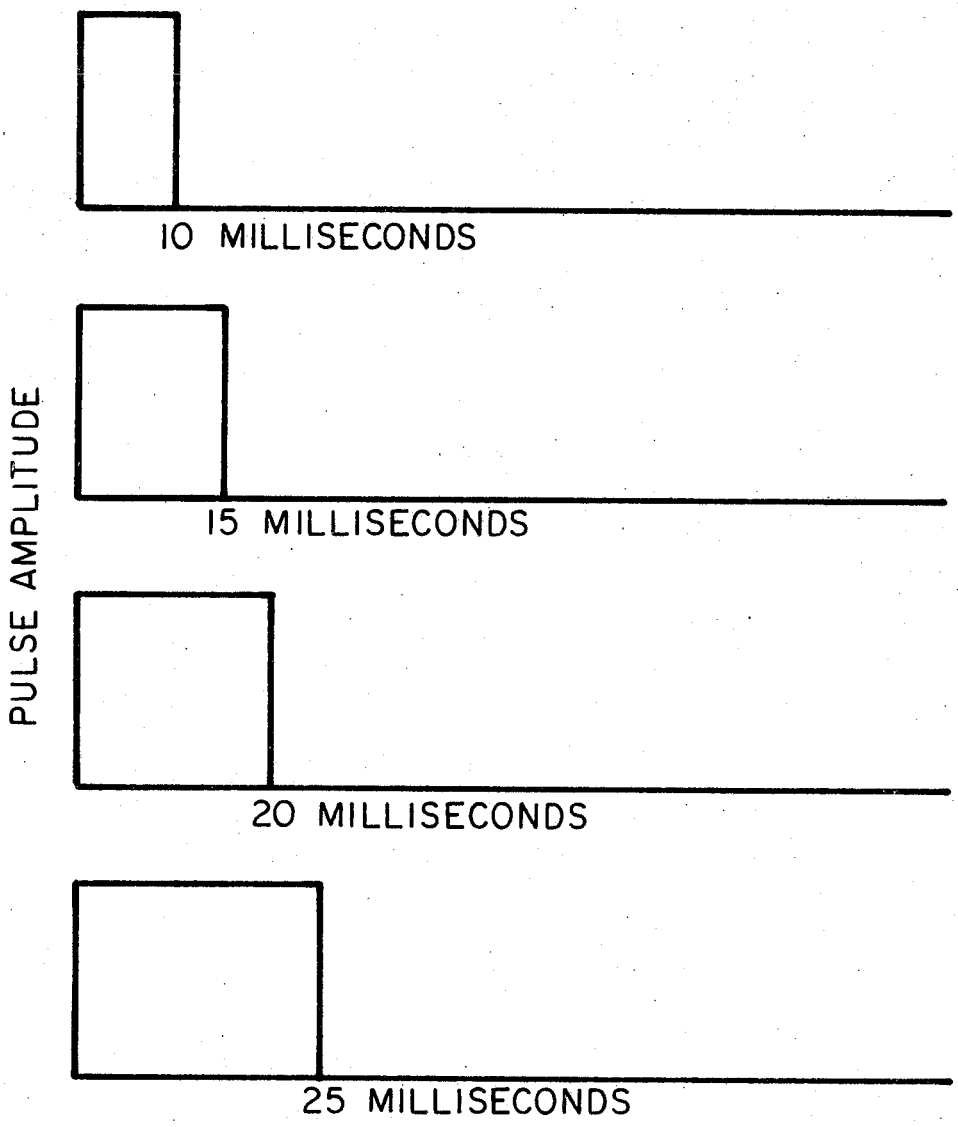

FIGURE 33. INPUT RECTANGULAR PULSE SHAPES TO THE CONTROL SYSTEM

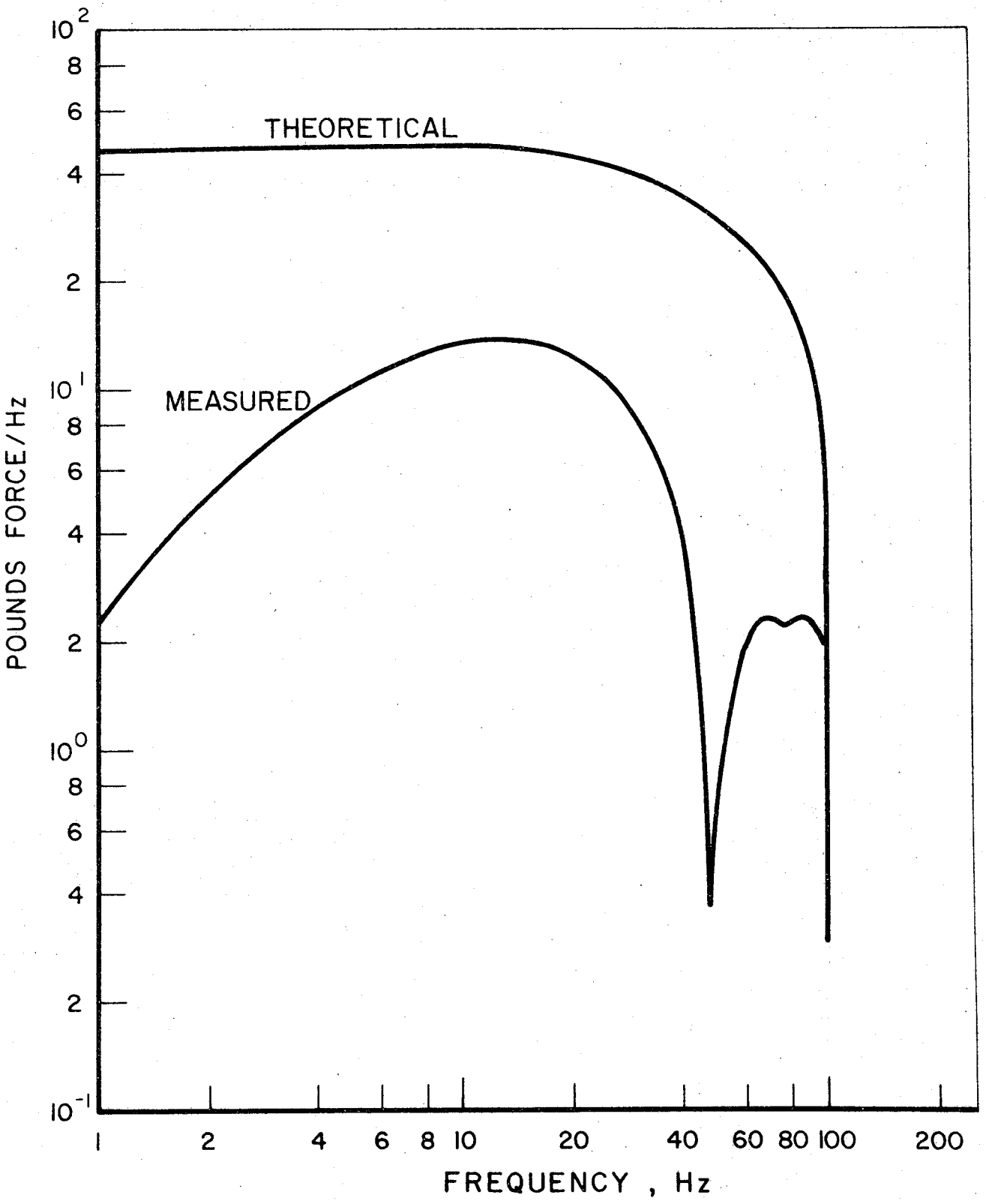

FIGURE 34. THEORETICAL AND MEASURED FREQUENCY CONTENT OF THE 10 MILLISECOND RECTANGULAR PULSE

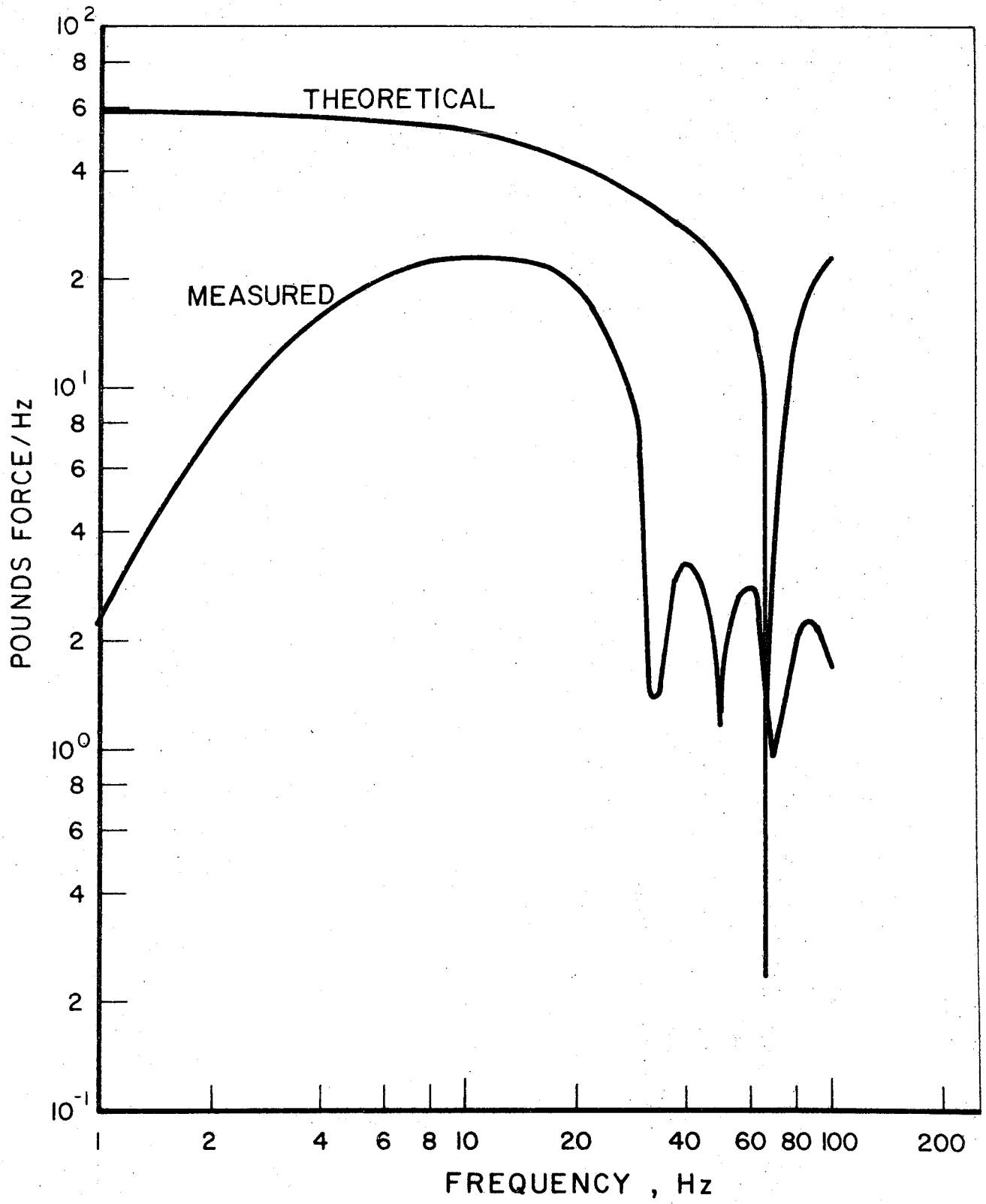

FIGURE 35. THEORETICAL AND MEASURED FREQUENCY CONTENT OF THE 15 MILLISECOND RECTANGULAR PULSE

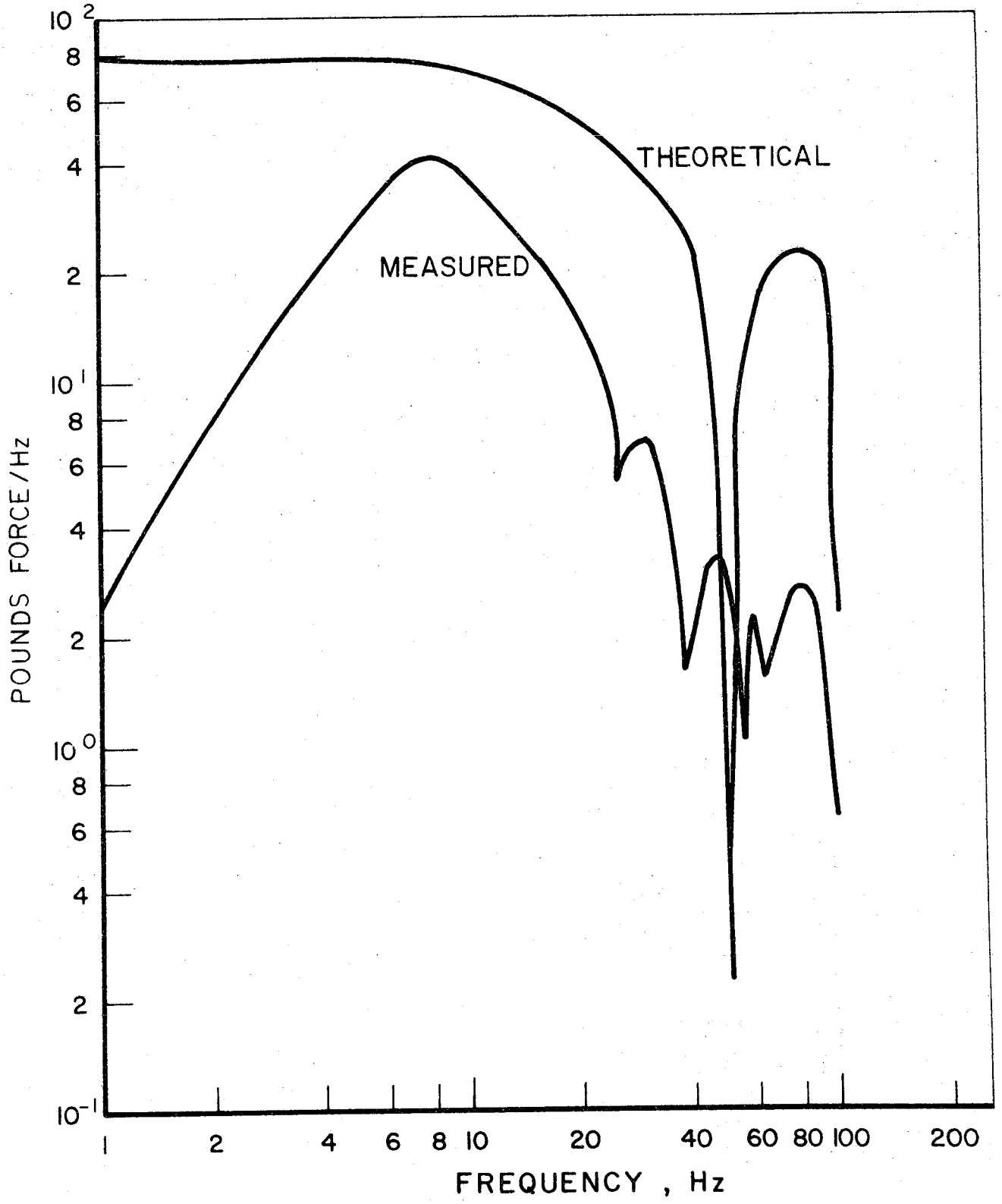

FIGURE 36. THEORETICAL AND MEASURED FREQUENCY CONTENT OF THE 20 MILLISECOND RECTANGULAR PULSE

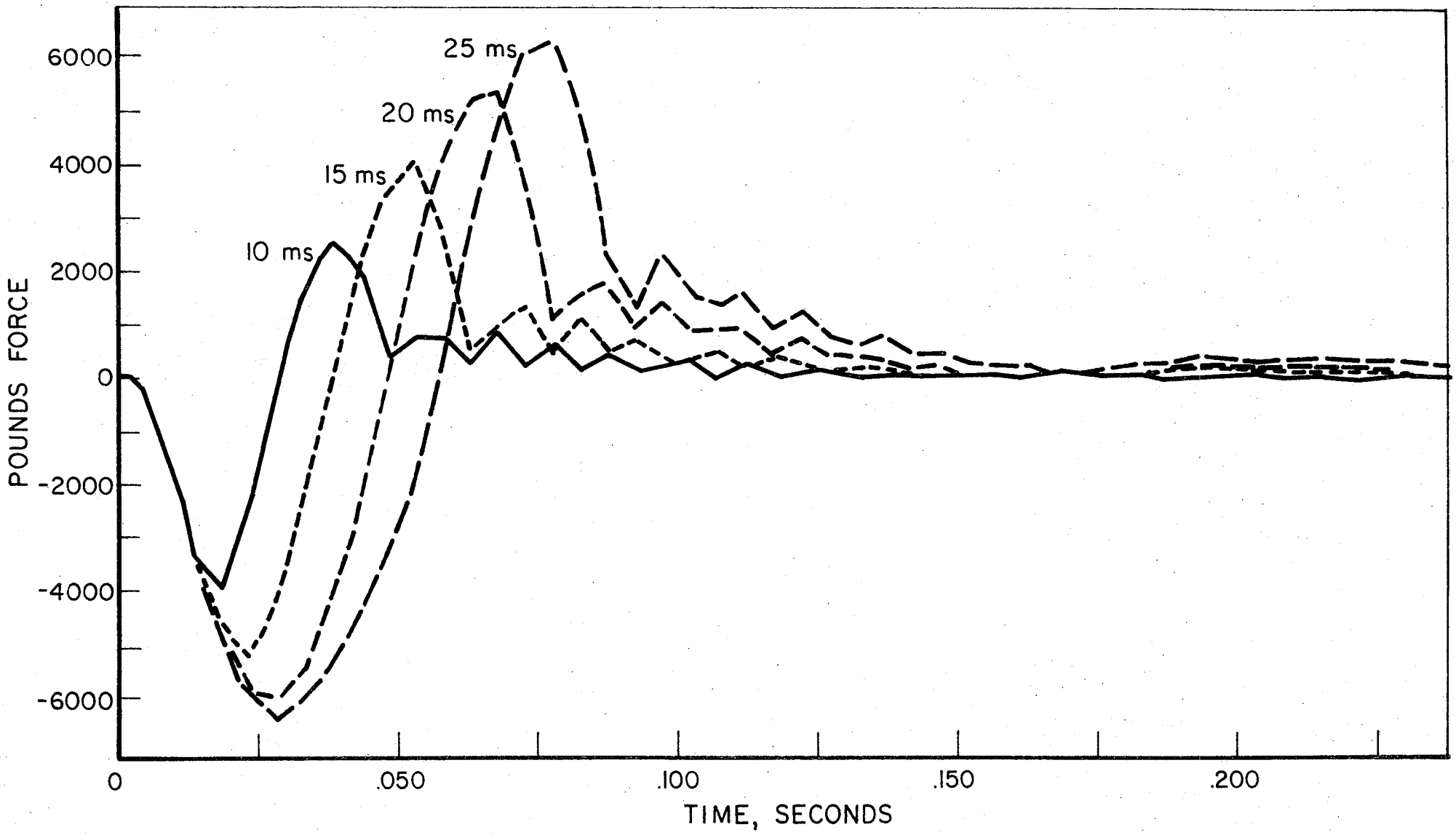

FIGURE 37. MEASURED UNLOADING PULSE INPUT TO THE RAIL STRUCTURE WITH 15,000-LB VERTICAL PRELOAD

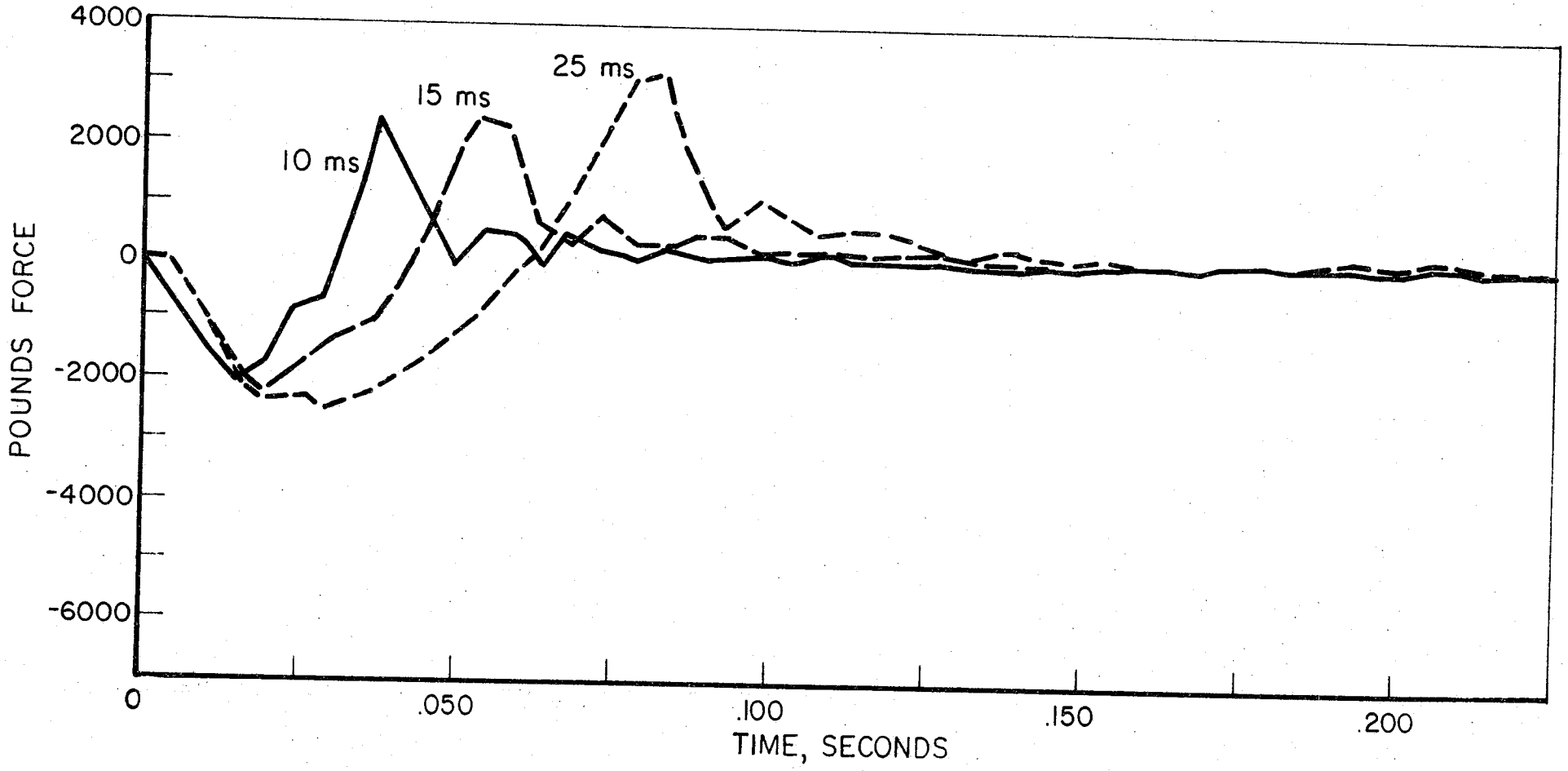

FIGURE 38. MEASURED UNLOADING PULSE INPUT TO THE RAIL STRUCTURE WITH 7,500-LB VERTICAL PRELOAD

An actuator system capable of providing large amplitude force pulses for short duration is needed for these track measurements.

Effect of Pulse Duration

Figure 39 shows vertical track compliance measurements for the four pulse durations with 15,000 lb vertical preload on each rail. These were unloading pulses, i.e., the load was quickly removed first, then reapplied. The figure shows four different vertical compliance plots for the same location and conditions, except that each pulse duration yields different force amplitudes. The input force amplitude increases as the pulse duration increases. Therefore, changing the pulse duration changes both the frequency content and the force level. The 25 millisecond pulse with a 6,200 lb peak force yielded a vertical stiffness of 220,000 lb/in., this increased to 398,000 lb/in. when the force level was reduced by the 10 millisecond pulse. None of these stiffness values is as high as the 500,000 to 600,000 lb/in. vertical stiffness obtained using the sine sweep or the random excitation.

Table 8 summarizes the parameters obtained using variable pulse duration excitation with 15,000 lb constant preload applied. For a linear system, all the stiffnesses and natural frequencies would have been the same, i.e., independent of the pulse amplitude and duration. This change in compliance values is due to the non-linear behavior of the track structure for these large amplitude unloading pulses. The input amplitudes were between 2,000 lb and 6,300 lb compared to a 15,000 lb constant preload.

It was shown previously that for small dynamic force levels, used for sinusoidal and random excitation, this large degree of non-linearity was not observed. This indicates the track structure is very dependent upon the type of loading. Next it will be shown that these compliance values are also a function of the sequence of loading direction, i.e., either loading or unloading.

At Location 2, the results from measurements using a loading pulse were compared to those using an unloading pulse. Figure 40 shows

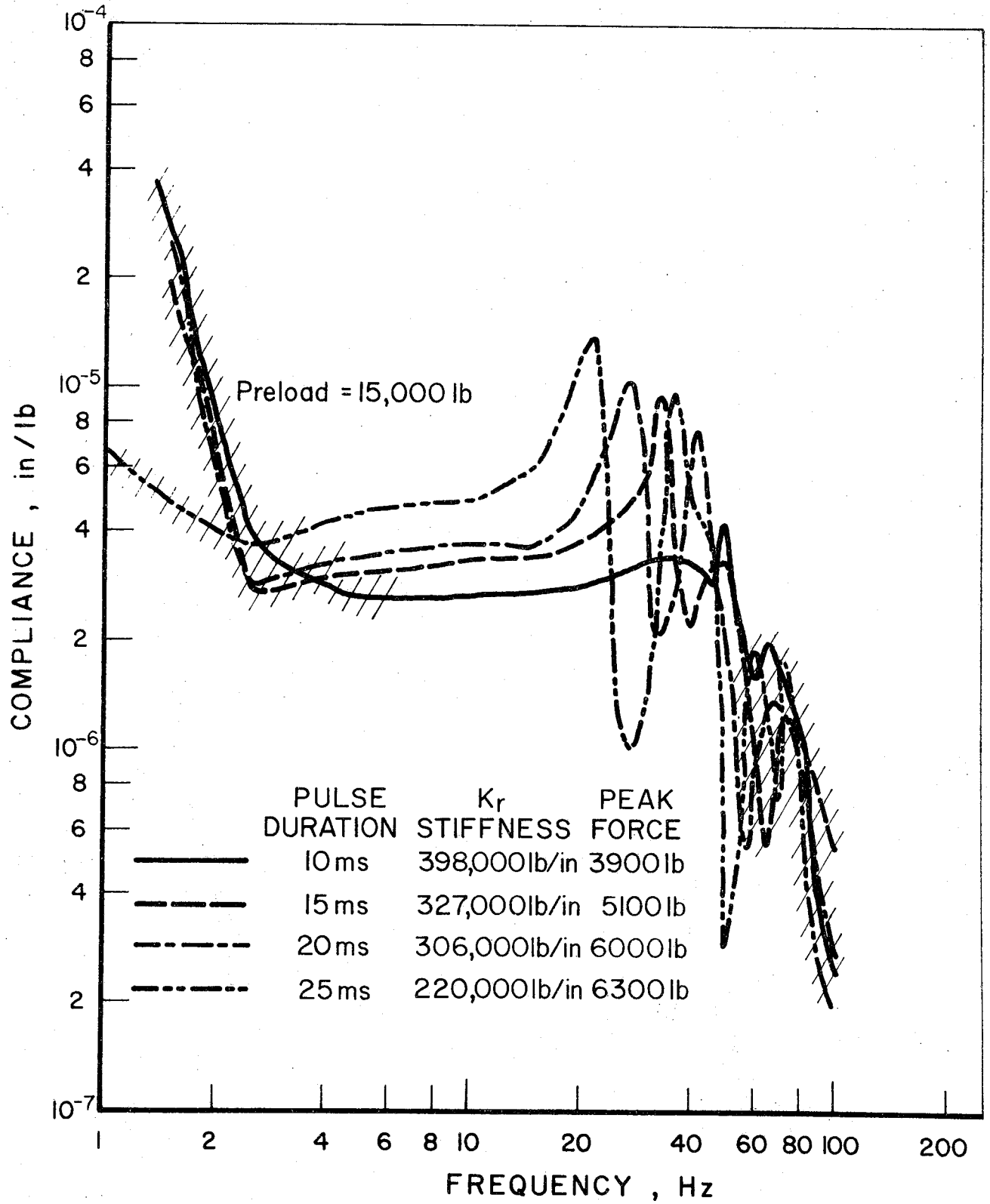

FIGURE 39. TRACK VERTICAL DYNAMIC COMPLIANCE OBTAINED BY USING PULSE EXCITATION AT A FIXED VERTICAL PRELOAD AND VARIABLE PULSE DURATIONS AT LOCATION 1

TABLE 8. SUMMARY OF VERTICAL COMPLIANCE MEASUREMENT USING PULSE EXCITATION WITH 15,000 LB VERTICAL PRELOAD FOR 5 PULSE DURATIONS AT LOCATION 1

Pulse Duration, ms	Peak Amplitude, lb	Dynamic Stiffness K_r, lb/in	Natural Frequency W_n, Hz	Damping , %	Mass M_r, lb
10	3900	398,000	47	31	1760
15	5100	327,000	34	16	2765
20	6000	306,000	28	16	3816
25	6300	220,000	20	15	5378

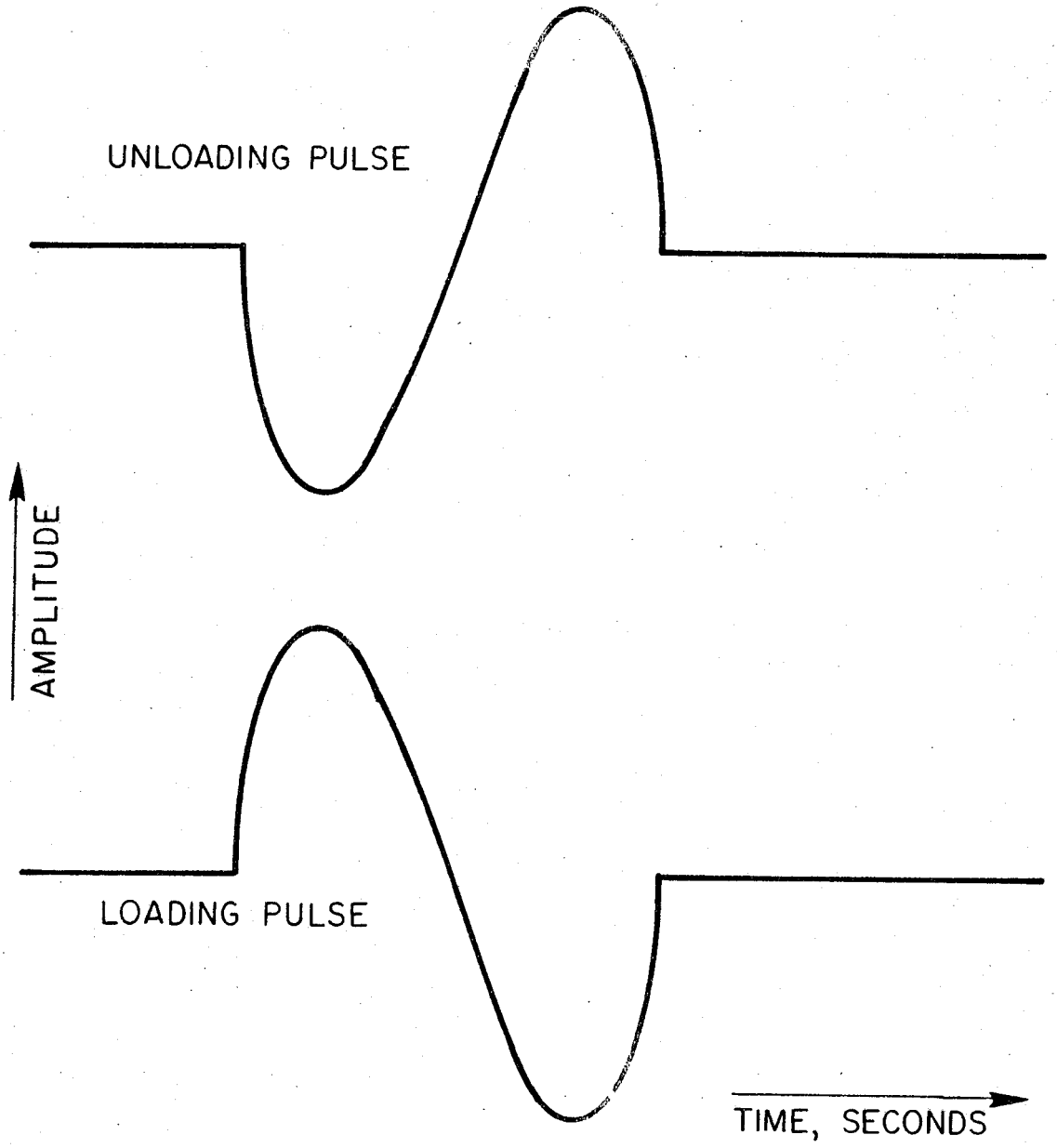

FIGURE 40. COMPARISON BETWEEN AN UNLOADING AND A LOADING PULSE SHAPE

the difference between the loading and the unloading pulses. A preload was applied to both rails, and excitation was applied to one rail. Figure 41 shows the difference between the loading and unloading compliance functions. Both pulses were 2,500 lb vertical preload nad both were 20 milliseconds in duration. The major difference was the sequencing of the compression and tension load and the magnitude; a 1,000 lb unloading pulse compared to a 2,000 lb loading pulse. The unloading pulse yielded a stiffness of 71,500 lb/in. while the loading pulse gave 167,000 lb/in. vertical stiffness. This demonstrates that pulse direction sequence is also a factor in the compliance function. Table 9 summarizes the parameters from the loading and unloading compliance plot.

Effect of Preload

A 25 millisecond pulse duration was used with an unloading pulse, and the preload was varied to obtain Figure 42. These track compliance measurements at Location 1 demonstrate the effect of preload and pulse amplitude using pulse excitation. For a 2,500 lb preload, the vertical stiffness obtained was 19,000 lb/in., and this is in good agreement with the results from the sine and random excitations, see Figure 43. The 7,500 lb preload gave a 55,000 lb/in. vertical stiffness, which is low compared with the other two methods of excitation. Preloading the rail to 15,000 lb yielded a vertical stiffness lf 213,000 lb/in., which is more than a factor of 2 less stiff than the random excitation. Table 10 summarizes the effect of preload on the dynamic compliance values using pulse excitation.

Figure 44 shows the effect of preload at Location 2 using the loading pulse on the east rail. The 15,000 lb vertical preload yielded a stiffness of 370,000 lb/in., which is similar in stiffness to that obtained using random excitation at Location 2. (Table 5)

Tables 11 and 12 give a summary of vertical compliance parameters measured at Locations 1 and 2 comparing all three dynamic methods of excitation. Figure 45 shows the (Table 12) stiffness values at Location 2 as a function of preload. The loading pulse gives consistently higher values of stiffness, whereas the stiffness for the unloading pulse was consistently

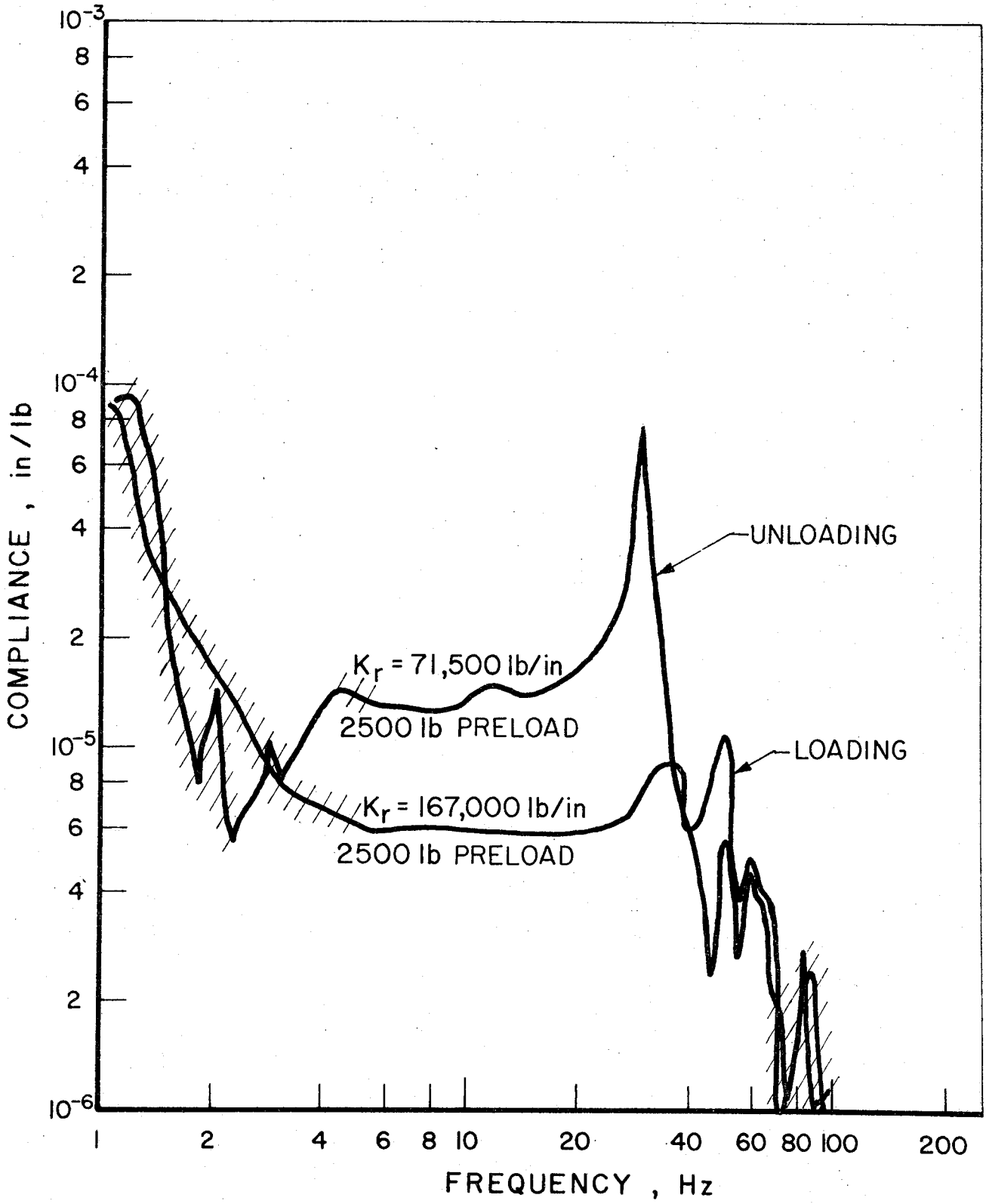

FIGURE 41. TRACK VERTICAL DYNAMIC COMPLIANCE OBTAINED BY USING A LOADING PULSE AND AN UNLOADING PULSE AT LOCATION 2

TABLE 9. SUMMARY OF VERTICAL COMPLIANCE PARAMETERS COMPARING LOADING PULSE AGAINST AN UNLOADING PULSE AT LOCATION 2 OF 20 ms DURATION

	Vertical Stiffness K_r, lb/in.	Natural Frequency W_n, Hz	Damping, %	Mass M_r, lb
1000 lb Unloading Pulse	71,500	30	9	776
2000 lb Loading Pulse	167,000	35	32	1333

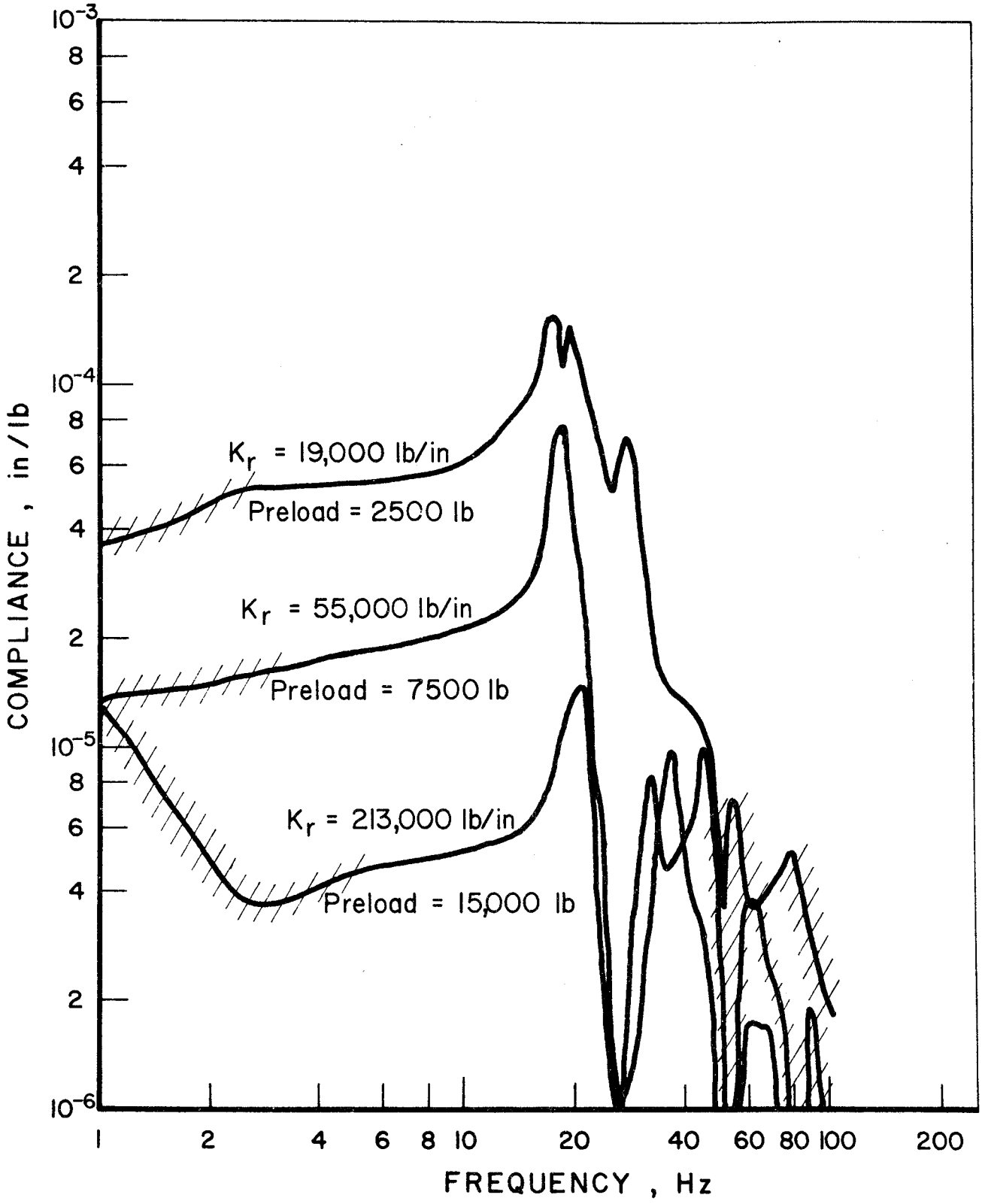

FIGURE 42. TRACK VERTICAL DYNAMIC COMPLIANCE OBTAINED BY USING A 25 MILLISECOND UNLOADING PULSE FOR THREE PRELOADS AT LOCATION 1

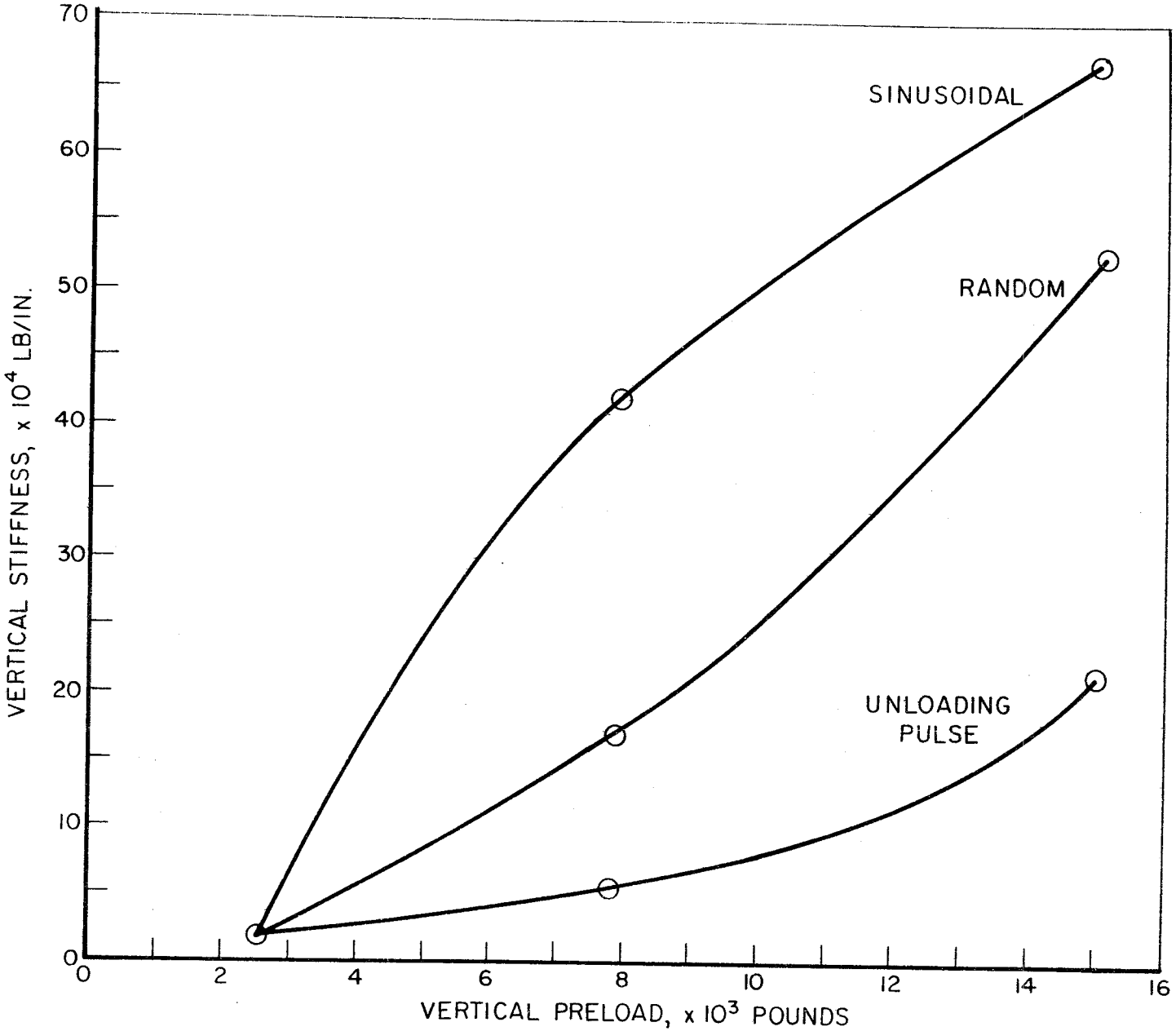

FIGURE 43. TRACK VERTICAL DYNAMIC STIFFNESS AT LOCATION 1 USING THREE METHODS OF EXCITATION

TABLE 10. SUMMARY OF VERTICAL COMPLIANCE MEASUREMENTS USING UNLOADING PULSE EXCITATION AT LOCATION 1

Vertical Preload, lb	Vertical Stiffness K_r, lb/in	Natural Frequency W_n, Hz	Damping , %	Mass M_n, lb
2500	19,000	18.0	18	573
7500	55,000	18.5	11	1571
15,000	213,000	21.0	31	4722

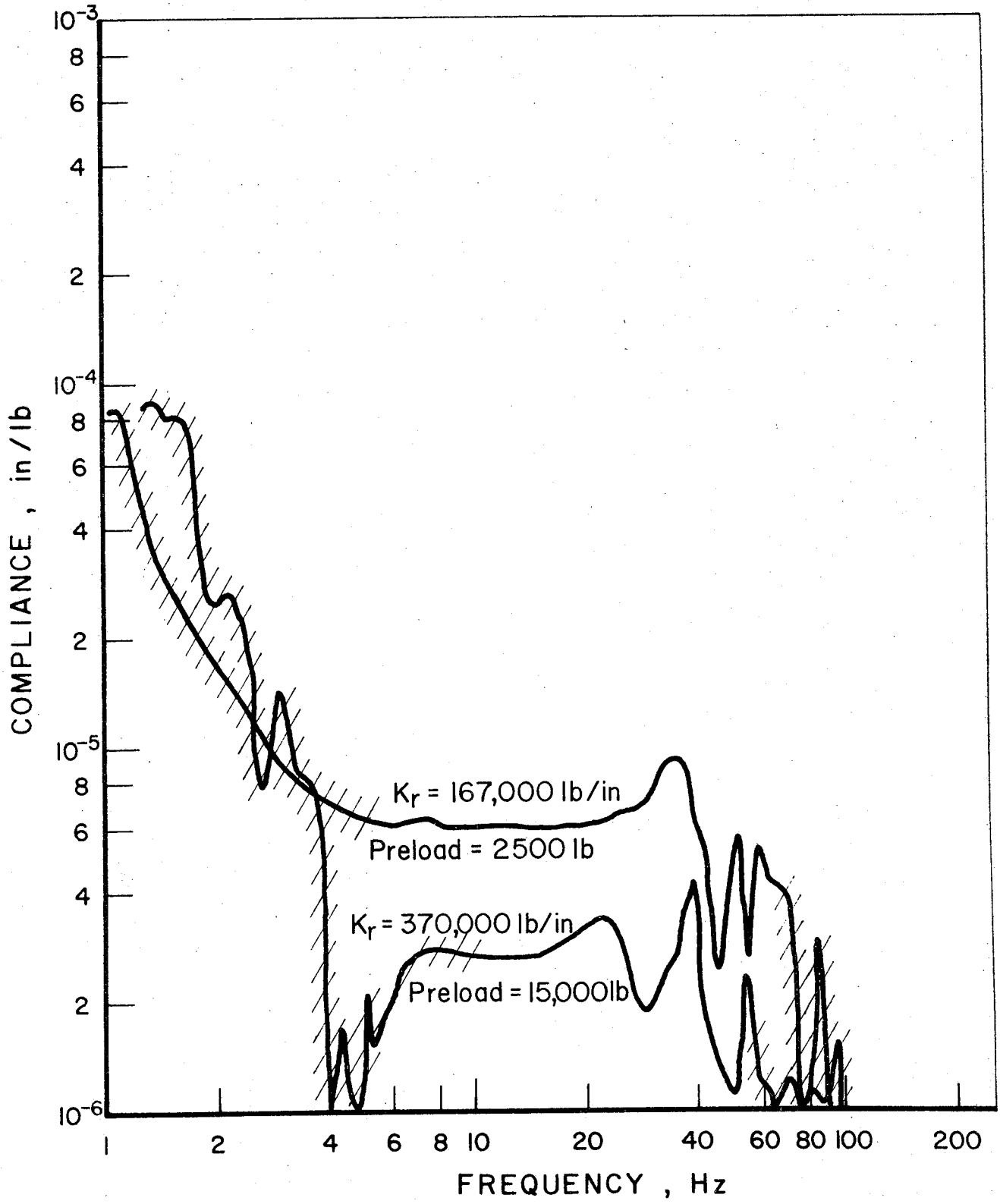

FIGURE 44. TRACK VERTICAL DYNAMIC COMPLIANCE OBTAINED BY USING A LOADING PULSE FOR TWO DIFFERENT PRELOADS AT LOCATION 2

TABLE 11. SUMMARY OF VERTICAL COMPLIANCE CHARACTERISTICS MEASURED AT LOCATION 1 USING THREE METHODS OF EXCITATION

Vertical Preload, lb	Sine	Pulse	Random
2500	K_r = 17,000 lb/in	19,000 lb/in	15,000 lb/in
	ω_n = 18 Hz	18 Hz	17.5 Hz
	ζ = 18 percent	18 percent	24 percent
	M_r = 510 lb	520 lb	480 lb
7500	K_r = 400,000 lb/in	55,000 lb/in	160,000 lb/in
	ω_n = 35 Hz	18.5 Hz	42 Hz
	ζ = 35 percent	11 percent	46 percent
	M_r = 3200 lb	1570 lb	880 lb
15,000	K_r = 670,000 lb/in	213,000 lb/in	526,000 lb/in
	ω_n = 37 Hz	21 Hz	36.5 Hz
	ζ = 30 percent	31 percent	39 percent
	M_r = 4780 lb	4720 lb	3860 lb

TABLE 12. SUMMARY OF VERTICAL COMPLIANCE CHARACTERISTICS MEASURED AT LOCATION 2 USING TWO METHODS OF EXCITATION

Vertical Preload, lb	Loading Pulse (2000 lb)	Random
2500	K_r = 167,700 lb/in	K_r = 33,000 lb/in
	ω_n = 30 Hz	ω_n = 23 Hz
	ζ = 32 percent	ζ = 28 percent
	M_r = 1810 lb	M_r = 610 lb
7500		K_r = 154,000 lb/in
		ω_n = 25 Hz
		ζ = 50 percent
		M_r = 2400 lb/in
15,000	K_r = 370,000 lb/in	K_r = 313,000 lb/in
	ω_n = 40 Hz	ω_n = 25 Hz
	ζ = 31 percent	ζ = 45 percent
	M = 2261 lb	M_r = 4896 lb

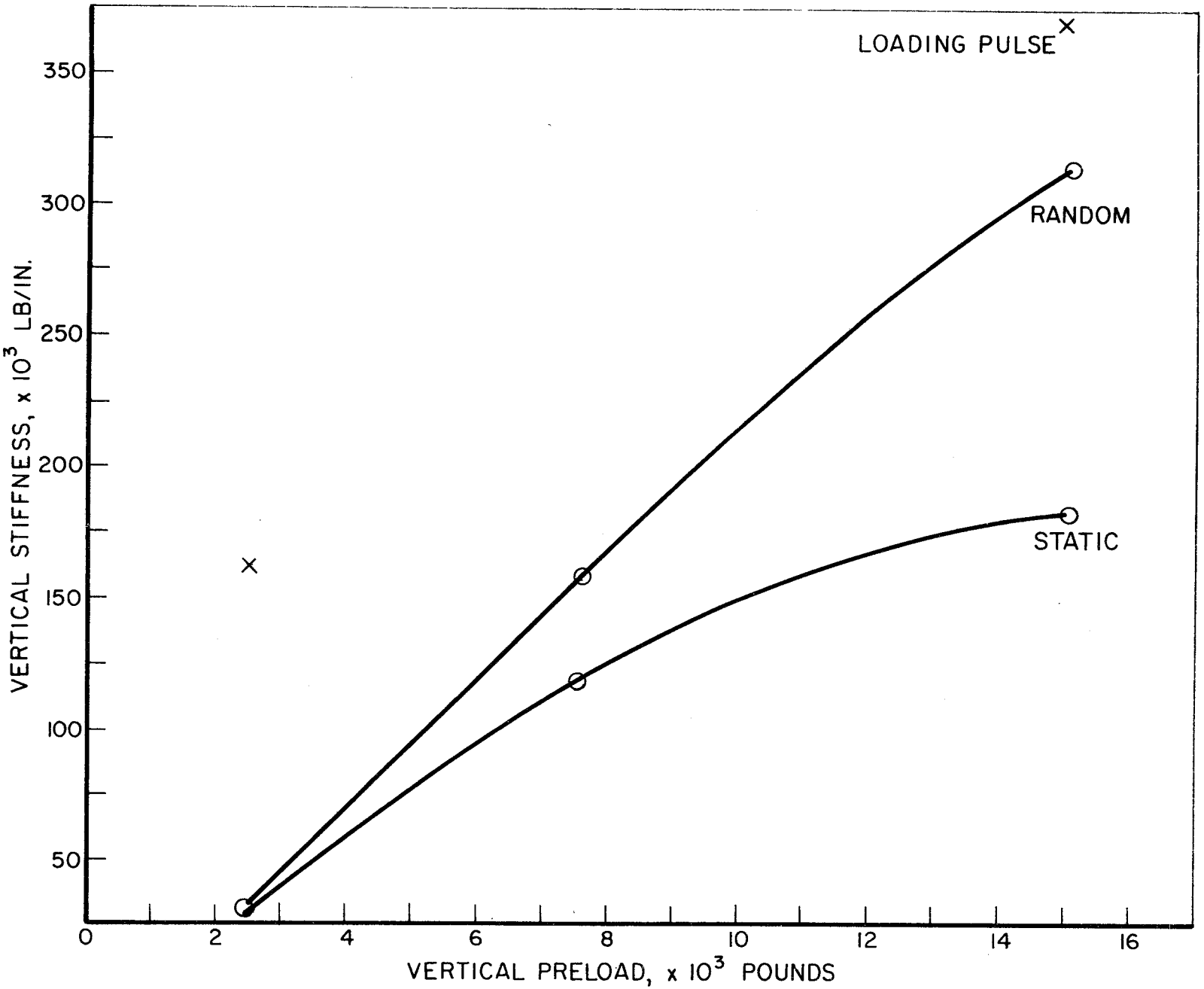

FIGURE 45. TRACK VERTICAL DYNAMIC STIFFNESS AT LOCATION 2 FOR TWO METHODS OF DYNAMIC EXCITATION

lower than that for random excitation, as shown in Figure 43.

Pulse Excitation at Location 3 in the Vertical Direction

Previously shown were compliance data taken using random excitation, and the phase the coherence were plotted and in addition to power spectrum of the input. Data in Figure 46 was obtained using pulse excitation. The pulse is a loading pulse at Location 3 for 2,500 lb vertical preload. Figure 47 is the averaged input power spectra of the measured pulse. Also shown in Figure 46 is the phase coherence plot.

Table 13 is a summary of compliance parameters in the vertical direction at Location 3 obtained by using pulse excitation. The stiffness values listed in the table are plotted in Figure 48.

To demonstrate the effect of averaging using pulse excitation, one 2-second sample of 256 Hz data was taken, and then 41 seconds of 256 Hz data was taken and averaged, see Figure 49. The static stiffness is not well defined for the unaveraged data, and the phase angle plot was very poor. It was determined that in the vertical direction under high preloads it was always necessary to average several pulses to get good coherence and phase information.

Pulse Excitation in Lateral Direction

A 20 millisecond loading pulse was used in the lateral direction to measure the lateral track compliance with zero lateral preload. Figure 50 shows lateral compliance plots for 5,000 and 15,000 lb vertical preloads. The stiffnesses obtained were 38,000 lb/in. for the 5,000 lb preload, and 200,000 lb/in. for the 15,000 lb preload. These values are compared in Table 14 and Figure 51 with those obtained using random excitation. The results for the lateral direction using the pulse and random excitation are in closer agreement than they were for the vertical measurements.

Comparison of Track Stiffness from Static and Dynamic Measurements

Track load-deflection curves were plotted by measuring the displacement of the rail using a LVDT or a linear potentiometer. The

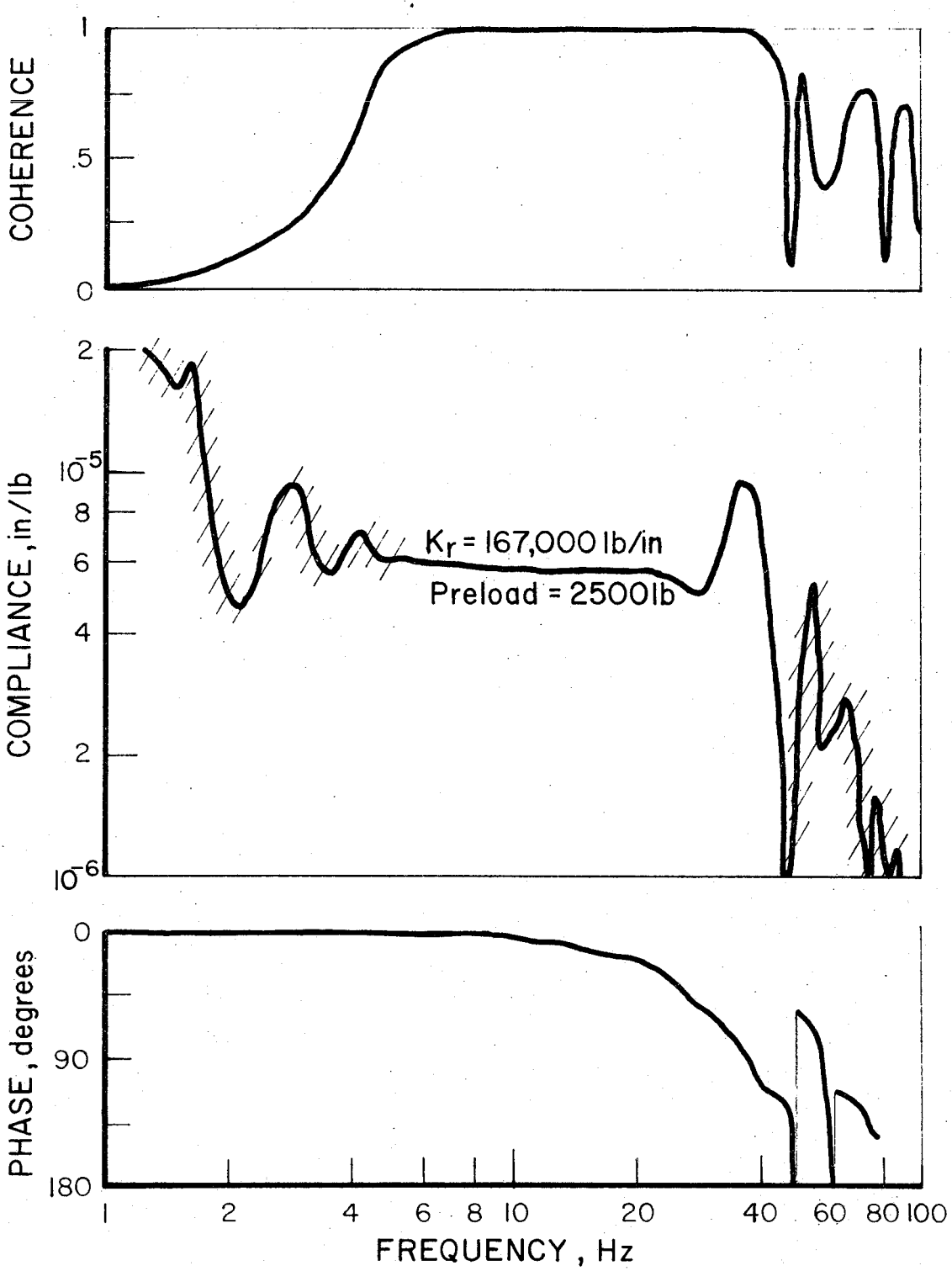

FIGURE 46. TRACK VERTICAL DYNAMIC COMPLIANCE (PHASE AND COHERENCE) OBTAINED BY USING LOADING PULSE EXCITATION WITH A 2500-LB VERTICAL PRELOAD AT LOCATION 3

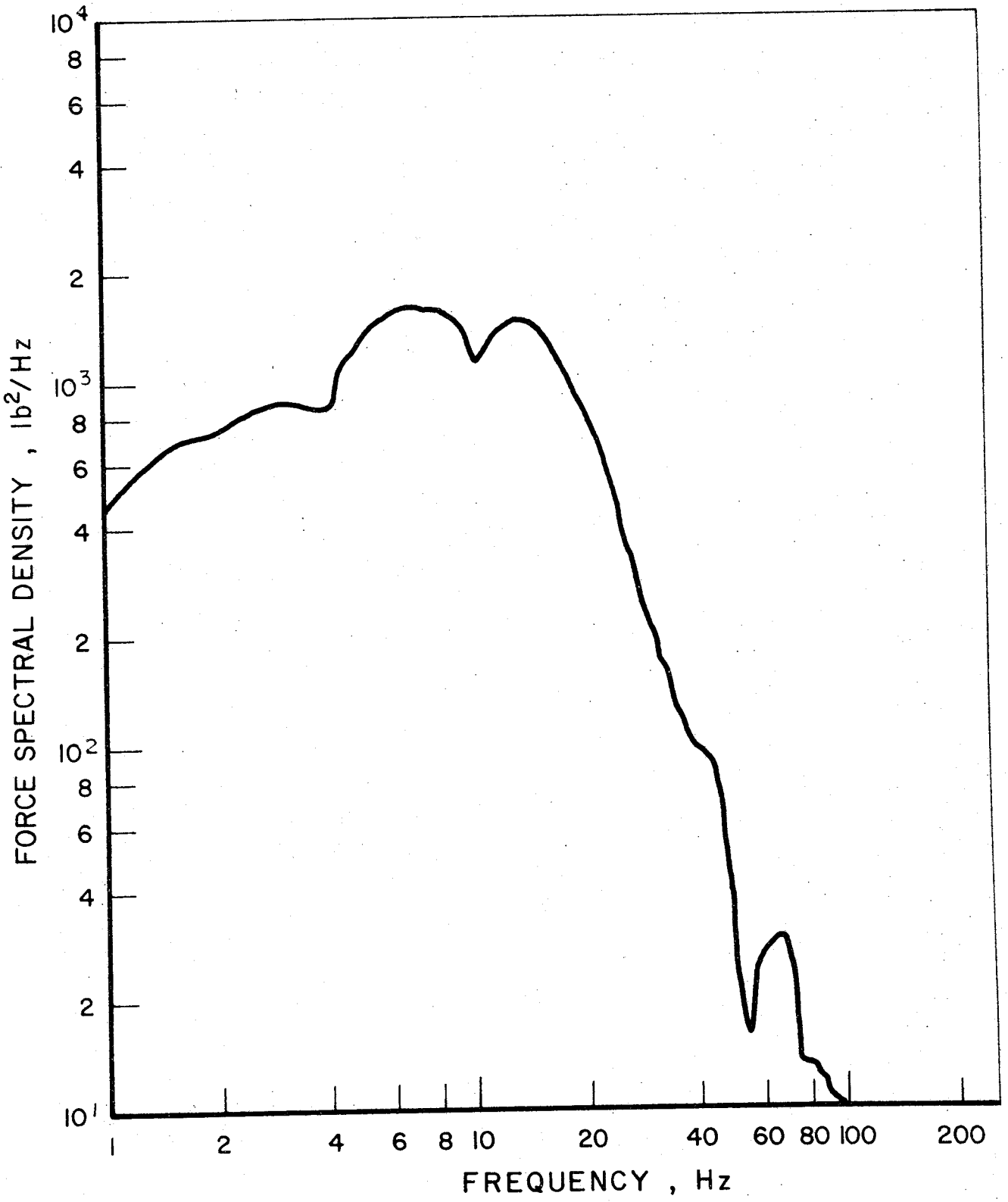

FIGURE 47. AVERAGED FORCE POWER SPECTRAL DENSITY OF THE PULSE EXCITATION AT LOCATION 3

TABLE 13. SUMMARY OF VERTICAL LOADING COMPLIANCE MEASUREMENTS AT LOCATION 3 LOADING USING PULSE EXCITATION (20 ms)

Vertical Preload, lb	Vertical Stiffness K_r, lb/in	Natural Frequency W_n, Hz	Damping Percent Critical, %	Effective Mass M_r, lb
2500	167,000	36	34	1260
7500	351,000	44	38	1770
15,000	500,000	42	45	2910

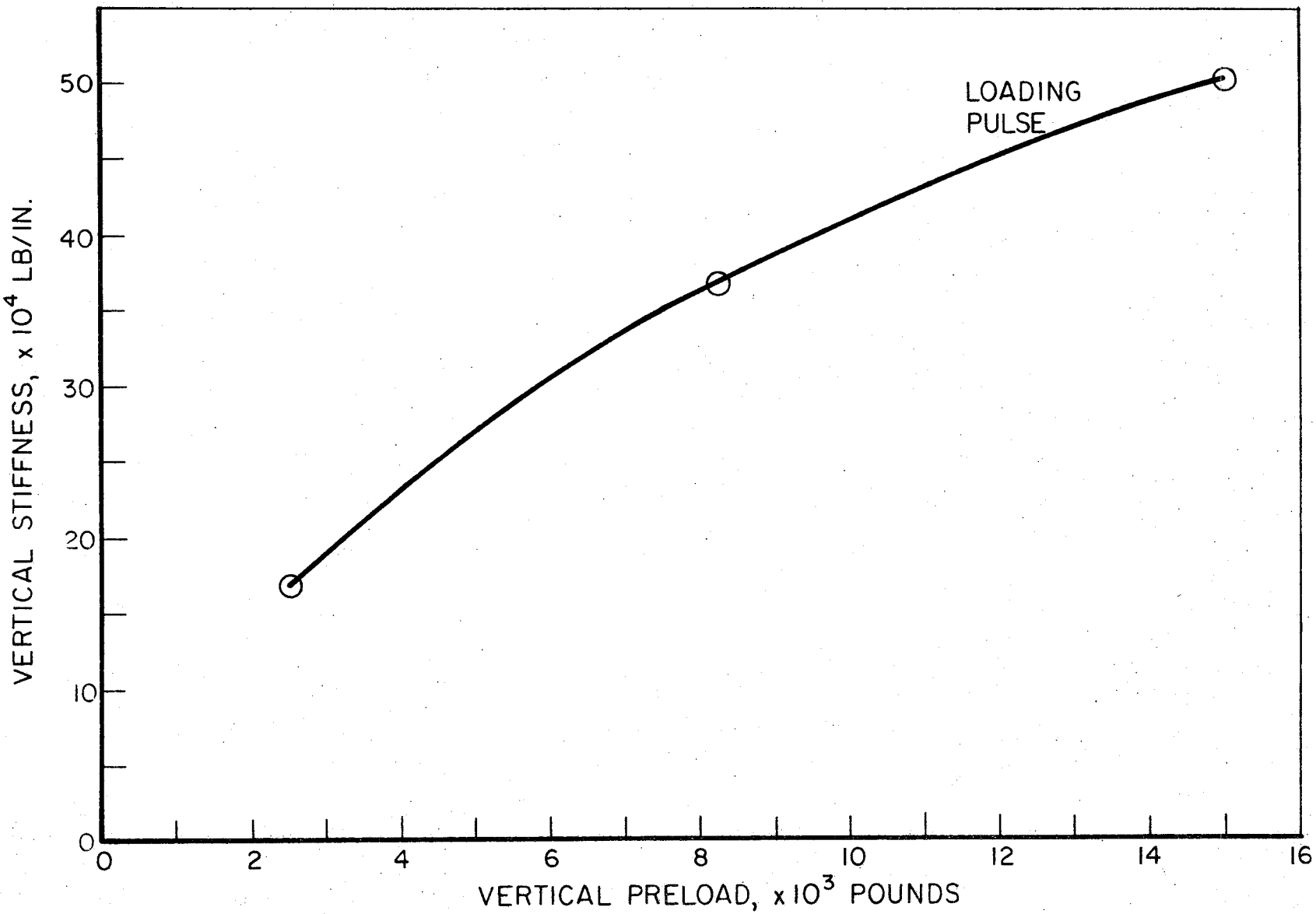

FIGURE 48. TRACK VERTICAL DYNAMIC STIFFNESS AT LOCATION 3 USING A LOADING PULSE

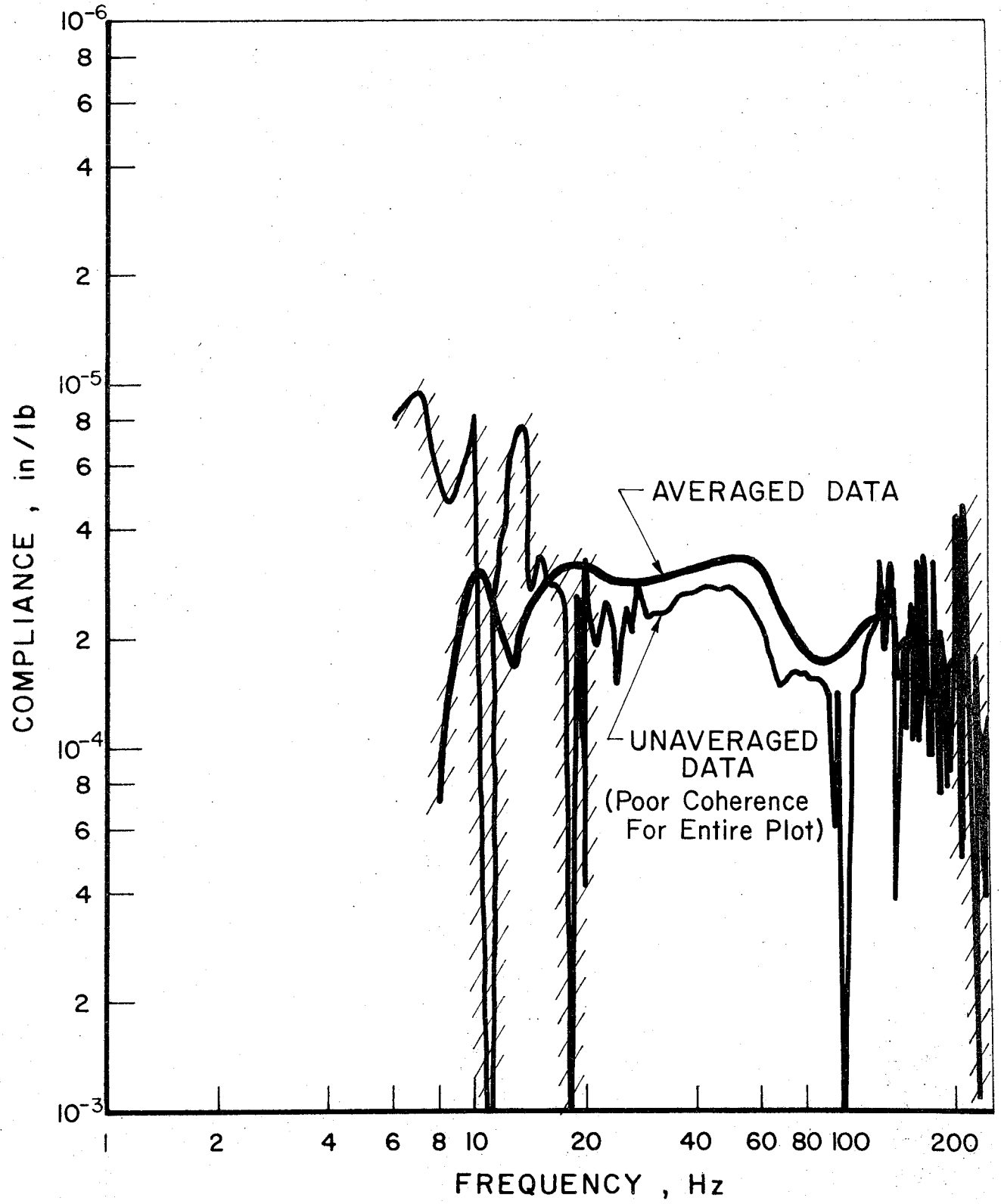

FIGURE 49. TRACK VERTICAL DYNAMIC COMPLIANCE TO DEMONSTRATE THE EFFECT OF AVERAGING USING PULSE EXCITATION WITH 15,000-LB PRELOAD AT LOCATION 1

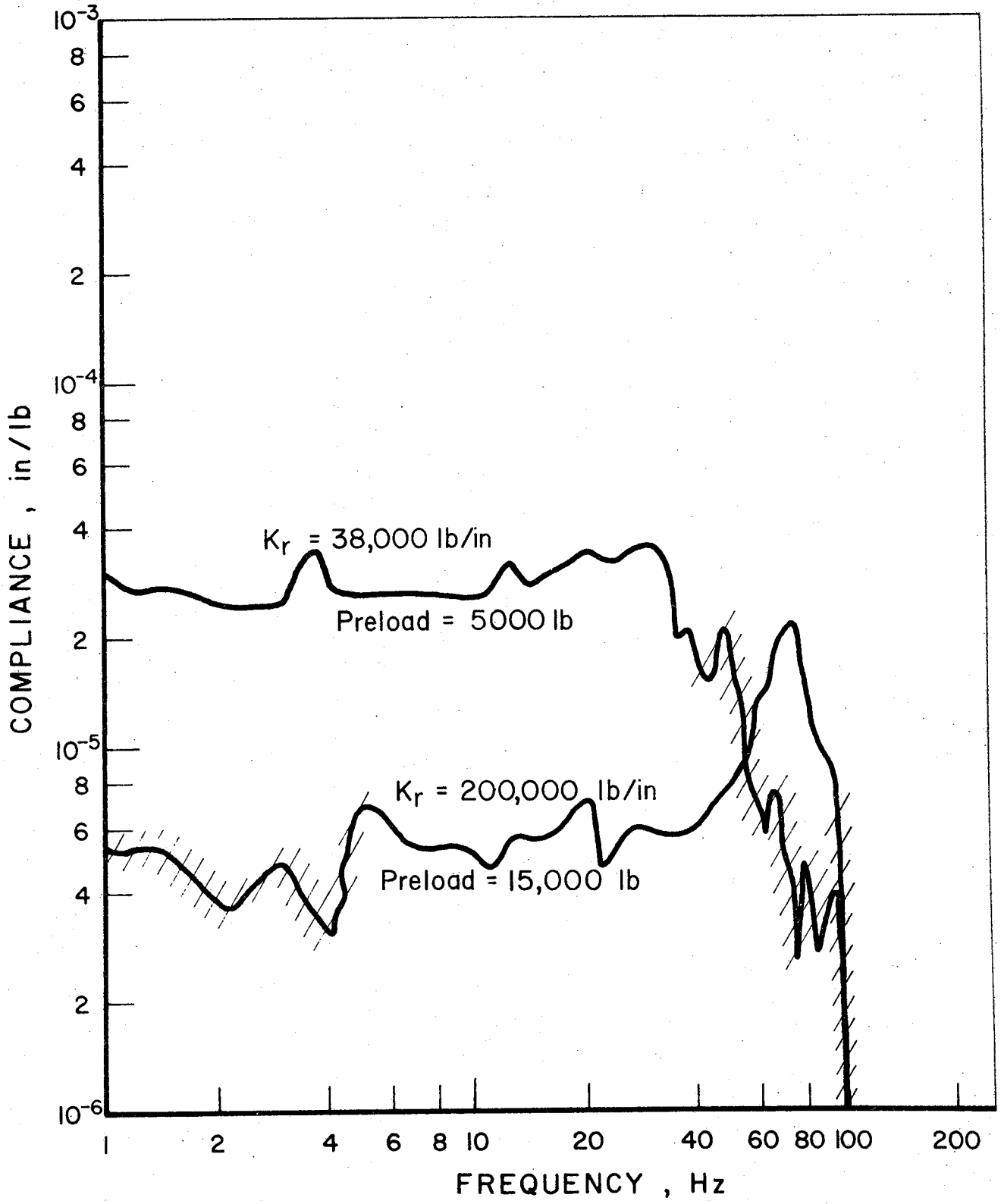

FIGURE 50. TRACK LATERAL DYNAMIC COMPLIANCE OBTAINED BY USING LOADING PULSE EXCITATION AT LOCATION 1

TABLE 14. COMPARISON OF LATERAL COMPLIANCE PARAMETERS OBTAINED USING RANDOM AND PULSE EXCITATION AT LOCATION 1

	Vertical Preload, lb	Lateral Stiffness K_r, lb/in	Natural Frequency W_n, Hz	Damping Percent
Random Excitation	2500	13,000	17.5	45.0
	5000	73,000	50.0	37.0
	15,000	250,000	90.0	31.0
Pulse Excitation	5000	38,000	30.0	37.5
	15,000	200,000	72.0	11.0

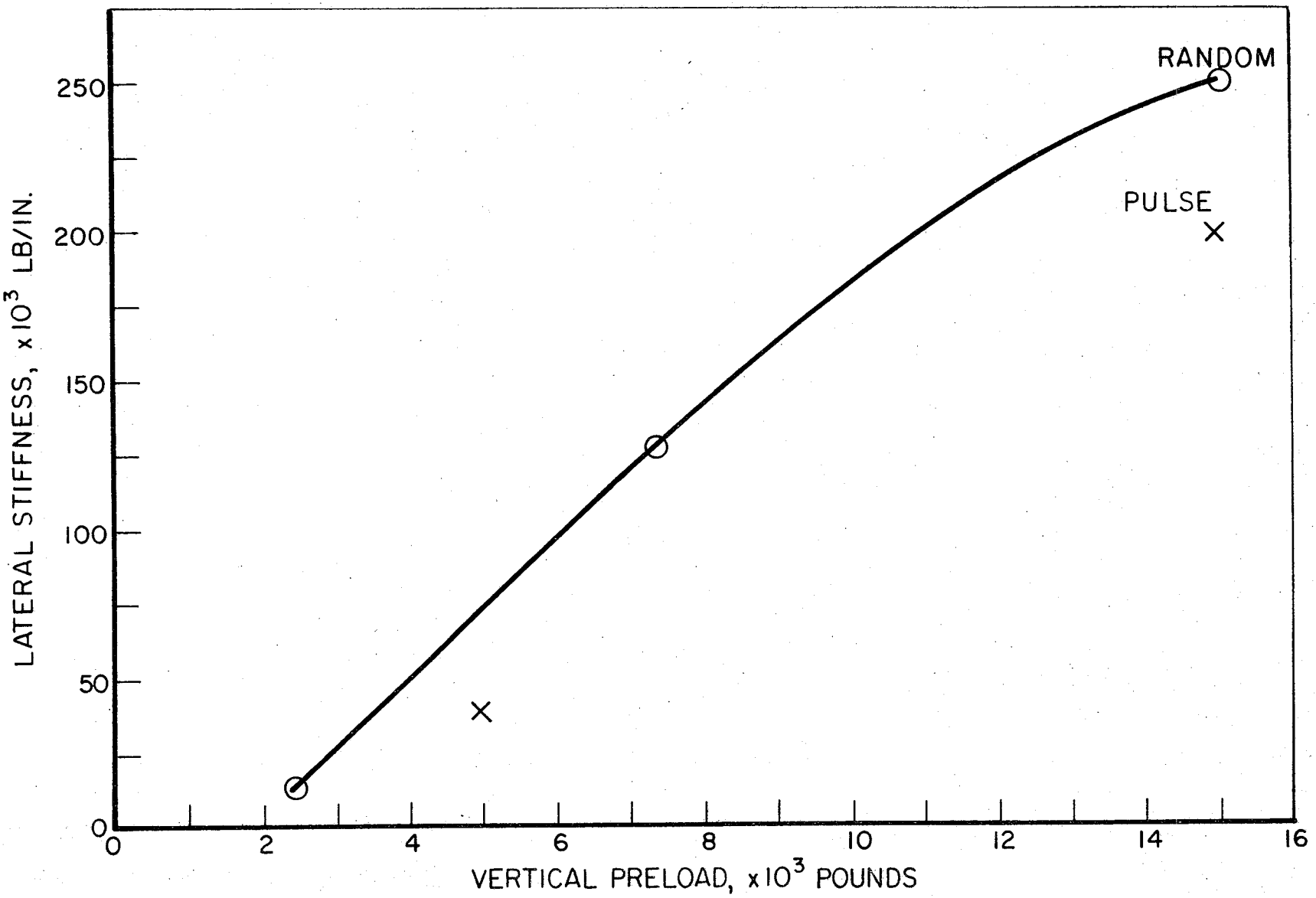

FIGURE 51. TRACK LATERAL DYNAMIC STIFFNESS AT LOCATION 1 FOR TWO METHODS OF EXCITATION

The load was applied by the hydraulic cylinders at a .05 Hz rate for a cyclic loading up to 20,000 lb. This "static" load-deflection measurement was made to compare with the low-frequency portion of the dynamic compliance data. Figure 52 shows a typical vertical load-deflection curve for Location 1.

The tangent stiffness values obtained from the slope of the load-deflection curve at the indicated preload are listed in Table 15. Also listed in this table are the dynamic stiffness values obtained using sine, pulse, and random excitation, and these are also plotted in Figure 53. If the track structure behaved as an ideal, linear system, these low-frequency values of dynamic stiffness would agree with the static stiffness values. However, our results show that the dynamic excitation gives consistently higher values of stiffness.

The mechanism that is causing this discrepancy appears to be a creep or settling of the ballast with the constant preload and repeated dynamic loads. The random excitation dynamic data were taken with a 15,000 lb preload applied throughout the test, which takes up to 4 minutes when averaging. When this load is first applied, the ballast and subgrade begin to creep until some equilibrium condition is reached. This was verified by running a strip chart recording of the displacement of the rail when a constant load is applied. This will cause a stiffening of the track structure due to this compaction. When the static load-deflection curves were made, the load was cycled from zero to about 20,000 lbs each time so the creep or settling phenomeenon didn't occur.

Figure 54 shows vertical-load deflection curves for all three track locations. The stiffness at high preloads is quite similar, but there is considerable difference in the non-linear behavior for low preloads.

Development of a Cyclic Preload/Pulse Excitation Technique

An excitation method was devised using pulse excitation where the preload is cycled from zero up to some value, then back to zero, and a dynamic pulse is superimposed when the preload is a maximum. Figure 55 shows a comparison of the cyclic preload/pulse excitation versus the constant preload. Results from the 20 pulses were averaged for both cases.

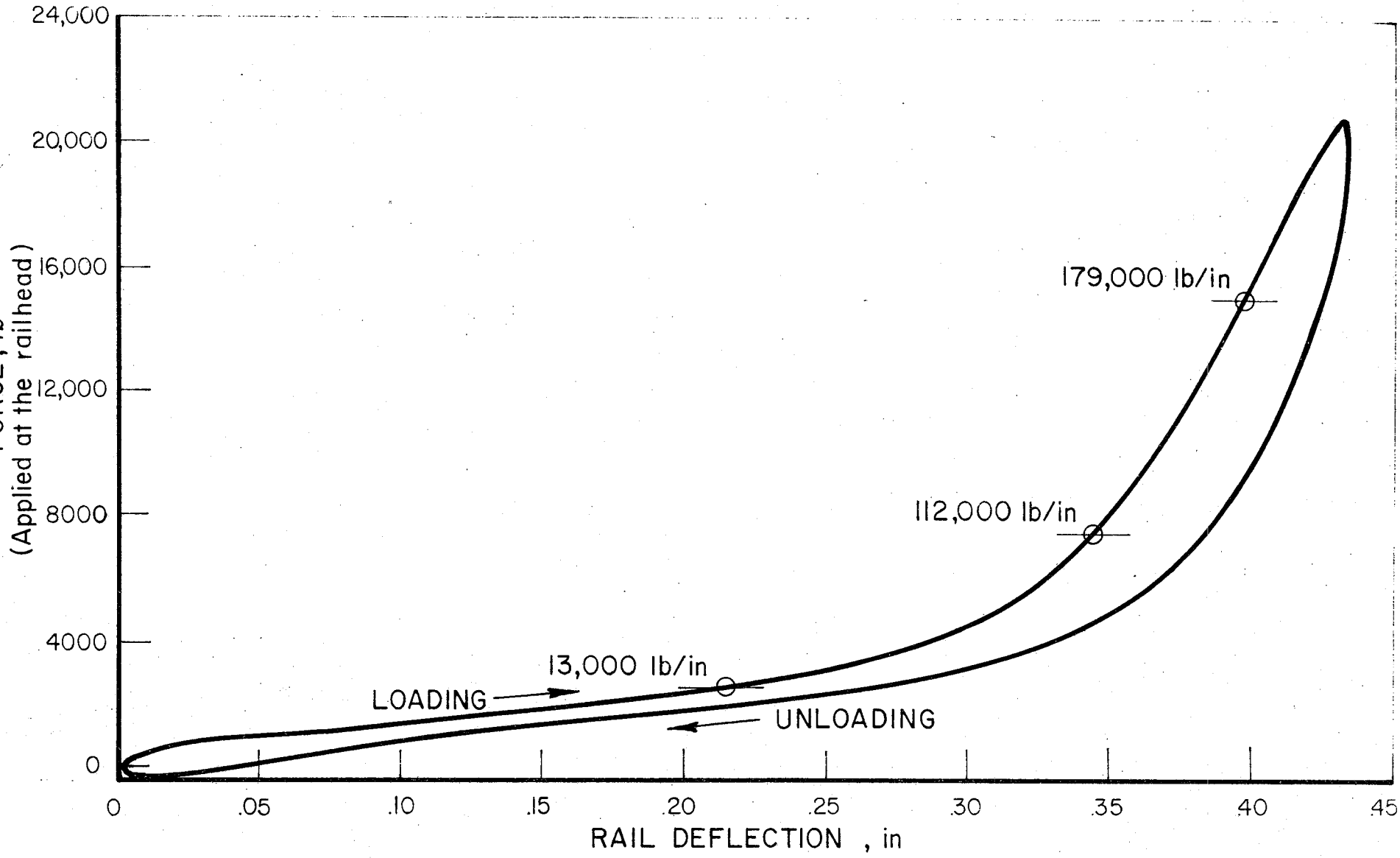

FIGURE 52. VERTICAL LOAD DEFLECTION CURVE FOR LOCATION 2

TABLE 15. SUMMARY OF THE VERTICAL STATIC AND DYNAMIC STIFFNESS DATA OBTAINED AT LOCATION 1

Vertical Preload, lb	Stiffness - Vertical			
		Dynamic		
	Static lb/in	Sine, lb/in	Random, lb/in	Unloading Pulse, lb/in
2500	12,500	17,000	15,000	19,000
5000	75,000	--	--	--
7500	121,000	400,000	160,000	55,000
15,000	180,000	670,000	526,000	213,000

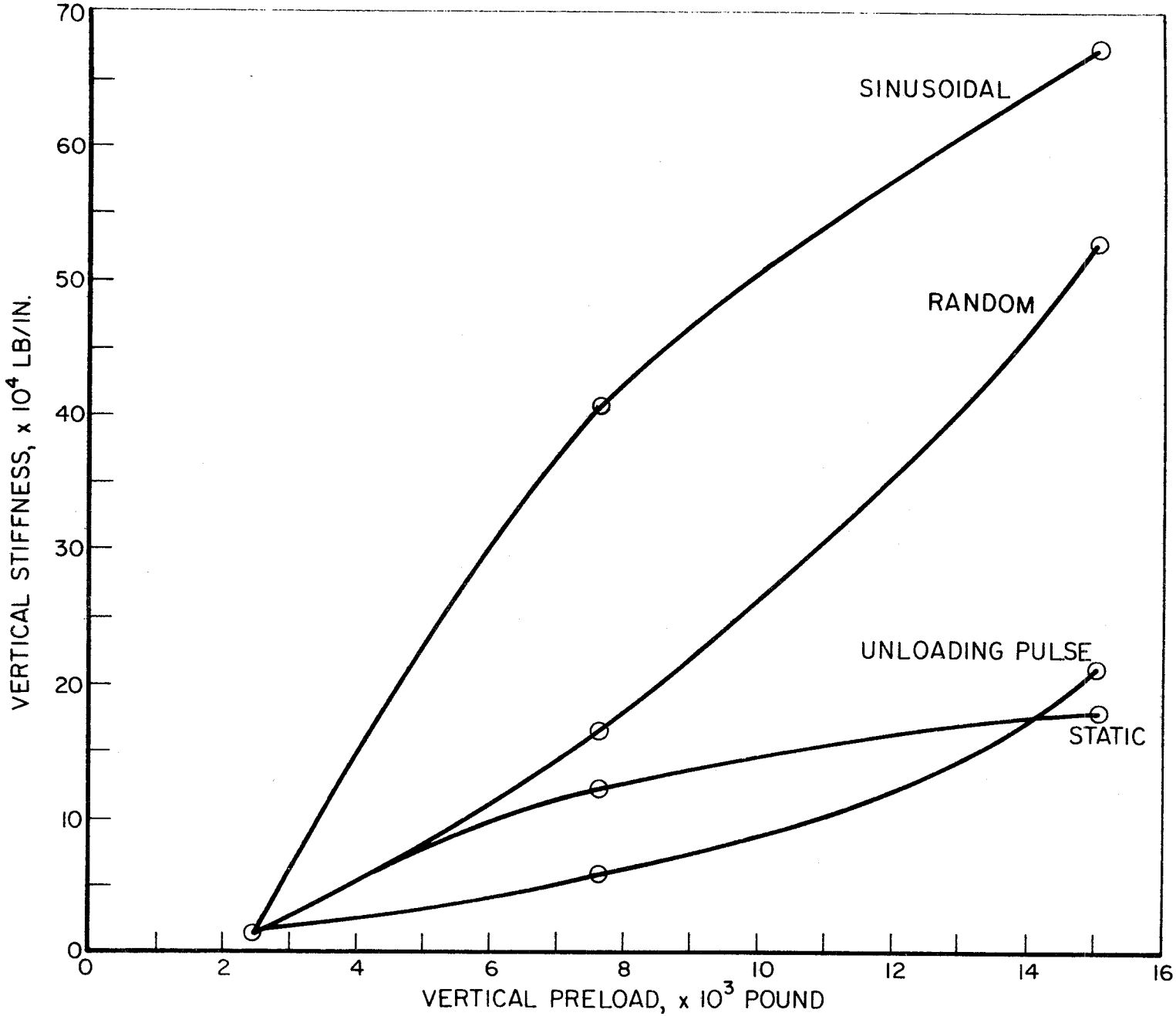

FIGURE 53. TRACK VERTICAL STATIC AND DYNAMIC STIFFNESS AT LOCATION 1

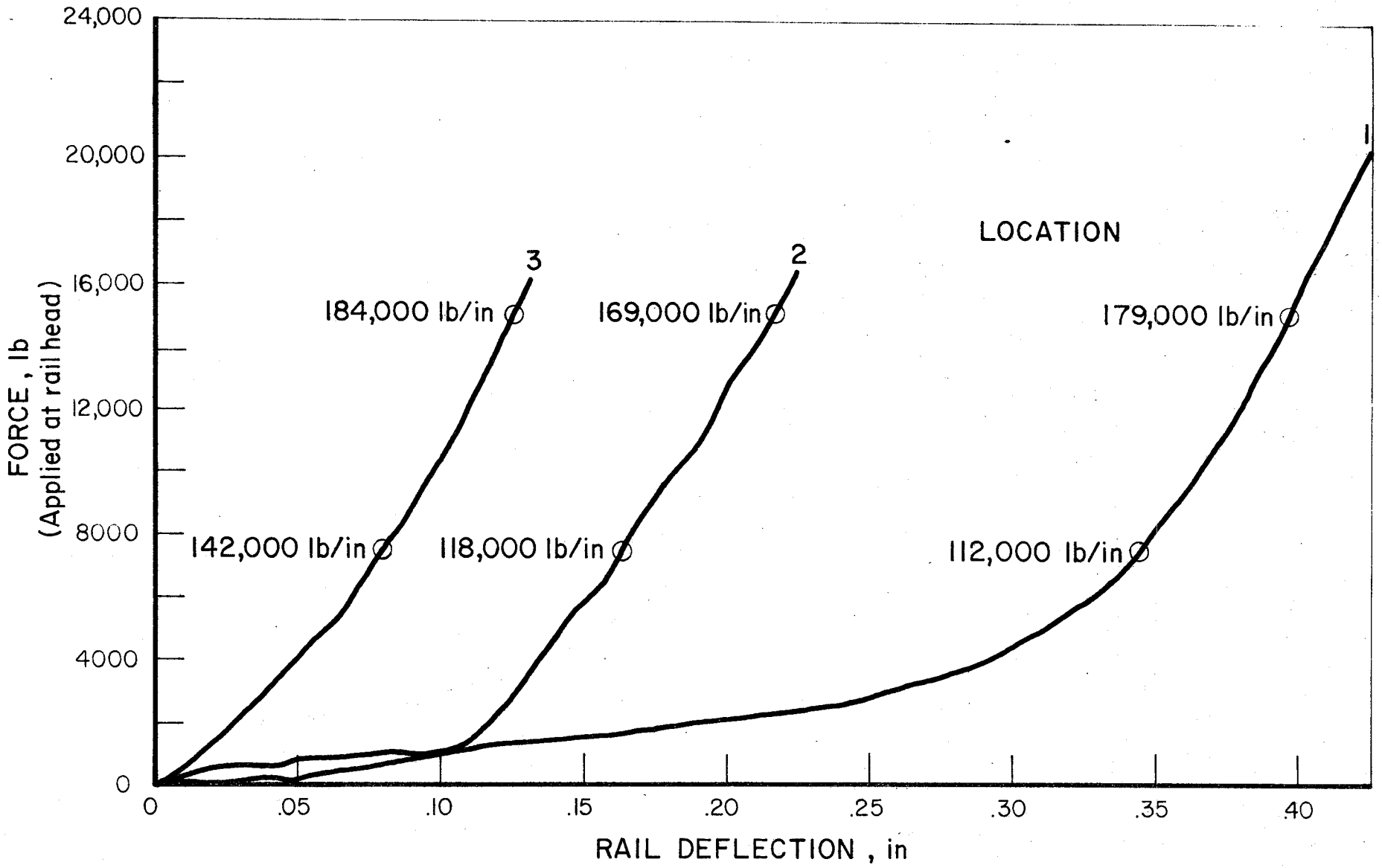

FIGURE 54. VERTICAL LOAD DEFLECTION CURVES FOR THE THREE TEST LOCATIONS

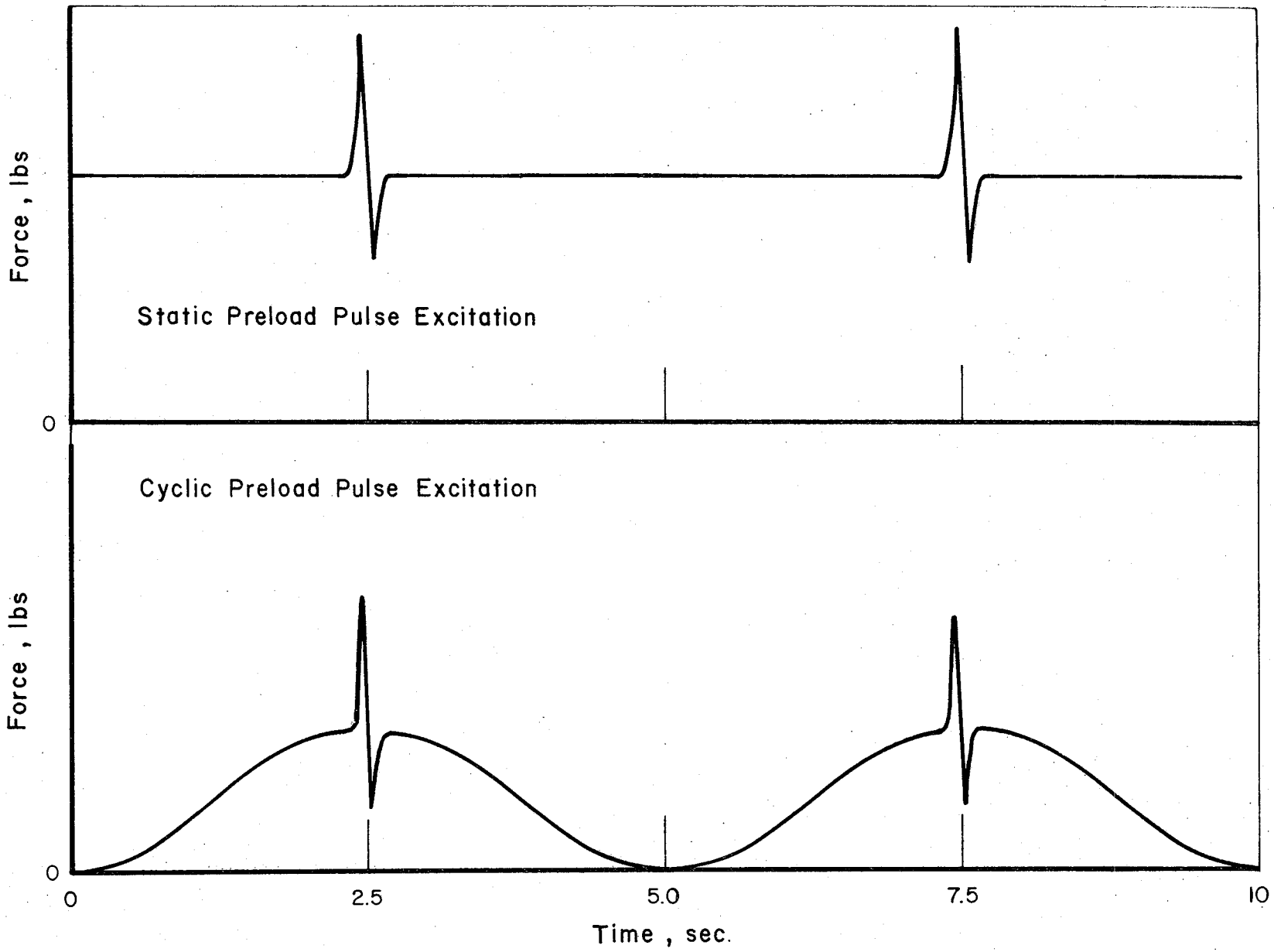

FIGURE 55. COMPARISON BETWEEN TWO METHODS OF EXCITATION, ONE USING A CONSTANT STATIC PRELOAD WITH PULSE EXCITATION, AND THE OTHER USING A CYCLIC PRELOAD WITH PULSE EXCITATION

Figure 56 shows vertical track compliance data for Location 1 using the cyclic preload pulse excitation. The peak preload was 8,000 lb and a loading pulse was superimposed. The stiffness was 170,000 lb/in., which can be compared to the 121,000 lb/in. reported in Table 15. Figure 56 also shows the track compliance for the same location, with a constant preload of 8,000 lb. This vertical compliance measurement shows a stiffness of 300,000 lb/in.

These data show that using a constant preload with repeated dynamic excitation gives higher stiffness values than are measured using a cyclic load. The service loading history of track is also cyclic from the individual truck loads, and the track is completely unloaded between the front and rear trucks of each passing car. Figure 57 is typical data for vertical tie plate load for a 4-car train, Reference 2. This figure shows the tie load is completely removed each loading cycle. Therefore, the stiffness that the wheel of a railroad car sees may be lower than if the track were loaded continuously. However, the cyclic preload/pulse results included in this report do not exactly duplicate the frequency and sequencing of actual track loads, so these are tentative conclusions. This stiffening effect, due to the constant preload and dynamic excitation, did not occur when the ballast was in a frozen condition. The static and the dynamic stiffness values agreed when the temperature measured 3 inches down in the ballast was below 32 F.

Track Lateral Static Stiffness at Location 1

Figure 58 shows a static (.05 Hz) load-deflection curve in the lateral direction with 15,000 lb vertical preload. Two distinct regions of stiffness are evident. The initial slope of 273,000 lb/in. extends up to approximately 1,500 lb applied load. Beyond this region, the stiffness drops to 102,000 lb/in., and it appears that the rail begins to slide on the tie. In this instance, the rail moved .080 inches laterally.

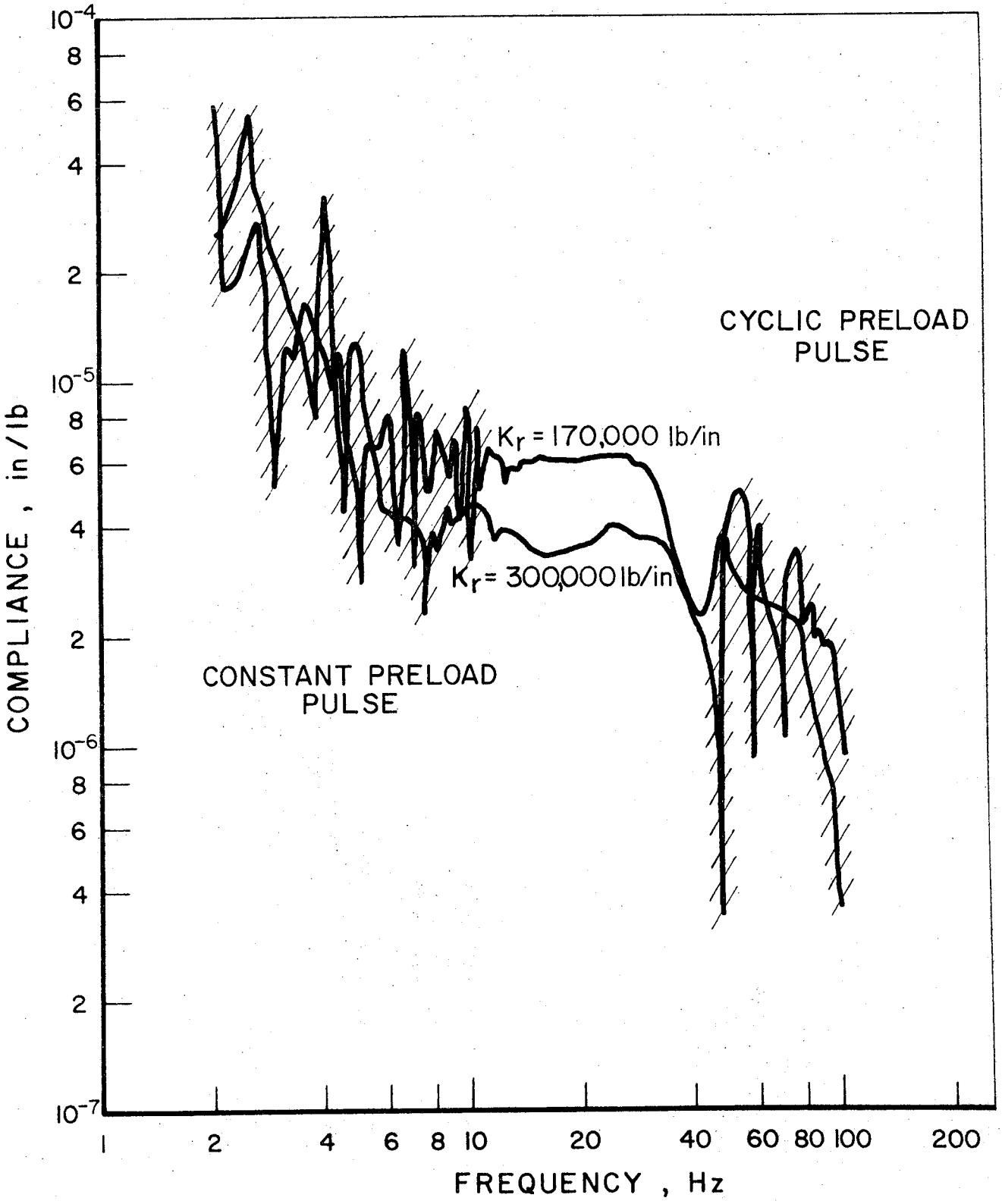

FIGURE 56. TRACK VERTICAL DYNAMIC COMPLIANCE OBTAINED BY USING A CYCLIC PRELOAD/PULSE AND A CONSTANT PRELOAD PULSE AT LOCATION 1

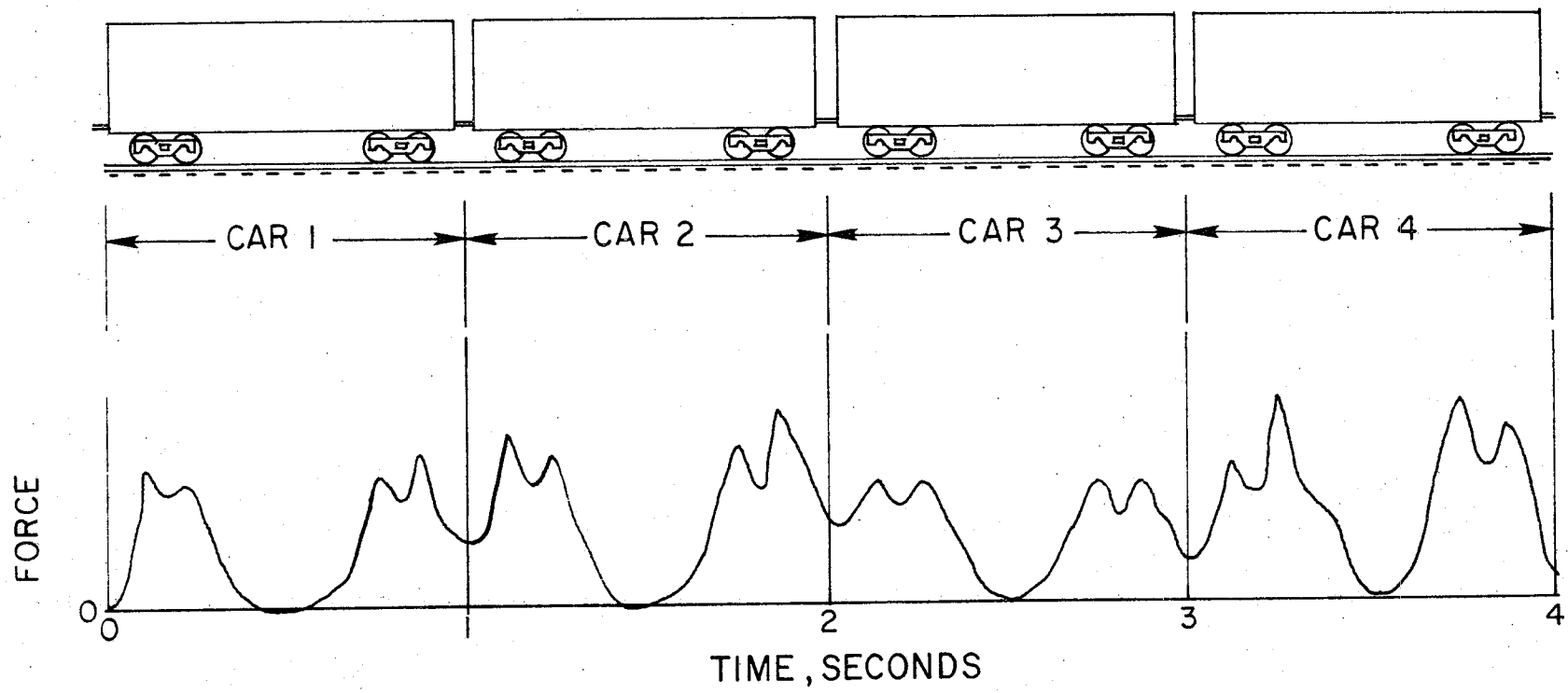

FIGURE 57. TYPICAL DATA FOR VERTICAL TIEPLATE FORCE FOR A 4-CAR TRAIN

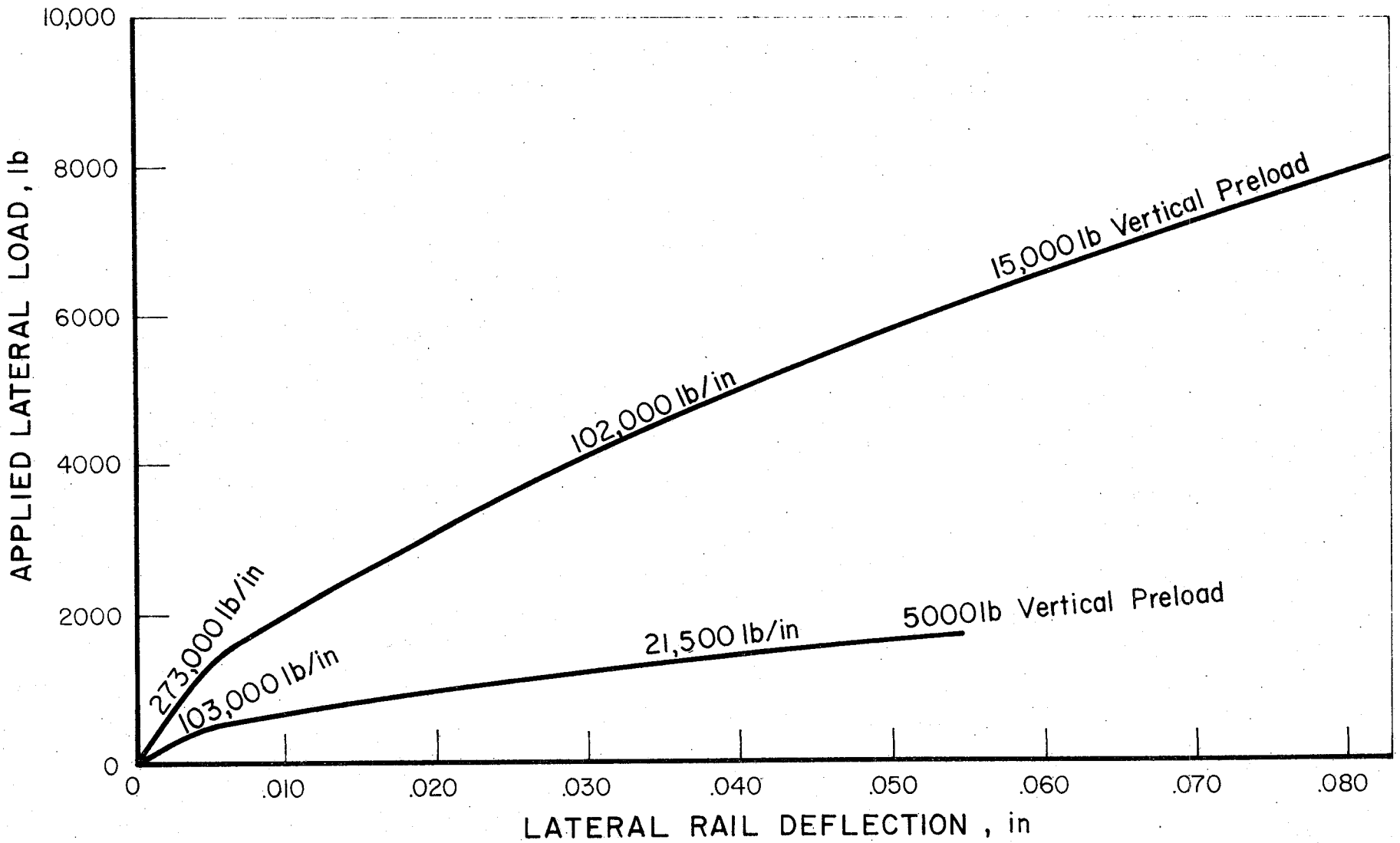

FIGURE 58. LATERAL LOAD DEFLECTION CURVES FOR LOCATION 1

Also shown in the figure is a load-deflection curve with 5,000 lb vertical load. In this case, the initial slope is 103,000 lb/in., and in the large deflection region, the stiffness is reduced to 21,500 lb/in. The higher stiffness values for small deflections compare fairly well to the 250,000 lb/in. lateral dynamic stiffness obtained with a 15,000 lb constant vertical preload and 80,000 lb/in. lateral stiffness for a 5,000 lb preload using random excitation, see Table 16. The deflections due to a random excitation of 100 lbs rms would be in the low-deflection region.

Effect of a Defective or Missing Tie

Location 3 was used to determine the sensitivity of the track compliance measurements for detecting a localized track anomaly such as a single defective or missing tie. This type of defect was simulated by measuring track compliance before and after the tie plates were removed from both rails on one tie. The track at this location was well compacted, and the maximum vertical load of 20,000 pounds applied directly over the missing tie plate did not deflect the rail enough to close the 1/2-inch gap left by the tie plate. Therefore, the compliance measurements actually represented the complete loss of support from one tie, irrespective of whether it was caused by a missing tie plate or a missing or defective tie.

Figure 59 shows a comparison of the vertical track compliance measured at Location 3 with the tie plate in place and removed. A comparison of stiffnesses is plotted in Figure 60. Removing the tie plates reduced the stiffness by 33 percent at the low preload, and by 45 percent at the high preload. Figure 61 is a comparison of vertical load deflection curves before and after the tie plates were removed. These static deflections show about the same change in stiffness as was shown with the dynamic data. Again, the static stiffness does not agree with the low-frequency dynamic stiffness, but using the cyclic preload/pulse gave better results. As shown in Figure 62, 227,000 lb/in. vertical dynamic stiffness on the west rail compared with 184,000 lb/in. vertical static stiffness at 8,000 lb load, and 154,000 lb/in. compared to 142,000 lb/in. static stiffness vertical at 8,000 lb load on the east rail.

TABLE 16. COMPARISON OF THE STATIC AND DYNAMIC LATERAL STIFFNESS MEASURED AT LOCATION 1

Preload - Vertical	Stiffness - Lateral		Dynamic, lb/in.
	Static, lb/in. Load Deflection Curve		
5,000 lb	Initial Slope	103,000	80,000
	Final Slope	21,500	
15,000 lb	Initial Slope	273,000	250,000
	Final Slope	102,000	

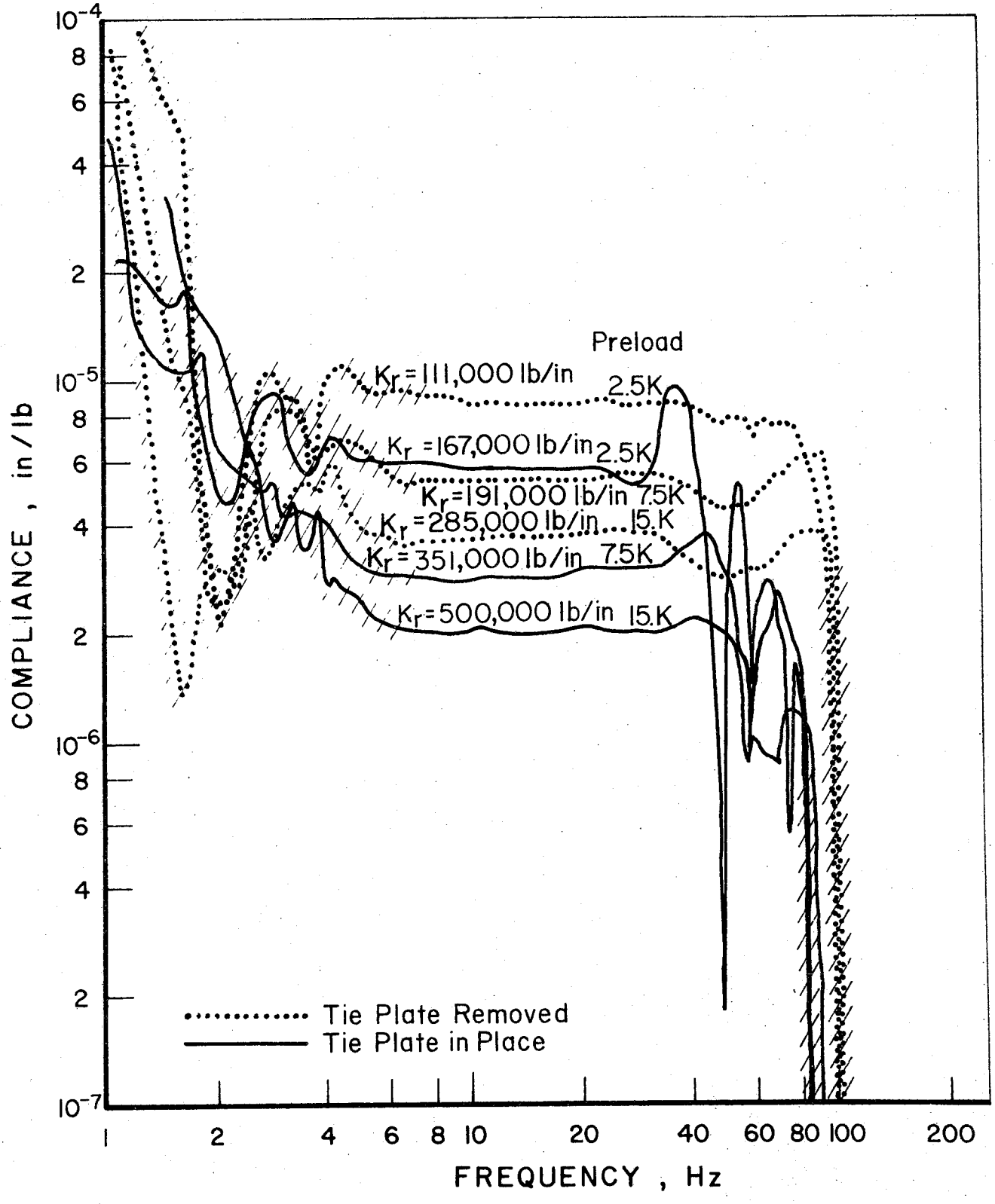

FIGURE 59. TRACK VERTICAL DYNAMIC COMPLIANCE MEASURED AT LOCATION 3 WITH AND WITHOUT THE TIEPLATE

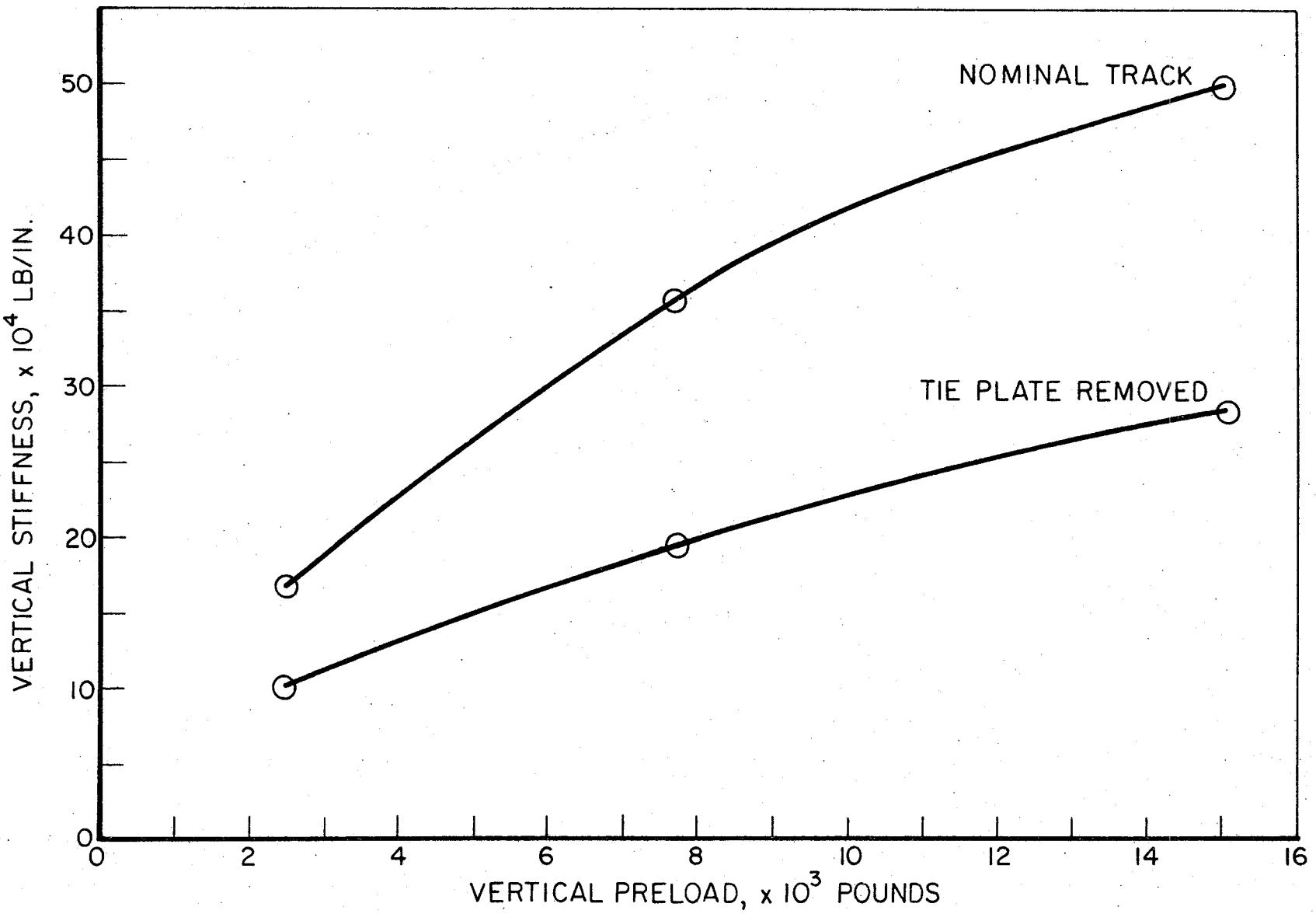

FIGURE 60. TRACK VERTICAL DYNAMIC STIFFNESS FOR NOMINAL TRACK AND TRACK WITH TIEPLATES ON ONE TIE REMOVED AT LOCATION 3

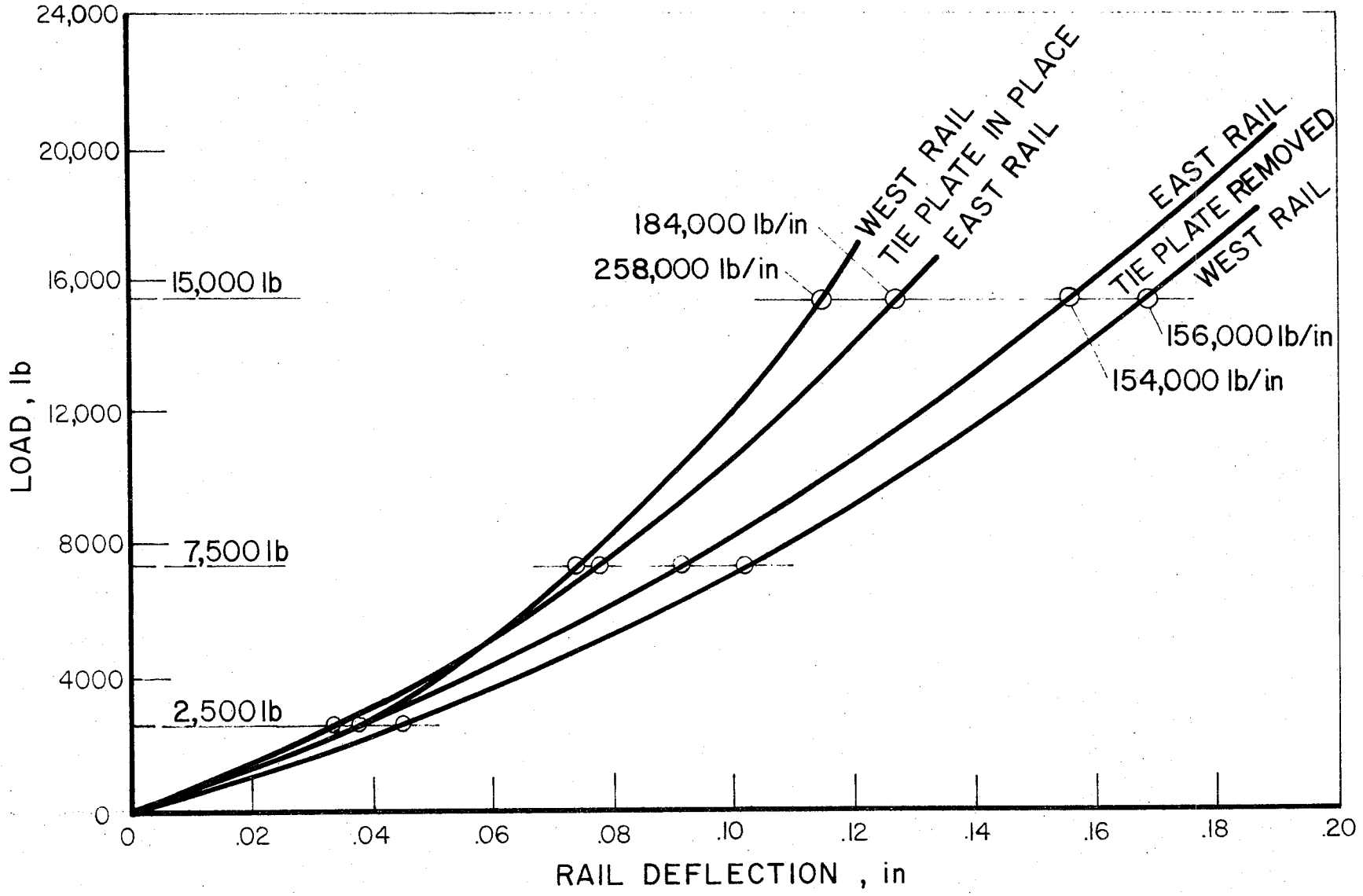

FIGURE 61. VERTICAL LOAD DEFLECTION CURVES FOR LOCATION 3 WITH AND WITHOUT TIEPLATES

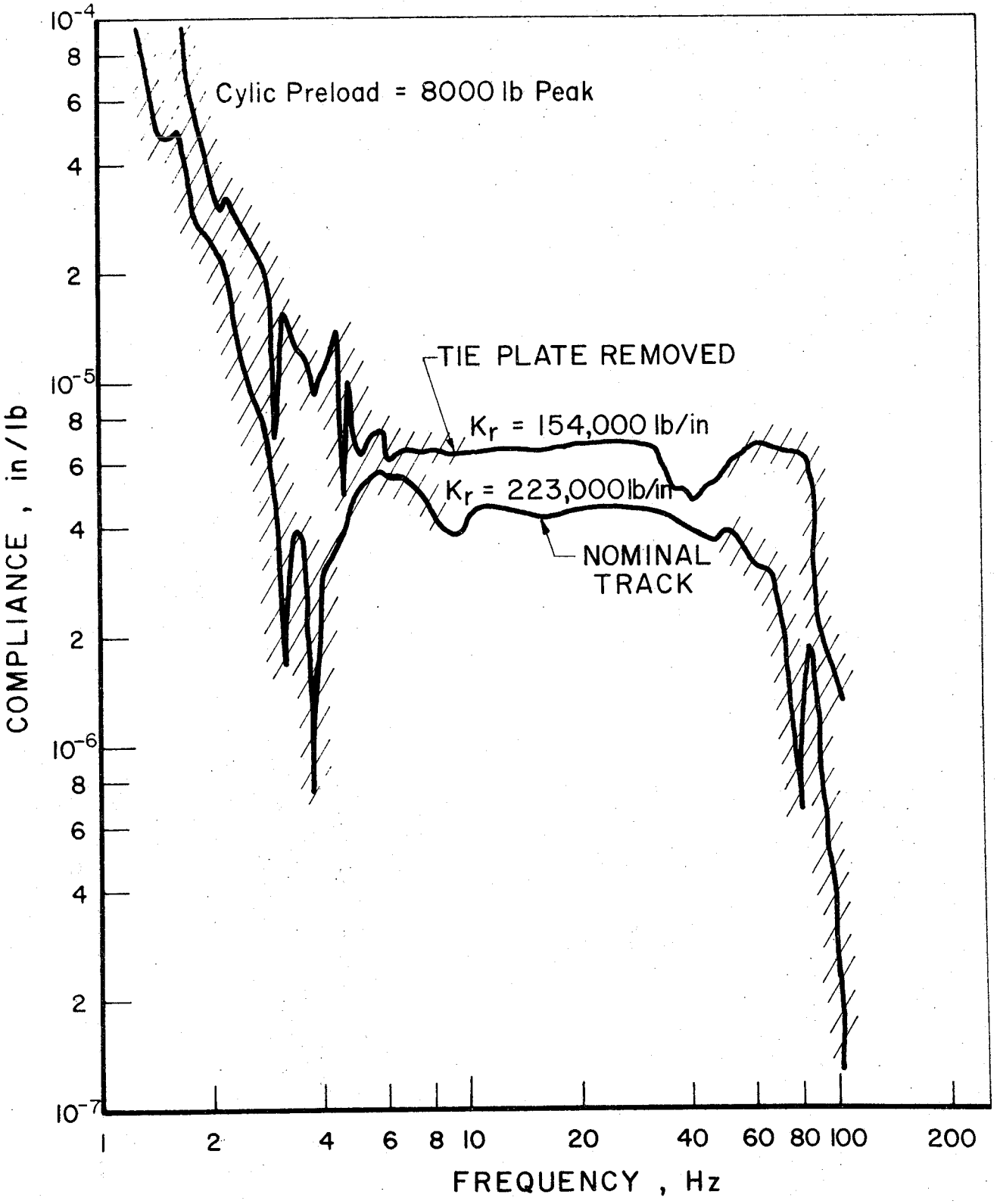

FIGURE 62. TRACK VERTICAL DYNAMIC COMPLIANCE OBTAINED BY USING A CYCLIC PRELOAD/PULSE TO DETERMINE THE EFFECT OF A MISSING TIEPLATE AT LOCATION 3

Figure 63 shows lateral track compliance measurements after the tie plate was removed. Table 17 lists the compliance parameters as a function of preload. Lateral static load-deflection measurements were also made and are shown in Figure 64; Also are listed in Table 17. These stiffness values are plotted in Figure 65. The two distinct stiffness regions can be seen in the stiffness curves. Since the horizontal dynamic excitation was below 1,000 lb, the stiffness measured should be the initial slope of 82,000 lb/in. at 5,000 lb vertical preload, 112,000 lb/in. at 10,000 lb vertical preload, and 128,000 lb/in. for 15,000 lb bertical preload. This is in good agreement with the dynamic data shown in Figure 63 and Table 17.

These results show that removing the tie plate does cause a measurable change in stiffness, static and dynamic, in both the lateral and vertical directions. The size of the change is approximately the same as that measured for wet track conditions in the vertical direction.

Load Affected Zone

Transfer compliance functions along the rail were obtained to describe the loading profile and the load affected zone from the point of application of the load. Compliance data were measured at the loading point and at 4,8, and 12 feet along the track. Compliance values can then be plotted, at a specific frequency, as a function of distance along the track. The phase angle is used to determine whether the rail is moving in phase with the force or out of phase. Figure 66 shows compliance values for 20, 25, 30, and 30 Hz plotted as a function of distance along the track. Table 18 tabulates the compliance values and the measured phase angle with respect to the force. The figure shows that the wavelength is decreasing with increasing frequency, and that the point of zero crossing changes from 7.75 feet at 20 Hz to 6.25 feet at 35 Hz. These compliance values would be a function of the track structure tested because these values measured are near and at the resonances of the track structure.

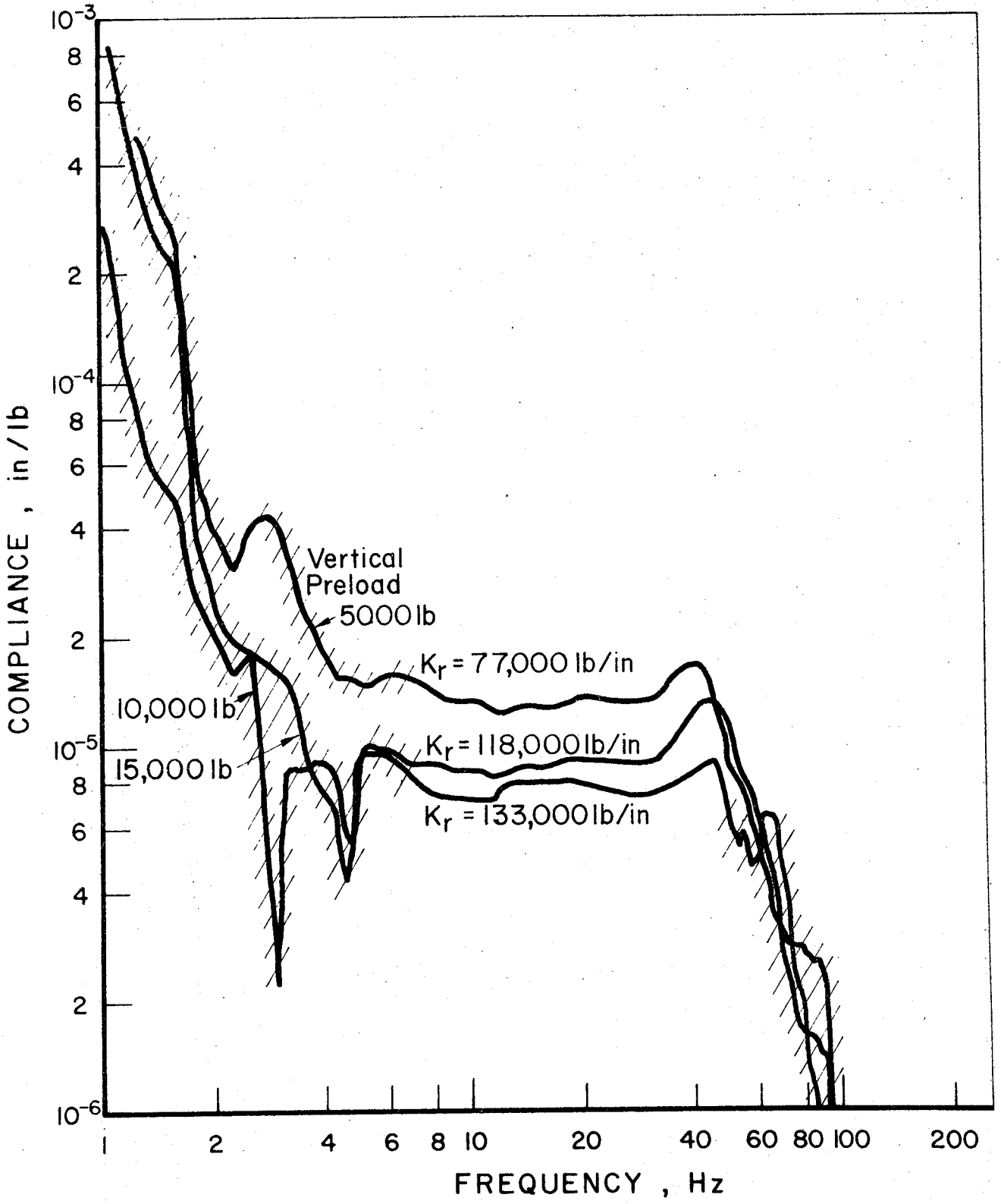

FIGURE 63. TRACK LATERAL DYNAMIC COMPLIANCE WITH THE TIEPLATES REMOVED

TABLE 17. SUMMARY OF TRACK LATERAL COMPLIANCE PARAMETERS AT LOCATION 3 USING RANDOM EXCITATION

Vertical Preload, lb	Dynamic Lateral Stiffness K_r, lb/in	Natural Frequency ω_n, Hz	Damping ζ, Percent	Effective Mass M_r, lb	Static Lateral Stiffness, lb/in
5,000	77,000	40	38.0	470	82,000
10,000	118,000	45	32.5	570	112,000
15,000	133,000	46	42.0	615	128,000

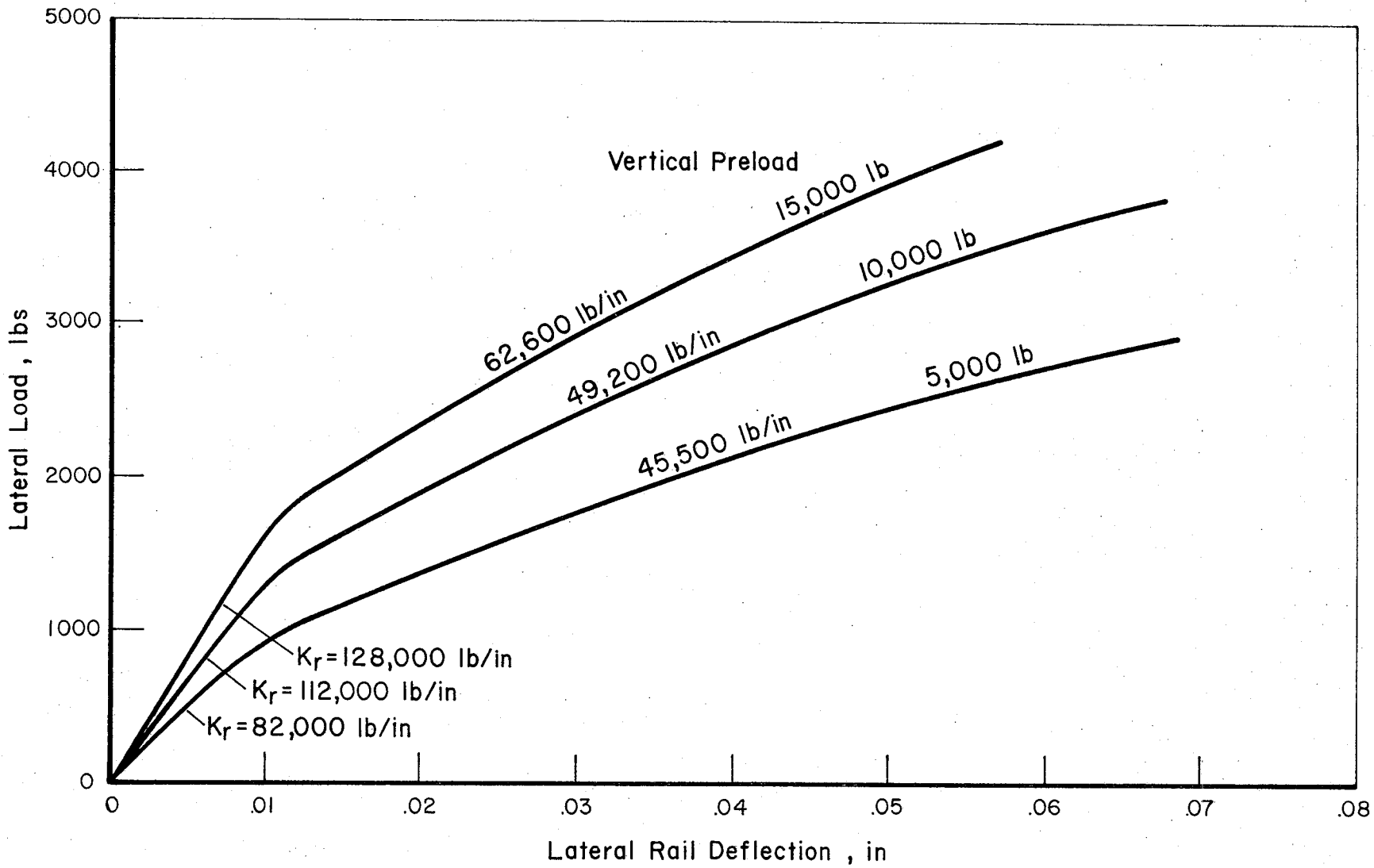

FIGURE 64. STATIC LOAD DEFLECTION CURVES IN THE LATERAL DIRECTION FOR THREE VERTICAL PRELOADS AT LOCATION 3

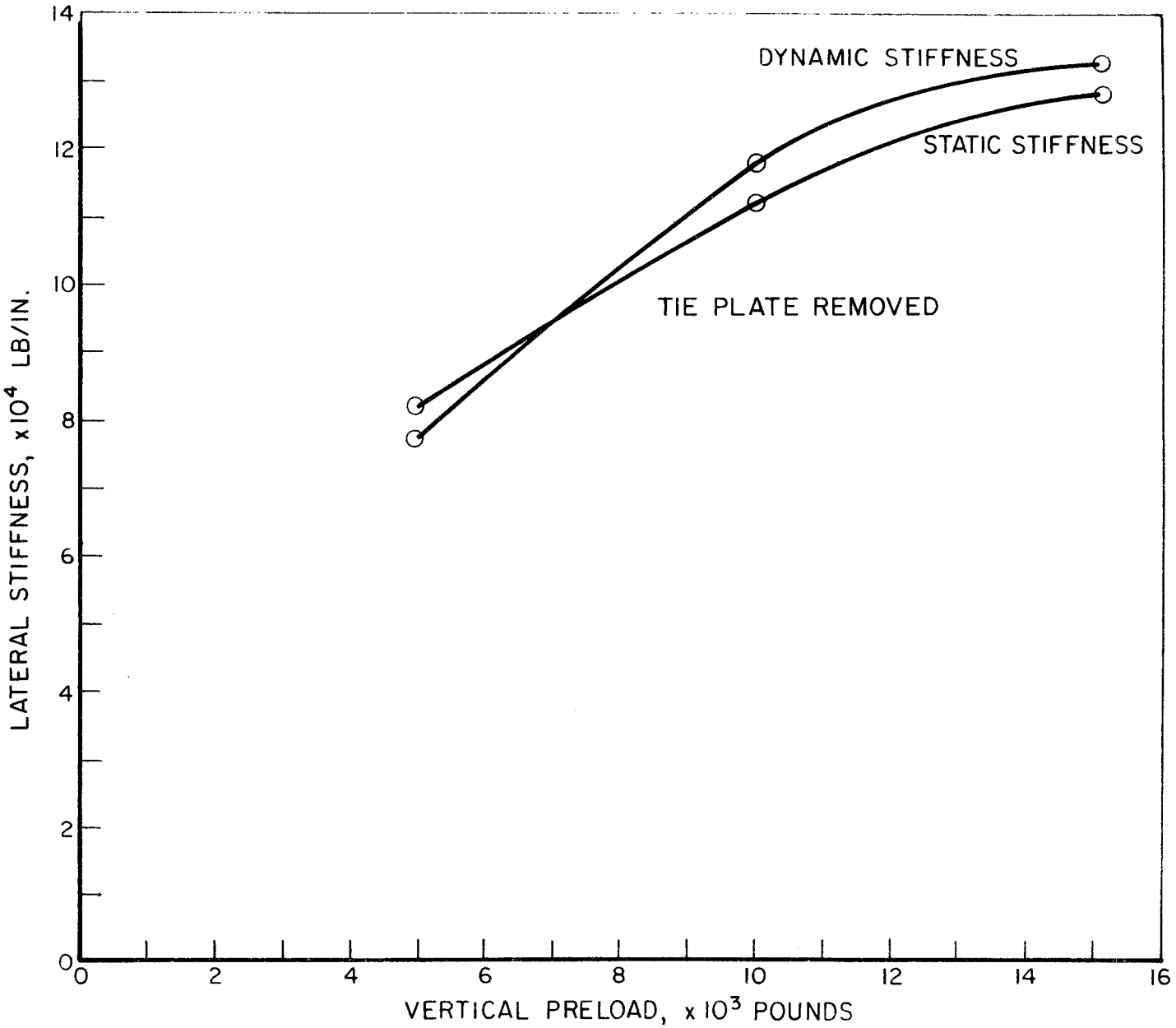

FIGURE 65. TRACE LATERAL STATIC AND DYNAMIC STIFFNESS AT LOCATION 3 WITH TIE PLATE REMOVED

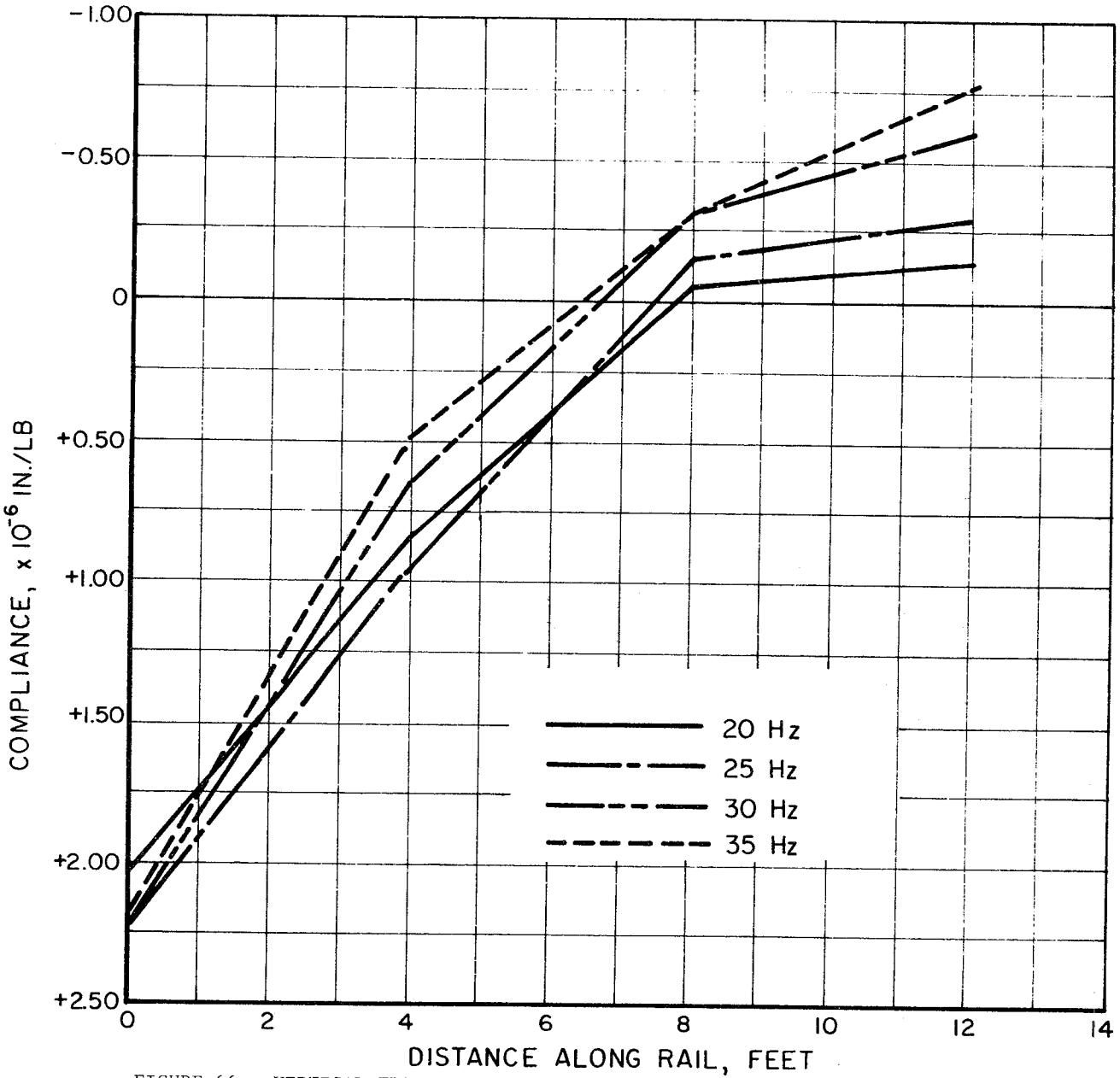

FIGURE 66. VERTICAL TRANSFER COMPLIANCE VALUES AT SPECIFIC FREQUENCIES AS A FUNCTION OF DISTANCE ALONG THE RAIL.

TABLE 18. TRANSFER COMPLIANCE VALUES ALONG THE RAIL

Frequency, Hz	Compliance, lb/in	Distance, ft	Basic Angle, deg
20	2.05×10^{-6}	0	13
20	8.5×10^{-7}	4	30
20	9.4×10^{-8}	8	160
20	1.3×10^{-7}	12	180
25	2.25×10^{-6}	0	23
25	9.4×10^{-7}	4	54
25	1.7×10^{-7}	8	149
25	2.4×10^{-7}	12	180
30	2.25×10^{-6}	0	30
30	6.5×10^{-7}	4	90
30	3.0×10^{-7}	8	192
30	6.0×10^{-7}	12	270
35	2.2×10^{-6}	0	0
35	5.0×10^{-7}	4	90
35	3.0×10^{-7}	8	192
35	7.6×10^{-7}	12	347

Figures 67 and 68 show the detailed amplitude and phase data for the compliance measurements at the different locations along the track. The phase angle at low frequencies indicates the zero crossing is probably between 4 and 8 feet, as shown in Figure 66, although the fluctuations in phase below 30 Hz are confusing. These fluctuations cause an apparent zero crossing between 8 and 10 feet. The amplitude data in Figure 67 is of particular interest because it shows a more dominant resonant behavior at distances of 8 and 12 feet from the loading point when the frequency approaches 35 Hz. It should be remembered, however, that the track is essentially unloaded by the static load at these low distances. Valid transfer compliance data for train wheels would require that the full wheel load be applied at each point where the compliance measurement is made.

Appendix A contains three tables that summarize the data listed in this report. Table A-1 is a summary table of the static stiffness measurements. Table A-2 is a summary table of the dynamic stiffness measurements obtained by using pulse, random and sine excitation. Table A-3 is a summary of the track vertical and lateral dynamic characteristics.

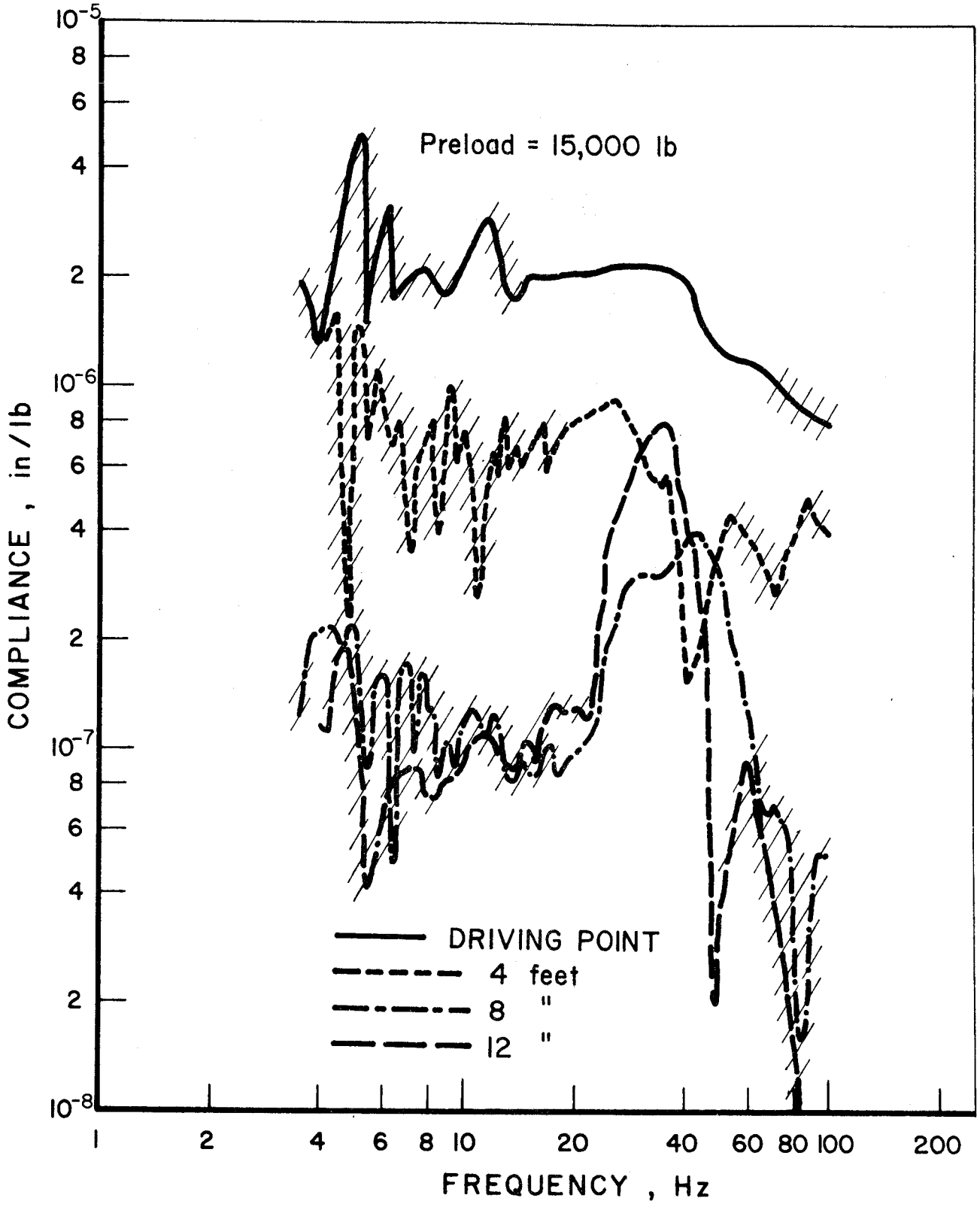

FIGURE 67. TRACK VERTICAL TRANSFER DYNAMIC COMPLIANCE AT FOUR LOCATIONS ALONG THE RAIL

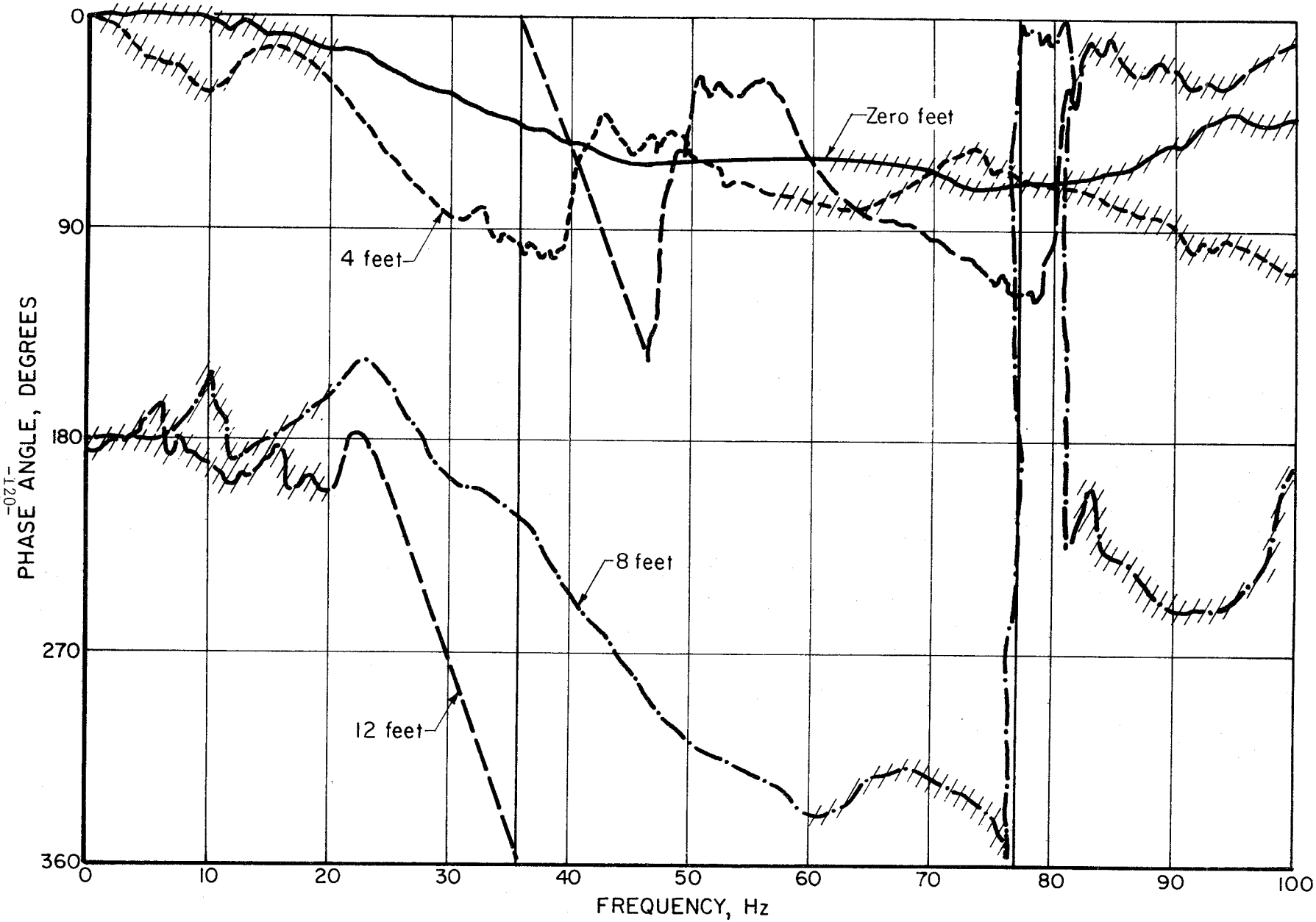

FIGURE 68. VERTICAL TRANSFER COMPLIANCE PHASE ANGLE FOR THE FOUR DISTANCES ALONG THE RAIL

REFERENCES

[1] Bendat, J.S. and Piersol, A.G., Random Data: Analysis and Measurement Procedures", John Wiley and Sons, Inc., New York, 1971, p 142.

[2] Prause, R.H. and Harrison, H.D., Data Analysis and Instrumentation requirements for Evaluating Rail Joints and Rail Fasteners in Urban Track, Report No UMTA-MA-06-0025-75-8, Prepared for U. S. Department of Transportation by Battelle Columbus Laboratories, February, 1975.

APPENDIX A

TABLE A-1. SUMMARY TABLE OF STATIC STIFFNESS MEASUREMENTS

Location	Vertical Preload, lb	Stiffness, lb/in	Direction/Rail
1	2500	12,500	Vertical
	5000	74,000	Vertical
	7500	121,000	Vertical
	15,000	180,000	Vertical
1 (cyclic preload pulse)	8000	102,400	Vertical
	5000	102,400	Lateral
		21,500	Lateral
	15,000	273,000	Lateral
		102,000	Lateral
2	2500	12,600	Vertical/East
		23,000	Vertical/West
	7500	118,500	Vertical/East
		90,000	Vertical/West
	15,000	169,000	Vertical/East
		138,000	Vertical/West
(Cyclic preload pulse)	8000	167,000	Vertical/East
3	2500	88,000	Vertical/East
		74,000	Vertical/West
	7500	142,000	Vertical/East
		184,000	Vertical/West
	15,000	184,000	Vertical/East
		258,000	Vertical/West
(cyclic preload pulse)	8000	227,000	Vertical/West
	2500	70,000	Vertical/East Tie Plate Out
		69,000	Vertical/West Tie Plate Out
	7500	108,000	Vertical/East Tie Plate Out
		98,000	Vertical/West Tie Plate Out
	15,000	154,000	Vertical/East Tie Plate Out
		154,000	Vertical/West Tie Plate Out
(cyclic preload pulse)	8000	154,000	Vertical/East Tie Plate Out
	5000	82,000	Lateral Tie Plate Out
		45,500	
	10,000	112,000	Lateral Tie Plate Out
		49,000	
	15,000	128,000	Lateral Tie Plate Out
		62,500	

TABLE A-2. SUMMARY TABLE OF DYNAMIC STIFFNESS MEASUREMENTS

Location	Vertical Preload, lb	Lateral Preload, lb	Stiffness, lb/in	Direction/Rail
1 Sine	2500		17,000	Vertical
	7500		400,000	Vertical
	15,000		670,000	Vertical
Random	2500		15,000	Vertical
	7500		160,000	Vertical
	15,000		526,000	Vertical
	2500		13,000	Lateral
	5000		73,000	Lateral
	15,000		250,000	Lateral
	5000		71,000	Lateral
	5000	2000	222,000	Lateral
	15,000		250,000	Lateral
	15,000	2000	244,000	Lateral
Unloading Pulse	2500		19,000	Vertical 25 ms
	7500		55,000	Vertical 25 ms
	15,000		213,000	Vertical 25 ms
	15,000		398,000	Vertical 10 ms 3900 lb peak force
	15,000		327,000	Vertical 15 ms 5100 lb peak force
	15,000		306,000	Vertical 20 ms 6000 lb peak force
	15,000		220,000	Vertical 25 ms 6200 lb peak force
Pulse	5000		38,000	Lateral 20 ms
	15,000		200,000	Lateral 20 ms
Cyclic Preload Pulse	8000		170,000	Vertical
2 Random	2500		33,000	Vertical/West
	7500		154,000	Vertical/West
	15,000		313,000	Vertical/West
Unloading Pulse	2500		71,500	Vertical/East
Loading Pulse	2500		167,000	Vertical/East 20 ms
Loading Pulse	15,000		370,000	Vertical/East 20 ms
Cyclic Preload Pulse	8000		167,000	Vertical/East
			118,000	Vertical/West
3 Loading Pulse	2500		167,000	Vertical 20 ms
	7500		351,000	Vertical 20 ms
	15,000		500,000	Vertical 20 ms
Cyclic Preload Pulse	8000		227,000	Vertical/West
Random	2500		111,000	Vertical Tie Plate Out
	7500		191,000	Vertical Tie Plate Out
	15,000		285,000	Vertical Tie Plate Out
Cyclic Preload Pulse	8000		154,000	Vertical/East Tie Plate Out
	5000		77,000	Lateral Tie Plate Out
Random	10,000		118,000	Lateral Tie Plate Out
	15,000		133,000	Lateral Tie Plate Out

TABLE A-3 SUMMARY OF TRACK VERTICAL AND LATERAL DYNAMIC CHARACTERISTICS

Location and Excitation	Direction	Vertical Preload, lb	Lateral Preload, lb	Stiffness, lb/in.	Natural Frequency, Hz	Effective Mass, lb	Damping Percent Critical	Remarks
1 Sine	Vertical	2500	0	17,000	18.0	513	18.0	
1 Random	Vertical	2500	0	15,000	17.5	478	24.0	
1 Random	Vertical	2500	0	18,500	18.0	560	30.0	
1 Unloading Pulse	Vertical	2500	0	19,000	18.0	573	18.0	
2 Unloading Pulse	Vertical	2500	0	167,000	30.0	1810	32.0	
2 Random	Vertical	2500	0	33,000	23.0	610	28.0	
3 Unloading Pulse	Vertical	2500	0	167,000	36.0	1260	34.0	
1 Sine	Vertical	7500	0	400,000	35.0	3200	35.0	
1 Unloading Pulse	Vertical	7500	0	55,000	18.5	1571	11.0	
1 Random	Vertical	7500	0	160,000	42.0	887	46.0	
2 Random	Vertical	7500	0	154,000	25.0	2400	50.0	
3 Unloading Pulse	Vertical	7500	0	351,000	44.0	1770	38.0	
1 Sine	Vertical	15,000	0	670,000	37.0	4700	30.0	
1 Random	Vertical	15,000	0	526,000	37.0	3760	39.0	
1 Unloading Pulse	Vertical	15,000	0	213,000	21.0	4722	31.0	
1 Unloading Pulse	Vertical	15,000	0	398,000	47.0	1760	31.0	3900 lb. peak force - 10 ms
1 Unloading Pulse	Vertical	15,000	0	327,000	34.0	2760	16	5700 lb. peak force - 15 ms
1 Unloading Pulse	Vertical	15,000	0	306,000	28.0	3816	16	6000 lb peak force - 20 ms
1 Unloading Pulse	Vertical	15,000	0	220,000	20.0	5378	15.0	6300 lb peak force - 25 ms
2 Random	Vertical	15,000	0	313,000	25.0	4896	45.0	
2 Unloading Pulse	Vertical	15,000	0	370,000	40.0	2261	31.0	
3 Loading Pulse	Vertical	15,000	0	500,000	41.0	2910	41.0	
1 Pulse	Lateral	2500	0	38,000	30.0	412	37.5	
1 Random	Lateral	2500	0	13,000	17.5	415	45.0	
1 Random	Lateral	5000	0	73,000	50.0	285	37.0	
1 Random	Lateral	5000	0	71,000	50.0	278	38.0	
1 Random	Lateral	5000	2000	220,000	65.0	509	21.0	
3 Random	Lateral	5000	0	73,000	40.0	470	38.0	
1 Pulse	Lateral	15,000	0	20,000	72.0	372	11.0	
1 Random	Lateral	15,000	0	250,000	90.0	301	31.0	
1 Random	Lateral	15,000	2000	244,000	70.0	486	29.0	
3 Random	Lateral	15,000	0	133,000	46.0	614	42.0	

TABLE A-3 SUMMARY OF TRACK VERTICAL AND LATERAL DYNAMIC CHARACTERISTICS

Location and Excitation	Direction	Vertical Preload, lb	Lateral Preload, lb	Stiffness, lb/in.	Natural Frequency, Hz	Effective Mass, lb	Damping Percent Critical	Remarks
1 Sine	Vertical	2500	0	17,000	18.0	513	18.0	
1 Random	Vertical	2500	0	15,000	17.5	478	24.0	
1 Random	Vertical	2500	0	18,500	18.0	560	30.0	
1 Unloading Pulse	Vertical	2500	0	19,000	18.0	573	18.0	
2 Unloading Pulse	Vertical	2500	0	167,000	30.0	1810	32.0	
2 Random	Vertical	2500	0	33,000	23.0	610	28.0	
3 Unloading Pulse	Vertical	2500	0	167,000	36.0	1260	34.0	
1 Sine	Vertical	7500	0	400,000	35.0	3200	35.0	
1 Unloading Pulse	Vertical	7500	0	55,000	18.5	1571	11.0	
1 Random	Vertical	7500	0	160,000	42.0	887	46.0	
2 Random	Vertical	7500	0	154,000	25.0	2400	50.0	
3 Unloading Pulse	Vertical	7500	0	351,000	44.0	1770	38.0	
1 Sine	Vertical	15,000	0	670,000	37.0	4700	30.0	
1 Random	Vertical	15,000	0	526,000	37.0	3760	39.0	
1 Unloading Pulse	Vertical	15,000	0	213,000	21.0	4722	31.0	
1 Unloading Pulse	Vertical	15,000	0	398,000	47.0	1760	31.0	3900 lb. peak force - 10 ms
1 Unloading Pulse	Vertical	15,000	0	327,000	34.0	2760	16	5700 lb. peak force - 15 ms

TABLE A-3 (CONTINUED)

Location and Excitation	Direction	Vertical Preload, lb	Lateral Preload, lb	Stiffness, lb/in.	Natural Frequency Hz	Effective Mass, lb	Damping Percent Critical	Remarks
1 Unloading Pulse	Vertical	15,000	0	306,000	28.0	3816	16	6000 lb peak force - 20 ms
1 Unloading Pulse	Vertical	15,000	0	220,000	20.0	5378	15.0	6300 lb peak force - 25 ms
2 Random	Vertical	15,000	0	313,000	25.0	4896	45.0	
2 Unloading Pulse	Vertical	15,000	0	370,000	40.0	2261	31.0	
3 Loading Pulse	Vertical	15,000	0	500,000	41.0	2910	41.0	
1 Pulse	Lateral	2500	0	38,000	30.0	412	37.5	
1 Random	Lateral	2500	0	13,000	17.5	415	45.0	
1 Random	Lateral	5000	0	73,000	50.0	285	37.0	
1 Random	Lateral	5000	0	71,000	50.0	278	38.0	
1 Random	Lateral	5000	2000	220,000	65.0	509	21.0	
3 Random	Lateral	5000	0	73,000	40.0	470	38.0	
1 Pulse	Lateral	15,000	0	20,000	72.0	372	11.0	
1 Random	Lateral	15,000	0	250,000	90.0	301	31.0	
1 Random	Lateral	15,000	2000	244,000	70.0	486	29.0	
3 Random	Lateral	15,000	0	133,000	46.0	614	42.0	